

**Aluminium uptake, translocation and accumulation in the
aluminium accumulating plant species buckwheat (*Fagopyrum
esculentum* Moench)**

Von der Naturwissenschaftlichen Fakultät der
Gottfried Wilhelm Leibniz Universität Hannover

zur Erlangung des Grades

Doktor der Gartenbauwissenschaften

Dr. rer. hort.

genehmigte Dissertation

von

Dipl.-Ing. agr. Benjamin Klug

geboren am 17.10.1977 in Miltenberg

2010

Referent: Prof. Dr. rer. agr. Walter J. Horst

Korreferent: Prof. Dr. rer. agr. Heiner Goldbach

Tag der Promotion: 01.07.2010

Abstract

Aluminium toxicity is the major factor limiting crop productivity on acid soils. These acid soils represent a significant share of the world's arable land. Most plant species are showing a pronounced root growth inhibition already at micro molar concentrations of Al in the soil solution which leads, as consequence thereof to reduced yield. Notwithstanding these severe effects of Al, there is a wide variation in Al resistance between plant species and even between genotypes within one species. Plant species like buckwheat are highly Al resistant and can even accumulate Al in above ground plant organs, whereas non Al accumulating plant species are showing only traces of Al in the leaf tissue. Buckwheat is only weakly affected by Al which is achieved by a combination of distinct resistance and tolerance mechanisms. However, under the common opinion resistance and tolerance mediating processes are acting in an opposite direction. On the one hand resistance mechanisms are keeping Al away from sensitive binding sites, thus preventing Al binding, uptake and resulting injury. On the other hand, processes participating in internal tolerance are enabling a plant to cope with Al which is taken up and to tolerate high symplastic Al concentrations. Due to the fact that this interrelation and the transport of Al itself are not understood this work focuses on the following objectives: I. How are resistance and tolerance mechanisms spatially organized? II. Does the in-situ analysis of Al distribution within the root tip provide information about the route of uptake and subsequent translocation? III. Are the Al uptake and translocation processes under metabolic control and do the resistance and tolerance mechanisms actually acting oppositional? IV. Is there a genotypic variation also in Al tolerance within the *Fagopyrum* genus and does this variation provide additional insights? The results show that Al is taken up by the 10 mm root apex is rapidly transferred to the xylem. Aluminium activates the resistance mechanism which is spatially overlapping with the zone of the most pronounced Al uptake. Furthermore, it is shown that a basipetal signal transduction for the transmission of resistance mediating stimuli is involved. The staining of Al in combination with LA-ICP-MS analysis of Al concentrations is an appropriate way for analysis of element distribution within cross sections of fresh root tip material. The results clearly indicate that Al is differentially localized in different distances from the root tip. The analysis of the uptake of Al into the water free space revealed that the Al-activated exudation of oxalate rapidly established a 1:1 ratio of oxalate and Al in the symplast, the Al concentration was 100 times higher than in the external solution, and the Al to oxalate ratio was 1:2. Loading and unloading of Al into and from the symplast has been clearly shown to be executed under metabolic control. Anion channel inhibitors reduced the constitutive and the Al-enhanced WFSF oxalate concentrations and intensified the Al-induced injury. The hypothesis is presented that an Al(Ox)^+ plasma-membrane transporter in the root cortex and a xylem-loading Al(Cit)^{3-} transporter in the xylem parenchyma cells represent key elements of Al accumulation in buckwheat. To achieve first genetic insights into Al hyperaccumulation a scope of 94 genotypes were screened. It is shown that these genotypes vary primarily gradually in the Al concentration in the xylem sap indicating that this trait is well conserved within this genus. A multiple correlation analysis provides circumstantial evidence for a positive correlation of Al resistance and tolerance mechanisms on a genotypic level.

Zusammenfassung

Auf sauren Böden wird die Pflanzenproduktion maßgeblich durch Aluminiumtoxizität beeinträchtigt, wobei diese Böden einen beträchtlichen Anteil der agrarisch nutzbaren Fläche der Welt bedecken. Die meisten Pflanzenarten zeigen, schon bei mikromolaren Konzentrationen von Al eine deutliche Inhibierung des Wurzelwachstums was letztendlich zu erheblichen Ertragseinbußen führt. Abgesehen von den schwerwiegenden Folgen von Al-Toxizität gibt es eine große Variabilität in der Aluminiumresistenz zwischen verschiedenen Pflanzenarten und Genotypen innerhalb einer Art. Buchweizen ist durch eine hohe Al Resistenz charakterisiert und transloziert, im Gegensatz zu anderen Pflanzenarten darüber hinaus Al in den Spross. Buchweizen zeigt nur geringe Beeinträchtigungen durch Al-Toxizität, was dadurch erreicht wird, Al-Toleranz- und Resistenzmechanismen kombiniert werden. Daraus ergibt sich dennoch ein gewisser Widerspruch, da diese Prozesse bisher so verstanden wurden, dass sie in entgegen gesetzter Richtung wirken. Auf der einen Seite sorgen Resistenzmechanismen dafür, dass Al von sensitiven Bindungsstellen im Wurzelapoplasten ferngehalten wird und somit Bindung, Aufnahme und daraus resultierende Schädigung unterbunden wird. Auf der anderen Seite sorgen Toleranzmechanismen dafür, dass große Mengen an symplastisch lokalisiertem Al toleriert werden können. Da diese Beziehung zwischen Resistenz- und Toleranzmechanismen und der Al Transport selbst, noch nicht verstanden wird, befasst sich die vorliegende Arbeit mit folgenden Fragen: I. Wie sind Al-Resistenz- und Toleranzmechanismus lokal organisiert? II. Ist es möglich über eine *in-situ* Al-Analyse nähere Aufschlüsse über die Al-Aufnahme und die anschließende Translokation zu bekommen? III. Sind die Al-Aufnahme und Translokation aktive, von metabolischer Aktivität abhängige Prozesse und wirken sie tatsächlich gegensätzlich? IV. Gibt es genotypische Variabilität in der Al-Toleranz innerhalb der Gattung *Fagopyrum*. Die Ergebnisse zeigen, dass Al von den apikalen 10 mm der Wurzelspitze aufgenommen und schnell ins Xylem transportiert werden. Dabei aktiviert Al den Resistenzmechanismus, der lokal auch in die Regionen mit hohen Al-Aufnahmeraten hereinreicht. Zusätzlich zeigte sich, dass eine basipetale Signaltransduktion in der Weiterleitung des resistenzvermittelnden Stimulus involviert ist. Die Fluoreszenzfärbung in Verbindung mit LA-ICP-MS Technologie hat sich als probates Mittel erwiesen, um die Al-Verteilung in radialer Richtung von Wurzelspitzenquerschnitten zu analysieren. Prinzipiell untermauern diese Ergebnisse, dass Al im Wurzelquerschnitt von Buchweizen sehr mobil ist. Al wird in verschiedenen Abständen von der Wurzelspitze in unterschiedlichen Zonen lokalisiert. Die Analyse der Al Aufnahme in den WFS zeigte, dass die Al aktivierte exsudation Oxalat von schnell zu einem Verhältnis von 1:1 (Al:Ox) im Apoplasten führt. Die Al Konzentration im Symplasten ist hingegen deutlich höher als im Apoplasten und das Al:Ox-Verhältnis liegt hier bei 1:2. Die Aufnahme und Abgabe von Al in und aus dem Wurzelsymplasten zeigte, dass diese Prozesse von metabolischer Aktivität abhängig sind. Der Einsatz von einem Anionenkanalinhibitor reduzierte die konstitutive und die Al-aktivierte Exsudation von Oxalat und führte zu einem verstärkten Al-induziertem Schaden. Die gezeigten Ergebnisse legen die Hypothese nahe, dass ein plasmamembrangebundener $Al(Ox)^+$ Transporter im Wurzelkortex und ein $Al(Cit)^-$ Transporter während der Xylembeladung die Schlüsselemente der Al-Akkumulation von Buchweizen darstellen. Um einen Überblick über die Variabilität der Al-Akkumulation bei Buchweizen zu bekommen wurden 94 *Fagopyrum* Genotypen einem Screening unterzogen. Dabei konnte gezeigt werden, dass die Al-Konzentration im Xylemsaft graduell variiert, was darauf hindeutet, dass es sich bei der Al-Akkumulation von Buchweizen um ein stark konserviertes Merkmal handelt. Eine multiple

Zusammenfassung

Regressionsanalyse erbrachte einen Indizienbeweis für eine positive Korrelation zwischen Al-Resistenz und Toleranzmechanismus

Keywords: Accumulator, Al resistance, Al detoxification

Schlagworte: Akkumulator, Al Resistenz, Al Entgiftung

Contents

Aluminium uptake, translocation and accumulation in the aluminium accumulating plant species buckwheat (*Fagopyrum esculentum* Moench)

Abstract	I
Zusammenfassung	II
Contents	IV
Abbreviations	7
General Introduction	9
Acid soils and Al toxicity	9
The physiology of Al toxicity in plants	10
How do plants cope with Al toxicity? - Al exclusion	11
How do plants cope with Al toxicity? – Al accumulation and Al tolerance mechanisms ...	14
Buckwheat – the combination of Al exclusion and Al accumulation/Al tolerance mechanisms	15

Spatial characteristics of aluminum uptake and translocation in roots of buckwheat (*Fagopyrum esculentum*)

Abstract	17
Introduction	18
Material and Methods	19
Plant material	19
Al and oxalate distribution along the root apex	20
Minirhizotron experiments	20
Determination of oxalate exudation from excised root segments	21
Al determination	21
Organic acid determination	22
Staining of suberin and lignin in root tips	22
Statistical analysis	23
Results	23
Discussion	28

Oxalate exudation into the root-tip water free space confers protection from Al toxicity and allows Al accumulation in the symplast in buckwheat (*Fagopyrum esculentum* Moench)

Abstract	33
Introduction	34
Material and Methods.....	35
Plant Material	35
Aluminium loading of intact adventitiously rooted cuttings.....	36
Aluminium loading and unloading of excised adventitious roots.....	36
Aluminium loading in presence of oxalate and phenylglyoxal.....	36
Fractionation of Al and organic acids in the root tissue.....	37
Aluminium determination	38
Determination of organic acids	38
Results	39
Discussion	46

Aluminium localisation in root tips of the aluminium-accumulating plant species buckwheat (*Fagopyrum esculentum* Moench)

Abstract	52
Introduction	53
Material & Methods	54
Plant Material	54
Fluorometry	55
Microscopy.....	55
Laser-ablation ICP-MS	56
Results:	57
Discussion:	68

Differences in aluminium accumulation and resistance between genotypes of the genus *Fagopyrum*

Abstract	73
Introduction	74
Material & Methods	75
Plant material.....	75
Plant cultivation.....	75
Substrate analysis	76
Genotypic comparison in nutrient solution	76
Sampling of xylem sap	76
Mineral element analysis.....	77
Determination of organic acids	77
Results	78
Discussion	86
Substrate parameters	86
Genotypic aspects.....	87
Xylem sap Al concentration the parameter of choice	88
Al transport.....	88
Association of Al resistance and tolerance	90
General Discussion	93
The role of the apoplast in Al-accumulating buckwheat.....	93
Al uptake and the symplastic contribution to Al resistance in buckwheat.....	97
Outlook.....	100
I. Expression analysis of physiologically determined candidate genes	101
II. Global gene expression profiling in buckwheat tissues.....	102
References	105
Supplemental material.....	127
Lebenslauf.....	130
Scientific Publications	131
Erklärung.....	132
Danke!	134

Abbreviations

Al	aluminium
ALMT1	aluminium-activated malate transporter
ANOVA	analysis of variance
°C	degree Celsius
Cit	citrate
CW	cell wall
EDTA	ethylenediamine tetra acetate
Fe	Iron
FRD3	ferric reductase defective 3 (member of the MATE family)
g	gram
µg	microgram
GF-AAS	graphite furnace atomic absorption spectrometer
h	hour
HPLC	high pressure liquid chromatography
ICP-OES	inductively coupled plasma optical emission spectroscopy
L	litre
LA-ICP-MS	laser ablation inductively coupled plasma mass spectroscopy
M	molar concentration
MATE	multi drug and toxic compound extrusion protein family
mg	milligram
min	minute
mL	millilitre
mm	millimetre
µm	micrometre
mM	millimolar
µM	micromolar
n	number of observations
nm	nanometre
nM	nanomolar
ns	nonsignificant
Ox	oxalate
PG	phenylglyoxal

Abbreviations

rpm	rotations per minute
SE	standard error
WFSF	water free space fluid
OA	organic acid
P	probability
qRT-PCR	quantitative real time polymerase chain reaction

General Introduction

Acid soils and Al toxicity

Aluminium is generally known as a light metal that makes up 8.3 % by weight of the earth's crust (Downs, 1993). This quantity makes Al the third most abundant element after oxygen and silicon. Al is more or less ubiquitous and plant roots are therefore almost always exposed to Al in some form. Aluminium is too reactive chemically to occur in nature as a free metal. Consequently, it is found combined in a huge number of different minerals and most Al in the soil is present in feldspares, alumino-silicate compounds, and usually exists as insoluble and non-rhizotoxic forms. On the one hand, Al rhizotoxicity is reported under alkaline soil conditions (Jones, 1961, Rees and Sidrak, 1955) and in alkaline nutrient solutions containing Al at a pH above 8 (Ma *et al.*, 2003, Stass *et al.*, 2006) where the aluminate ion is the primarily prevailing species of Al (Martin, 1988). However, it is not yet clear whether the aluminate ion is the toxic Al species leading to rhizotoxicity in the alkaline pH range (Stass *et al.*, 2006). On the other hand, Al hydroxides are very insoluble around neutrality, but their solubility increases drastically as pH decreases (Marion *et al.*, 1976). Al becomes toxic at low soil pH and the trivalent octahedral hexahydrate of Al (Al^{3+}) is most abundant at a pH below 5 (Martin, 1988).

Acidic soils are a much more important agronomical problem than alkaline soil conditions. Most acid soils are saturated with aluminium rather than hydrogen ions. The acidity of the soil is therefore often a result of hydrolysis of aluminium compounds (Turner and Clark, 1966). Estimations of the global spread of acid soils, which are defined by a pH lower than 5.5 in their surface layers, comprise nowadays about 30 % of the total ice free land (von Uexkull and Mutert, 1995). The phenomenon of acidic soils is primarily found in two major global areas which are located in one northern belt, in regions with cold, humid temperate climate, and in one southern belt with warm, humid conditions. Soil acidification is mainly depending on the reservoir of alkaline cations and the leaching potential of these ions under certain soil conditions. Therefore, high rainfall, the removal of cations by harvested crops, acid precipitation from polluted air (Ulrich, 1980) and organic matter decay (Carver and Ownby, 1995), or certain cropping practices as repeated application of reduced nitrogen compounds particularly if overshooting the demand of the crop (Adams, 1984) significantly accelerate the process of soil acidification.

The physiology of Al toxicity in plants

Aluminium toxicity is the major constrain limiting crop production on acid soils. The toxic octahedral hexahydrate of Al (following mentions will refer to this Al species) directly and immediately interferes with the root tip and leads to a rapid inhibition of root growth (Delhaize and Ryan, 1995; Taylor 1988). The process of root-growth inhibition could be analysed within 1-2 h of Al contact to roots, thus it is supposed to be a primary effect of Al toxicity (Sivaguru *et al.*, 1999; Horst, 1995). However, the primary cause of Al toxicity is not consistently determined (Delhaize and Ryan, 1995; Kochian, 1995; Matsumoto, 2000). Nevertheless, there is accumulating evidence that the root-tip apoplast is the main compartment for the development of Al toxicity (Horst, 1995) where it reduces cell-wall plasticity and elasticity (Ma *et al.*, 2004) and thereby interacts directly with the apoplastic site of the cell wall-plasma membrane-cytoskeleton continuum (Horst *et al.*, 1999). For example Al binds to the pectic residues and proteins in the cell wall decreasing the extensibility, it could displace other ions from critical sites in the cell wall or the plasma membrane, it binds to the lipid bilayer or membrane-bound proteins which could interfere with transport processes of essential nutrients, or it possibly disrupts the intracellular metabolism from the apoplastic compartment by triggering secondary-messenger pathways (Haug, 1984; Taylor, 1988; Bennet and Breen, 1991; Rengel, 1992, Haug *et al.*, 1994)

Application of Al to defined apical root zones revealed an outstanding role of the distal transition zone (DTZ) for the development of Al toxicity in maize (Kollmeier *et al.*, 2000, Ryan *et al.*, 1993). The application of Al to both the meristematic zone and the elongation zone showed not the particularly same inhibitory effect as the application in the DTZ. It is indicated that Al induces alterations in the secretory pathway which interrupts the basipetal auxin flow being implicated in cell elongation. Based on these results it was proposed that the Al-induced callose formation represents a possible candidate for the inhibition of the auxin signalling pathway by plugging symplastic transport via plasmodesmata (Sivaguru *et al.*, 2000).

Some studies suggest symplastic events to be related to the development of Al toxicity (Lazof *et al.*, 1996; Silva *et al.*, 2000; Taylor *et al.*, 2000), where Al was proposed to inhibit vital functions of symplastic ligands as enzymes, calmodulin, tubulin, ATP, GTP and DNA or the Al-ligand complex induces toxic reactions and interferes with the metabolism. Furthermore, Al exposure leads to the induction of reactive oxygen species (ROS) as well as peroxidative

damage to membranes. Even though, the peroxidation of lipids is rather likely to be not a primary mechanism of Al toxicity (Horst *et al.*, 1992; Yamamoto *et al.*, 2001). However, the symplastic relevance of Al toxicity is still matter of debate. Ions, and especially polyvalent ions as Al^{3+} , are virtually insoluble in lipid bilayers which indicates that the plasma membrane represents a significant barrier for Al entry into the symplast (Delhaize and Ryan, 1995).

How do plants cope with Al toxicity? - Al exclusion

It is known for a long time that there is a wide variation in the Al resistance between plant species and genotypes within species (Magistad, 1925; Maclean and Gilbert, 1927). Particularly during the last two decades the physiological and molecular understanding of Al resistance has made far reaching progress. Generally the physiological mechanisms leading to detoxification of Al are divided by their site of action. There is one class of mechanisms that operate to exclude Al from the root apex, which are called external resistance mechanisms and another class that enables plants to tolerate Al in their symplast that are called internal tolerance mechanisms (Barcelo and Poschenrieder, 2002; Ma and Furukawa, 2003; Kochian, 2004). The majority of Al resistant plants use external resistance mechanisms by root exudation of organic acid anions which are known to chelate and thereby detoxify rhizotoxic Al. For example wheat (*Triticum aestivum*) was shown to exude, specifically induced by Al, malate (Delhaize *et al.*, 1993), maize (*Zea mays*) and common bean (*Phaseolus vulgaris*) citrate (Miyasaka *et al.*, 1991; Kollmeier *et al.*, 2001) and *Fagopyrum esculentum* oxalate (Zheng *et al.*, 1998). However, different organic acid anions lead to the same benefit for the particular plant species. Al is excluded from both the root cell wall and the root symplast.

The exudation process is induced or activated by Al in different plants in different patterns. Al activates a rapid exudation of malate in wheat (Pattern I), but a lag phase between onset of exudation and the exposure to Al spanning time frames of 4-10 h was observed in rye and common bean (Pattern II) (Li *et al.*, 2000; Rangel *et al.*, 2009). There is a proposed model how these differential responses are achieved. In pattern I-type responses the Al-induced exudation could occur in three different ways: i) Al interacts directly with a channel protein to trigger its opening; ii) Al interacts with a specific receptor protein on the membrane surface or with the membrane itself to initiate a secondary messenger cascade that then activates the channel, or iii) Al enters the cytoplasm and activates the channel directly or indirectly via secondary messengers. In contrast, in pattern II plant species Al is proposed to interact with

the cell, possibly via a receptor protein on the plasma membrane, to activate the transcription of genes that encode proteins involved in the transport of organic acid anions across the plasma membrane and possibly also with the metabolism of organic acids. This process will take some time (hours), which is responsible for the lag phase in pattern II plants (Ma *et al.*, 2001; Ryan and Delhaize., 2001).

The exudation of organic acid anions could explain genotypic differences in the Al sensitivity for example in wheat (Delhaize *et al.*, 1993) where resistant genotypes are characterized by an enhanced Al-activated exudation rate compared to the Al-sensitive genotypes. The excretion of organic acid anions, localized at the root tip particularly protecting the most sensitive root zones, facilitates to sustain normal root growth rates by preventing harmful effects of Al. For example an Al-resistant cultivar of wheat is able to maintain 80 % of the root-growth rate under Al toxicity, whereas a sensitive genotype is heavily inhibited and shows only growth rates of 12 % compared to the root growth rate without Al supply (Table 1). The resistant genotype is characterized by an enhanced malate exudation and this forms the basis of a first hypothesis to explain Al tolerance in wheat. Sasaki *et al.* (2004) cloned a wheat gene, an Al-activated malate transporter (ALMT1) which co-segregated with Al resistance in the progeny of two near-isogenic wheat lines differing in Al resistance. This approach was the first evidence that ALMT1 confers an Al-activated malate efflux and revealed that this gene encodes a protein constitutively expressed in root apices of the resistant line which is higher abundant than in the sensitive line. These results were further substantiated by Delhaize *et al.* (2004) who showed that this gene derived from wheat conferred Al resistance in transgenic barley plants. This gene transfer provided first evidence that the trait Al resistance can be transferred to important crop plants. Recently, a homolog of the wheat aluminium-activated malate transporter (AtALMT1) was shown to be critical for Al resistance in *Arabidopsis* and encodes as well an Al-activated root malate efflux transporter which is associated with resistance but is not a major Al-resistance quantitative trait loci in *Arabidopsis* (Hokenga *et al.*, 2006). Parallel work with *Sorghum bicolor* identified a gene encoding a member of the multi drug and toxic compound extrusion (MATE) family, by positional cloning. This MATE gene product is an Al-activated citrate transporter which represents the major *Sorghum* Al tolerance locus (Magalhaes *et al.*, 2007). Subsequently, Liu *et al.*, (2009) revealed that STOP1, a transcription factor, is also required for the expression of this MATE gene and consequently for Al-activated citrate exudation. However, not all listed genotypic differences are exclusively explained by differences in the exudation pattern of organic acid anions.

General introduction

Table 1. Overview over differences in Al resistance and/or tolerance between species and genotypes.

	Al-resistance classification	Genotype	Relative root growth inhibition	Al concentration [μM]	Nutrient solution	Reference
<i>Triticum aestivum</i>	resistant	Atlas	20 %	20	100 μM CaCl_2 ; pH 4.5	Pellet <i>et al.</i> , 1996
	sensitive	Scout	88 %			
<i>Zea mays</i>	resistant	Cateo	5 %	40	calculated activity	Piñeros <i>et al.</i> , 2005
	sensitive	11*723	75 %			
<i>Phaseolus vulgaris</i>	resistant	Quimbaya	18 %	20	5 mM CaCl_2 ; 0.5 mM KCl ; 8 μM H_3BO_3 ; pH 4.5	Rangel <i>et al.</i> , 2005
	sensitive	Vax-1	68 %			
<i>Oryza sativa</i>	resistant	Koshihikari	40 %	50	0.5 mM CaCl_2 ; pH 4.5	Ma <i>et al.</i> , 2002
	sensitive	Kasalath	70 %			
<i>Sorghum bicolor</i>	resistant	SC283	50-45 %	27	calculated activity	Magelhaes <i>et al.</i> , 2003
	sensitive	BR007	95-90 %			
<i>Arabidopsis thaliana</i>	resistant	Alr-104	35 %	20	Complete nutrient solution; 200 μM KH_2PO_4 ; pH 4.2	Larsen <i>et al.</i> , 1998
	sensitive	Columbia _(wt)	83 %			
<i>Secale cereale</i>	resistant	Bates	20 %	50	0.5 mM CaCl_2 ; pH 4.5	Yang <i>et al.</i> , 2005
	sensitive	Dongmu 70	60 %			
<i>Brachiaria spec.</i>	resistant	<i>B. decumbens</i>	55 %	60	calculated activity	Wenzl <i>et al.</i> , 2001
	sensitive	<i>B. ruzizensis</i>	95 %			
<i>Fagopyrum esculentum</i>	resistant	Jiangxi	45 %	50	0.5 mM CaCl_2 ; pH 4.5	Zheng <i>et al.</i> , 2005
	sensitive	Shanxi	78 %			

Furthermore, it has been shown that specific cell-wall properties are involved in differential Al resistance of genotypes. On the one hand, root tip Al contents are negatively correlated with root growth rates and consequently with Al resistance (Schmohl and Horst, 2001). Root tips with higher pectin contents accumulate more Al in their cell walls leading to a higher Al sensitivity. Moreover, the degree of methylation of pectic polysaccharides, affecting the negative charge of the cell wall, leads to changes in the Al binding capacity and is additionally shown to participate in genotypic differences in Al resistance in various plant species (Stass *et al.*, 2007; Eticha *et al.*, 2005b). On the other hand, certain cell-wall properties were mentioned to enable Al immobilization in the cell wall which prevent Al to enter the symplast and affect Al-sensitive sites in that compartment (Taylor *et al.*, 1991).

Some plants show an Al-induced pH barrier which leads to precipitation of Al in the rhizosphere (Larsen *et al.*, 1998; Table 1.). The Al-resistant *Arabidopsis* mutant alr-104 showed an increased net H^+ influx into the root cells that significantly increased the pH of the surrounding nutrient solution which represents a resistance mechanism based on an Al-induced increase in root-surface pH (Degenhardt *et al.*, 1998).

How do plants cope with Al toxicity? – Al accumulation and Al tolerance mechanisms

Generally, there is a wide range of plant species which accumulate Al in their above ground plant organs (Table 2) and thus exhibit an extraordinary degree of Al tolerance. Jansen *et al.*, (2002) suggested that Al contents of 1000 ppm Al or more in dried leaf tissue are a suitable criterion for defining Al hyperaccumulation in plants. However, the total accumulated amounts differ, but even small concentrations of Al within certain tissues demand for effective internal tolerance mechanisms.

Table 2: Al accumulation in leaf dry matter of Al accumulating plant species after several month of growth on acidic soils

Species	Leaf Al concentration [mg g ⁻¹ dry matter]	Reference
<i>Camellia sinensis</i>	30	Matsumoto <i>et al.</i> , 1976
<i>Hydrangea macrophylla</i>	3	Ma <i>et al.</i> , 1997
<i>Melastoma malabathricum</i>	10	Watanabe and Osaki, 1998
<i>Fagopyrum esculentum</i>	15	Ma <i>et al.</i> , 2001
<i>Richeria grandis</i>	1	Cuenca <i>et al.</i> , 1990

The mechanisms which enable specific plants to tolerate symplastic Al without interference with essential metabolic processes, need to be high efficient since Al is characterized by a high affinity to O-donor compounds. Despite the fact that a cytosolic pH of approximately 7.5 less than nanomolar concentrations of free Al are supposed to induce drastic consequences (Martin, 1988) due to an interaction of Al with sites regulated by Mg²⁺. These sites are involved in ATP-mediated phosphate transfer, cytoskeletal interactions and signal transduction. Al tolerance mechanisms primary involve complexation with organic acid anions within the cytosol, the compartmentation of Al within the vacuole or enzyme adaptation, either showing advanced tolerance or increased activity to produce for example more Al detoxifying ligands (Kochian, 1995).

Al accumulation in *Hydrangea macrophylla* is well documented because of the ornamental value of blue sepals. This colour formation from pink to blue is obtained by a translocation of Al into the sepals, a compartmentation within vacuoles of subepidermal cells (Naumann,

2001) and by a complex formation between delphinidine 3-glucoside, Al and 3-caffeoylquinic acid (Takeda *et al.*, 1985).

Buckwheat – the combination of Al exclusion and Al accumulation/Al tolerance mechanisms

A model organism for Al accumulation is buckwheat (*Fagopyrum esculentum* Moench) which is known for being Al resistant and furthermore Al-tolerant on a high level. Buckwheat responds to Al supply by immediate exudation of oxalate (Pattern I, Yang *et al.* 2006). In Pattern I plant species the Al resistance mediated by the release of organic acid anions is constitutively expressed and does not require an Al-induced protein biosynthesis process. The analysis of the Al-activated exudation process provided hints for the involvement of anion channels in efflux of oxalate. In *Polygonum aviculare* L. (You *et al.*, 2005) and buckwheat (Zheng *et al.*, 1998) the application of phenylglyoxal (PG), an anion channel inhibitor, which did not directly interfere with root growth, effectively inhibited the exudation of oxalate in the Al treatment. On the other hand, the application of cycloheximid (CHM), a protein synthesis inhibitor, led to a cessation of exudation in *Cassia tora* L., a Pattern II plant, but not in buckwheat, indicating a constitutively expressed metabolic “machinery” in buckwheat (Yang *et al.* 2006).

Nonetheless, Al exclusion and Al accumulation mechanisms and their possible interrelation are not fully understood. Only a mechanistic model for the involved mechanisms exists. Ma and co-workers developed a framework for Al uptake and translocation in buckwheat. Briefly, Al is suggested to be taken up as Al^{3+} . Once it crosses the plasma membrane, the Al^{3+} is chelated with oxalate to form a 1:3 Al:oxalate complex. When Al is translocated from the roots to the shoots, a ligand-exchange reaction occurs in the xylem to form Al citrate (Ma and Hiradate, 2000; Ma *et al.*, 1998; Zheng *et al.*, 1998). This complex is transported into above-ground plant parts where again a ligand exchange is proposed to take place, and an Al oxalate complex will be reformed. If the Al concentration exceeds a certain limit, especially in the leaf margins, an Al-citrate complex will be additionally formed (Shen *et al.*, 2004). Al is transported exclusively into transpiring organs and does not accumulate in the seeds (Shen *et al.*, 2006). Buckwheat shows characteristics that qualify it as a model organism for further unravelling of the process of Al accumulation. Buckwheat has a short vegetative period, it is

an herbaceous plant, and the availability of ecotypes adapted to strongly acid Al-toxic soils may represent a powerful tool for the identification of novel genes responsible for a high level of Al resistance. Al resistance related genes had not yet been identified in buckwheat but the application of genotypes which have not been selected for suitable agronomic characteristics in the past (You *et al.*, 2005) will represent a promising gene pool for tracking of genes conferring Al resistance and Al accumulation. Buckwheat also shows other important features. It is one of the few non-*Poaceae* cereals and as such it is often referred to as a “pseudocereal” which has been cultivated for a long time in several countries of Asia, Europe and North America for human and livestock consumption. Its production has, however, strongly decreased over the last decades and has almost disappeared in many western European countries. Only two cultivars were protected under plant breeders right in Germany, despite several attractive crop properties such as (I) short vegetative period, (II) resistance against most cereal diseases (III) high contents of lysine, an essential amino acid for the human diet, (IV) high rutin contents, a secondary metabolite which shows medicinal applications and (V) absence of gluten which is important for Coeliac disease patients. Buckwheat performs well on poor soils, and can be grown where wheat or even rye cannot be grown with profit (Sure, 1955). It shows high phosphorus efficiency (Zhu *et al.*, 2002; Amann and Amberger 1989). In addition buckwheat and other *Polygonum* species grow well on acid soils (You *et al.*, 2005). Therefore, this study will concentrate on buckwheat to characterize processes and interrelations that are not yet understood such as Al exclusion and Al accumulation.

Four physiological approaches were experimentally explored: 1. Spatial characteristics of aluminium uptake and translocation in roots, 2. Characterization of aluminium uptake, 3. In-situ aluminium localization in root tips, 4. Genotypic differences in aluminium accumulation of *Fagopyrum* accessions.

Spatial characteristics of aluminum uptake and translocation in roots of buckwheat (*Fagopyrum esculentum*)

Benjamin Klug, Walter J. Horst

Published in: *Physiologia Plantarum* (2010) 139, 181-191.

Abstract

The detoxification of aluminum (Al) in root tips of the Al accumulator buckwheat by exudation of oxalate leading to reduced Al uptake (Al resistance) is difficult to reconcile with the Al accumulation (Al tolerance). The objective of this study was to analyze resistance and tolerance mechanisms at the same time evaluating particularly possible stratification of Al uptake, Al transport and oxalate exudation along the root apex. The use of a minirhizotron made it possible to differentiate between spatial responses to Al along the root apex with regard to Al uptake and organic acid anion exudation, but also to measure at the same time Al and organic acid transport in the xylem. Al accumulates particularly in the 3-mm root apex. The study showed that Al taken up by the 10-mm root apex is rapidly transferred to the xylem which differentiates in the 10 to 15-mm root zone as revealed by a microscopic study. Al induces the release of oxalate from the root apex but particularly from the subapical 6–20 mm root zone even when Al was applied only to the 5-mm root apex suggesting a basipetal signal transduction. Citrate proved to be the most likely ligand for Al in the xylem because Al and citrate transport rates were positively correlated. In conclusion, the data presented show that the Al-induced release of oxalate, and Al uptake as well as Al accumulation are spatially not separated in the root apex.

Introduction

Aluminum (Al) is naturally occurring as aluminosilicate (Brady and Weil 2008). The solubility of this clay mineral-bound Al increases exponentially with decreasing pH below 4.5 with the resultant increase in abundance of the phytotoxic Al_3^+ species (Dalal 1975). Soil acidity is a widespread problem constraining plant growth on more than 50% of the non-irrigated arable land of the world (Miller *et al.* 1992) with Al toxicity as the major factor limiting crop production (Kochian, 1995). The human population is increasing hyperexponentially on a macrohistorical scale (Varfolomeyev and Gurevich 2001) particularly in the developing countries of the subtropics and tropics where acid soils are wide spread and food production is suboptimal. However, crop species, and genotypes within species, differ in their productivity on acid, Al-toxic soils. Therefore, it is important to unravel Al resistance and tolerance mechanisms naturally occurring in plants adapted to these conditions. Ecotypes evolved on strongly acidic soils represent a valuable source of Al resistance and tolerance genes that may be used to improve Al-sensitive crop plants (You *et al.* 2005).

Buckwheat (*Fagopyrum esculentum* Moench), combines Al exclusion and Al tolerance (Ma *et al.* 1998, Zheng *et al.* 1998) accompanied with high phosphorus (P) efficiency (Amann and Amberger 1989, Zhu *et al.* 2002). However, the interrelationships and relative importance of these traits are not yet fully understood. It has been suggested by Ma and Hiradate (2000) that Al^{3+} is taken up by buckwheat, but that once it crosses the plasma membrane it is chelated with oxalate to form a 1:3 Al-oxalate complex (Ma *et al.* 1998). Further, when Al is translocated from the roots to the shoots, a ligand-exchange reaction occurs in the xylem to form Al citrate (Ma and Hiradate 2000). However, controversial results exist about the process of xylem loading. The concentration of Al in the xylem sap by far exceeds that in the external medium (Ma and Hiradate 2000) suggesting an actively driven process. Controversially, hydroxylamine, an inhibitor of respiration, did not affect the Al concentration in the xylem sap (Ma and Hiradate 2000) suggesting a passive process. Thus the mechanisms contributing to Al tolerance and Al accumulation of buckwheat are not well understood so far. In addition, they do not explain the comparatively low Al sensitivity of buckwheat root growth when exposed to Al_3^+ because this requires the protection of the root-tip apoplast from Al binding (Horst *et al.* 2007, Ryan *et al.* 2001). In this regard the exudation of organic acid anions complexing and thus detoxifying Al is of major importance (Li *et al.* 2009a, Ma *et*

al. 2001). It has been demonstrated that Al supply triggers oxalate exudation particularly in the 10-mm root tip without a lag phase. For that reason buckwheat has been classified among the Pattern I responders which release organic acid anions in response to Al by opening a plasma membrane anion-permease without a lag phase (Zheng *et al.* 1998). This mechanism is constitutively expressed and, thus, does not need protein synthesis or gene activation. The exudation of oxalate proved to be inappropriate to explain differences in Al resistance of buckwheat genotypes (Zheng *et al.* 2005). However, Peng *et al.* (2003) concluded that both the constitutive oxalate exudation and the internal oxalate content contribute to Al detoxification and to genotypic Al resistance (Peng *et al.* 2003). Another hypothesis suggests an alternative resistance mechanism, relating Al resistance to the precipitation of Al by P and the accumulation of Al–P in the root tissue (Zheng *et al.* 2005). The detoxification of Al in the root tips of buckwheat by exudation of oxalate leading to reduced Al uptake (Al resistance) is difficult to reconcile with the Al accumulation (Al tolerance). It has been suggested that Al exclusion and Al accumulation are spatially separated along the root apex (Ma and Hiradate 2000).

The objective of this study was to analyze resistance and tolerance mechanisms at the same time taking particularly a possible stratification of Al uptake, Al transport and oxalate exudation along the root apex into consideration.

Material and Methods

Plant material

Buckwheat (*F. esculentum* Moench) cultivar ‘Lifago’ (Deutsche Saatveredelung AG, Lippstadt, Germany) was germinated in a peat substrate with 30% clay (Einheitserde, Balster Einheitserdenwerk GmbH, Fröndenberg, Germany). Plants were grown for 4 weeks in a green house at 25/20°C day/night temperature. After this growth period the shoots were cut 10 mm below the first node exhibiting first adventitious root initials and above the primary leaf to reduce evaporation. The cuttings were transferred to low ionic strength nutrient solution for 4 days, keeping the shoots at 100% relative humidity until adventitious roots had emerged. Subsequently, the plants were adapted to lower relative humidity by reducing air humidification. Finally, the pH of the nutrient solution was reduced to 4.3 in three steps, enabling an adaptation to low pH over at least 12 h before beginning the Al treatment. Adventitious roots have been used for this study because these roots are thicker than seminal roots and, thus, better suited for the rhizotron experiments.

Al and oxalate distribution along the root apex

Rooted cuttings were grown for 24 h in complete nutrient solution at pH 4.3 with the following composition [μM]: 500 KNO_3 , 162 MgSO_4 , 30 KH_2PO_4 , 250 $\text{Ca}(\text{NO}_3)_2$, 8 H_3BO_3 , 0.2 CuSO_4 , 0.2 ZnSO_4 , 5 MnSO_4 , 0.2 $(\text{NH}_4)_6\text{Mo}_7\text{O}_{24}$, 50 NaCl and 30 Fe-EDDHA . Addition of 75 μM Al resulted in a mononuclear Al concentration of 40 μM . Segments of adventitious roots were excised using a knife with 10 razor blades fixed in a distance of 1 mm.

Minirhizotron experiments

Compartmented rhizotrons were built and modified based on the model of Pitman (1971) (Fig. 1). These minirhizotrons were made of 2-mm thick acrylic glass plates. All elements were fixed with liquid glue for plastics (Revell GmbH & Co. KG, Bünde, Germany). Then 45-mm root tips of adventitious roots of low pH-adapted buckwheat cuttings were excised and washed in control nutrient solution to remove symplastic contamination from the cut surface. After this washing step eight roots were placed in a rhizotron containing minimal nutrient solution composed of 500 μM CaCl_2 , 5 μM H_3BO_3 , 100 μM K_2SO_4 and $\pm 200 \mu\text{M}$ AlCl_3 at pH 4.3. Minimal nutrient solution was chosen to avoid interactions with Al, namely precipitation or complexation (e.g. with phosphate). The Al concentration was set to 200 μM in order to prevent depletion in the small volume of 2 ml, amounting to only 400 nmol Al per rhizotron. Single compartments were sealed with silicon grease to avoid Al contamination between the chambers. A leak between the compartments can be excluded based on the analysis of Al and organic acids in the protection compartment. Al was either applied in the first compartment to the apical 5 mm (or 10 mm) of the root or in the second compartment to the subapical 6–10 mm (or 11–20 mm) zone. Al and organic acid anion concentrations were determined in the solution of each compartment. To analyze the Al contents of different root-tip zones, 3-mm segments (0–3 and 6–9 mm) or 8-mm segments (1–9 and 11–19 mm) were cut out of each zone to avoid contamination by silicon grease. Exudates were analyzed by combining the volumes of three compartments to one composite sample. Every treatment was performed in nine rhizotrons resulting in three composite samples.

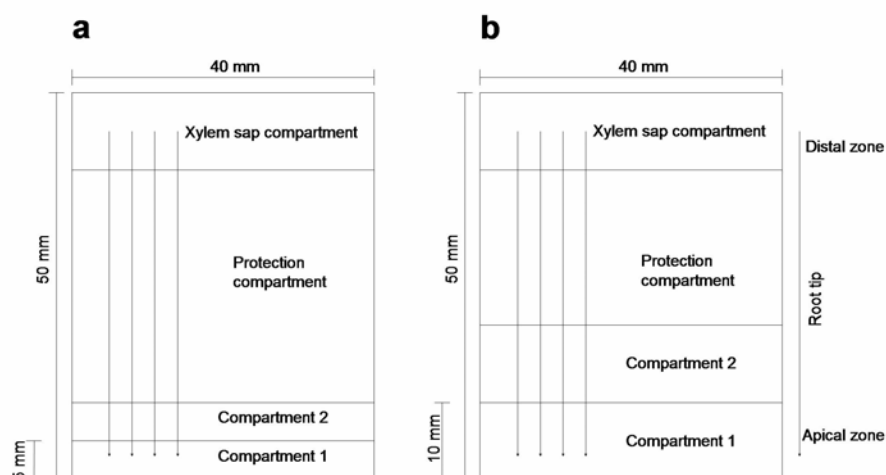


Figure 1. Schematic structure of a minirhizotron. Eight adventitious root tips of buckwheat with a length of 45 mm were placed in each rhizotron with (A) 5-mm compartments or with (B) 100-mm apical compartmentation. Incubation occurred for 6 h in minimal nutrient solution $\pm 200 \mu\text{M}$ Al at pH 4.3. Three rhizotrons were combined to one sample. Three replicates, therefore, comprise nine rhizotrones per treatment.

Determination of oxalate exudation from excised root segments

Low pH-adapted root tips from adventitious roots of buckwheat cuttings were excised 30 mm behind the root tip. These root tips were again subdivided into six 5-mm segments. Ten segments from each zone were placed within one well of a 96-well plate. Root tips were washed three times by changing the control-nutrient solution without Al to remove cytoplasmic contaminations. Each well contained 300 μl nutrient solution (500 μM CaCl_2 , 5 μM H_3BO_3 , 100 μM K_2SO_4 and $\pm 200 \mu\text{M}$ AlCl_3 at pH 4.3). The root-tip segments containing microplate was placed on a platform shaker (Heidolph, Polymax 1040, Schwabach, Germany) at 20 rpm for 6 h. The nutrient solution was aerated by pipetting the solution up and down every 10 min. Organic acids were analyzed using high pressure liquid chromatography (HPLC; see below).

Al determination

Al was determined by GF-AAS (Unicam 939 QZ, Analytical Technologies Inc., Cambridge, UK) at a wavelength of 308.2 nm, an ashing phase of 20 s at 1500°C and an atomisation phase of 3 s at 2300°C . Each sample was measured twice. Root tips were digested over night in 500 μl double-distilled ultrapure nitric acid under continuous shaking at room temperature. After digestion the samples were appropriately diluted with double deionised water.

Organic acid determination

The organic acid concentrations in the root exudates as well as in the extracts of root tissue were measured by isocratic HPLC (Kroma System 3000, Kontron Instruments, Munich, Germany). The organic acids were injected through a 20 μ l loop-injector (Auto-sampler 360), separating different organic acids on an Animex HPX-87H (300 x 7.8 mm) column (BioRad, Laboratories, Richmond, California, USA), supplemented with a cation H^+ micro-guard cartridge, using 10 mM perchloric acid as eluant at a flow rate of 0.5 ml per minute, constant temperature of 35 °C (Oven 480) and 74 hPa of atmospheric pressure. Measurements were performed at a wavelength of $\lambda = 214$ nm (UV Detector 320).

Prior to the analysis of exuded organic acids the nutrient solution samples were exchanged using a cation exchange column (hydrochloric form) (AG® 50W-X8; Biorad; Life science group; Hercules; CA), followed by concentration to dryness via vacuum centrifugal evaporation (RCT 10-22T; Jouan; Saint-Herblain, France). Extracts of root tips were analyzed according to Wenzl *et al.* (2002) with modifications. Samples were homogenized in 500 μ L 70 % (v/v) EtOH using a swing mill (MM 200, Retsch GmbH & Co. KG; Haan, Germany) and incubated for 1 h at 45 °C. Samples were centrifuged at 15.000 rpm for 10 min in order to get a pellet. Subsequently, EtOH was evaporated to dryness by a vacuum centrifugal evaporator. The dry pellet was resuspended in 200 μ L 10 mM perchloric acid, homogenized in an ultra sonic bath (Bandelin Sonorex super RK105; Bandelin electronic, Berlin; Germany) and finally filtrated using a filter unit with a pore size of 0.45 μ m (GHP Nanosep®; MF Centrifugal device; Pall Life Sciences; Ann Arbor; MI). The filtrate was analyzed by HPLC.

Staining of suberin and lignin in root tips

Staining of suberin and lignin depositions in cell-wall material in root tips of adventitious roots of buckwheat cuttings was performed following the procedure described by Brundett *et al.* (1988). Root tips were embedded in 5 % (w/v) agarose with a low gelling temperature of 31-39 °C. Sections were obtained by free hand sectioning using a razor blade. Sections were directly mounted on a slide and stained at first with 0.1 % (w/v) berberine in deionised water (dH₂O) for one hour in darkness at room temperature. The solution was gently blotted off using tissue paper. Sections were rinsed three times with dH₂O and again blotted dry. For counterstaining, a drop of 0.5 % (w/v) aniline blue was placed on each section for 0.5 h.

Afterwards, the sections were rinsed and blotted of as mentioned before. Sections were covered by a 0.1 % (w/v) FeCl₃ solution (in 50 % glycerine). Sections were observed under ultraviolet (UV) illumination with an Axioscope microscope (Zeiss, Jena, Germany).

Statistical analysis

The ANOVA procedure of the statistical program SAS 9.2 (SAS Institute, Cary, NC) was used for analysis of variance. Means were compared using the Tukey test.

Results

After 24 h Al supply the profile of the Al contents along the root tip in mm segments revealed a steep decreasing gradient from the root apex to the more basal segments (Fig. 2). The first three mm contributed about 60 % to the Al content of the 10 mm root apex.

The contents of organic acids measured in the bulk root tissue were oxalic > succinic >> malic > citric acids (data not shown). After 24 h Al supply the oxalic acid contents did not differ between the Al treatments. In contrast to the Al contents (see Fig. 2), the oxalic acid contents increased from the root apex to the more basal root segments independent of the Al treatment (highly significant segment effect only).

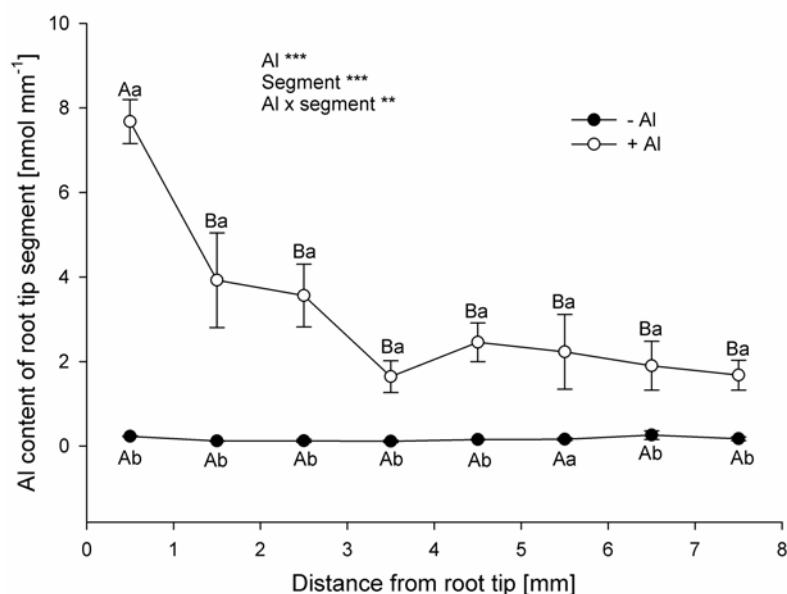


Figure 2. Al contents of adventitious root tips of buckwheat after 24 h Al treatment in P (30 μM) and NO₃⁻ (250 μM) reduced complete nutrient solution with and without 75 μM AlCl₃ at pH 4.3 in mm-segment resolution. Cuttings were rooted for 4 days followed by 1 day pH adjustment. Data represent means \pm SE, n = 4. For the ANOVA, **, *** denote probability levels at $P < 0.01$ and 0.001, respectively. Means with the same letter are not significantly different (Tukey test, $P < 0.05$). Capital letters denote the comparison of root-tip segments within Al treatments; small letters denote the comparison between Al treatments.

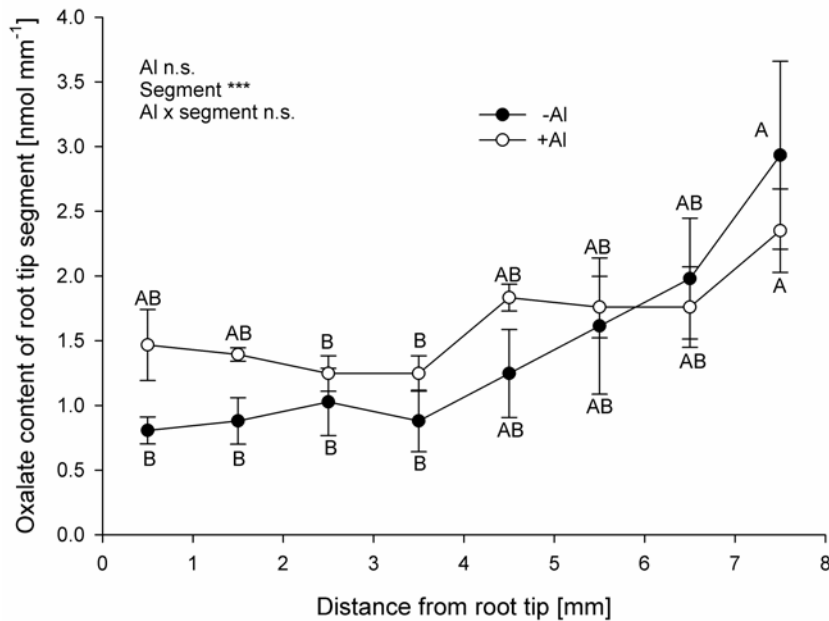


Figure 3. Oxalate contents of adventitious root tips of buckwheat after 24 h treatment in P (30 μM) and NO_3^- (250 μM) reduced complete nutrient solution with and without 75 μM AlCl_3 at pH 4.3 in mm-segment resolution. Cuttings were rooted for 4 days followed by 1 day pH adjustment. Data represent means \pm SE, $n = 4$. For the ANOVA, **, *** denote probability levels at $P < 0.01$ and 0.001, respectively. Means with the same letter are not significantly different (Tukey test, $P < 0.05$). Capital letters denote the comparison of root tip segments within Al treatments.

The use of mini-rhizotrons (Fig. 1) facilitated a more detailed study of the spatial characteristics of Al uptake and translocation along the root tip. This appeared to be necessary and promising on the basis of the results described above, showing gradients in Al and oxalate contents along the root. In a first approach the focus was on a differentiation between the 0-5 and the 6-10 mm root zone (Fig. 4a). Application of Al in compartment 1 led to high Al accumulation, particularly in the 5 mm root apex in contact with Al (Fig. 4a). The Al contents of the more basal root zones were slightly enhanced (not significantly or significantly for zones 2 and 3 not in contact with Al, respectively). Aluminium transport via the xylem indicated rapid transfer of Al from the external solution to the xylem in the root apex. Aluminium application to the sub-apical 5-10 mm root zone in compartment 2 led to Al accumulation particularly in zone 2. But this accumulation was less than in zone 1 when Al was applied to the same zone. The Al contents of the adjacent apical and basal root zones were only slightly enhanced (not significantly or significantly for zones 1 and 3, respectively). Application of Al to zone 2 increased xylem Al transport to the same extent as application to the apical 5 mm zone.

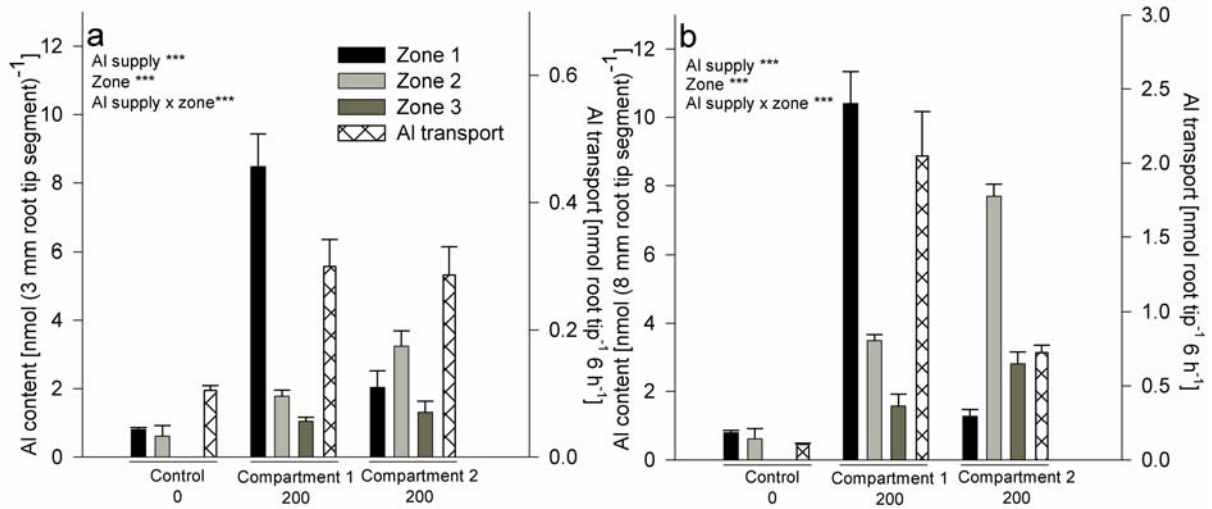


Figure 4. Aluminium contents in different root sections and xylem aluminium transport rates of excised 45 mm apical zones of adventitious buckwheat roots after 6 h Al treatment (0 or 200 μM) in 5 (a) or 10 (b) mm compartmented mini-rhizotrons allowing application of Al to the specific root zones. After the Al treatment for (a) the root zones 0-3 mm (compartment 1), 6-9 mm (compartment 2), and 12-15 mm (compartment 3) and for (b) the root zones 0-10, 10-20 and 20-30 mm were analysed, respectively. Aluminium transport-rates in the xylem flow were calculated from the Al accumulation in the xylem-sap compartment (Fig. 1) when Al (200 μM) was applied to the specific root zone. For the ANOVA, *** denotes significant effects at $P < 0.001$. Bars represent means \pm SE, $n = 9$.

When Al was applied to 10 mm root sections (Fig. 4b), again the Al content was particularly increased in the root zone in contact with Al, more when applied to the apical than to the subapical root zone. There was little, but significant transfer of Al to the adjacent basal root sections. Xylem Al transport was largely enhanced by Al application to the 10 mm root apex but lower when Al was applied to the 10-20 mm root zone. Oxalate exudation was sampled from both compartments irrespective of the Al treatment zone (Fig. 5). The oxalate exudation was generally higher from the 5-10 compared to the 0-5 mm zone (Fig. 5a). Aluminium supply enhanced the oxalate exudation from the root zone which was in direct contact with Al. However, Al application to zone 1 also enhanced oxalate exudation from zone 2. When Al was applied to the 0-10 mm root zone (Fig. 5b) also the oxalate exudation from the non Al-treated 10-20 mm zone was induced to a similar extent compared to the Al-treated root zone. However, application of Al to the sub-apical root section triggered exclusively the oxalate exudation from the Al-treated 10-20 mm root zone.

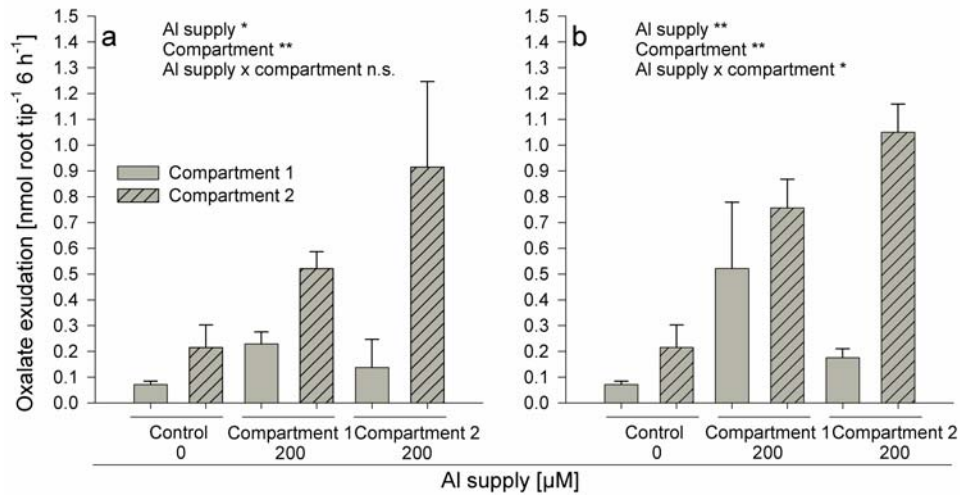


Figure 5. Oxalate exudation from two apical root zones of excised 45 mm apical zones of adventitious buckwheat roots after 6 h Al treatment (0 or 200 µM) in 5 (a) or 10 (b) mm compartmented mini-rhizotrons allowing application of Al to the (a) 0-5 or 5-10 mm and (b) 0-10 or 10-20 mm root zones. Oxalate was collected in both compartments. For the ANOVA, * and ** denote significant effects at $P < 0.05$ and 0.01, respectively, ns nonsignificant. Bars represent means \pm SE, $n = 9$.

Studying the oxalate exudation using 5 mm excised apical root zones (Fig. 6) confirmed the oxalate exudation pattern along the root apex shown above with intact plants. Aluminium treatment enhanced oxalate exudation from the 20 mm root apex, particularly from the 11-15 and 16-20 mm root zones. Beyond the 20 mm root tip (21-30 mm) the Al-induced oxalate exudation quickly reached the constitutive exudation of Al non-treated roots.

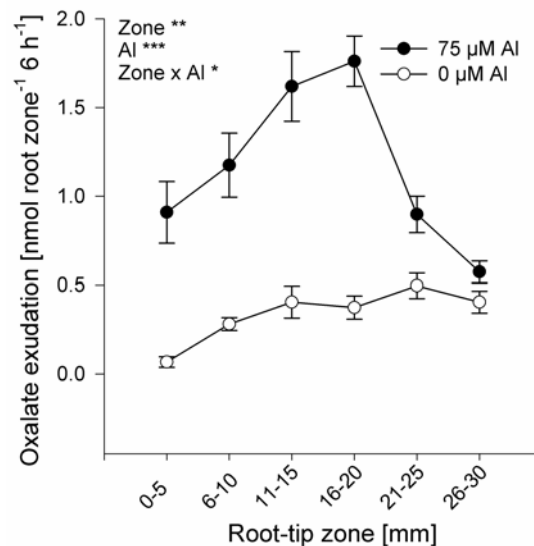


Figure 6. Oxalate exudation profile of adventitious buckwheat roots. For the collection of the root exudates excised 5 mm apical root zones were treated without and with 200 µM Al in simplified nutrient solution in 300 µL micro-plate wells. For the ANOVA, *, ** and *** denote significant effects at $P < 0.05$, 0.01 and 0.001 respectively, ns non significant. Data represent means \pm SE, $n = 4$.

In the xylem compartment not only Al but also organic acids could be determined, and the xylem transport-rate could be calculated. Oxalic acid could not be found in the xylem sap. The concentrations of other organic acids were succinic > citric > malic acid. Only citric acid responded to the Al supply. Therefore, only the correlation of the Al and citrate transport-rates is shown. Generally, citrate and Al transport-rates in the xylem were significantly correlated (Fig. 7). The citrate transport-rate of the controls without Al supply and the positive value for the intercept of the regression with the y-axis clearly showed that citrate was constitutively transported independent of the Al supply. However, Al transport to and in the xylem induced an increased citrate transport. The Al and citrate transport-rates reflect the efficiency of Al xylem loading according to the root section exposed to Al: 0-5 mm < 6-10 mm < 0-10 mm < 11-20 mm. With increasing Al transport the Al: citrate ratio decreased approaching a ratio of 1:1. Since it has been shown that Al accumulation and transport, and oxalate exudation differ between root-tip sections the question arises whether this could be related to morphological particularities of the buckwheat root.

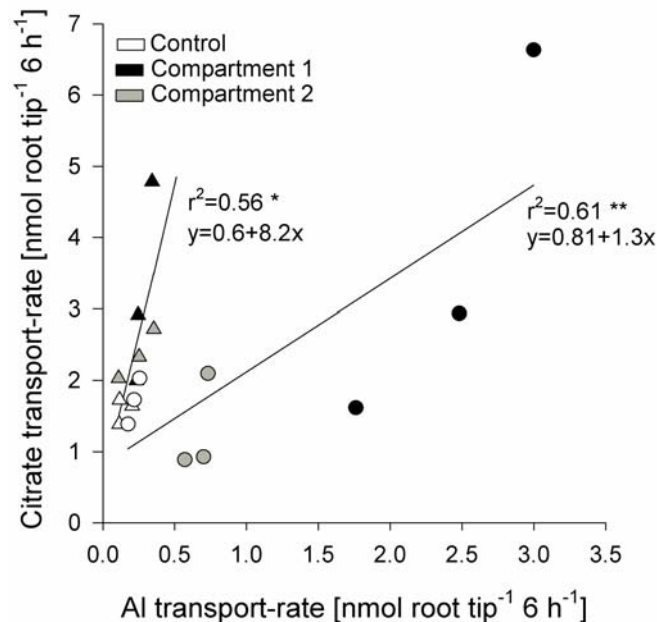


Figure 7. Correlation of Al and citrate transport-rates in the xylem sap without Al application (white symbols) or after Al application to the apical zone in compartment 1 (black symbols) or to the subapical zone in compartment 2 (grey symbols). Aluminium was applied either to the root zones 0-5 and 6-10 mm (triangles) or the root zones 0-10 and 10-20 mm (circles). Citrate and Al were collected in the xylem-sap compartment. Incubation of 45 mm apical root sections for 6 h in minimal nutrient solution +/- 200 μ M Al at pH 4.3. For the ANOVA, * and ** denote significant effects at $P < 0.05$ and 0.01, respectively.

Therefore, a systematic microscopic analysis of the development of hydrophobic barriers and the differentiation status of the vascular system from the root tip in distinct 5 mm zones of the 0-30 mm root tip was undertaken (Fig. 8) applying a berberine aniline-blue fluorescent staining procedure. The first 0-5 mm zone could be characterized by undifferentiated

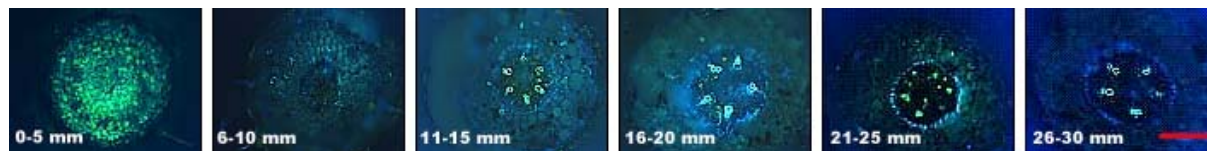


Figure 8. Berberine aniline -blue counterstaining of buckwheat free-hand cross sections embedded in 5 % agarose gel. Exposure time and magnification were 79 ms and 200 fold, respectively. Sections were obtained after embedding of 5 mm root tip zones in a distance of 0–5, 6–10, 1 – 15, 16– 20, 21-25 and 26 –30 mm from the root tip. Sections were examined under UV-light. Green, light blue and yellow fluorescence indicate meristematic cells, suberin and lignin depositions, respectively. The white bar represents a scale of 100 μ m.

meristematic cells showing strong autofluorescence. The second 5-10 mm zone showed first signs of differentiation between cortex and central cylinder, however, without any hydrophobic barrier. In the 11-15 mm zone, the first fully differentiated lignified xylem vessels were visible and the endodermis showed beginning suberin staining of the Casparian strip. All more basal root zones >15 mm from the root apex showed clear formation of fully differentiated lignified xylem vessels and a suberinized endodermal layer.

Discussion

The distribution of Al along the root axis clearly showed a steep decreasing gradient from the root apex to the 4th mm (Fig. 2). The high Al accumulation capacity of the root apex was confirmed by experiments in which the Al accumulation of the apical 5 mm (Fig. 4a) or 10 mm (Fig. 4b) was compared with the corresponding adjacent basal root segments. This higher Al accumulation by the root apex was not specific for buckwheat because similar gradients of Al contents along the root apex have been demonstrated for other plants species such as maize (*Zea mays*, Eticha *et al.* 2005 a), faba bean (*Vicia faba*, Horst *et al.* 2007) loblolly pine (*Pinus taeda*, Moyer-Henry *et al.* 2005) and wheat (*Triticum aestivum*, Tice *et al.* 1992). Thus it appears that this pattern is not different between Al accumulators and Al excluders.

The main reason for the Al accumulation particularly in the root apex is most likely a corresponding gradient of the pectin content as it has been shown for maize (Eticha *et al.* 2005 b) and bean (Rangel *et al.* 2009, Stass *et al.* 2007) . The main binding sites for Al in the cell wall are the negative charges of the pectic matrix (Horst *et al.* 1999, Blamey *et al.* 2001).

Differences in the negativity of the root-tip cell-walls contribute to genotypic differences in Al resistance in rice (Yang *et al.* 2008), maize (Eticha *et al.*, 2005b, Li *et al.* 2009a), but also in buckwheat (Zheng SJ, personal information, 2009). The Al content in the root tissue is a function of Al uptake into and Al translocation out of the tissue. One of the main advantages of the applied mini-rhizotron (Fig. 1) was that it allowed differentiating between spatial responses to Al along the root apex with regard to Al uptake and organic acid anion exudation. Additionally, it rendered possible to measure at the same time Al and organic acid transport in the xylem. The Al uptake and binding to the pectic matrix in the cell wall is strongly modified by the release from the symplast of organic acid anions which form complexes with Al. The capacity to release organic acid anions in response to Al supply is the main mechanism explaining genotypic differences in Al resistance within Al excluders (Delhaize *et al.* 2007). But the same principle also applies to the Al accumulator buckwheat which releases oxalate in response to Al (Ma *et al.* 1997, Figs. 5, 6). The Al-induced release of oxalate was greater from the sub-apical than from the apical root zone (Figs. 5, 6) which is in agreement with a lower Al accumulation in the sub-apical root sections (see above). The enhanced exudation of the sub-apical root tip zone might be due to the higher oxalate contents compared to the root apex (Fig. 3). However, the relationship between the root contents and exudation of organic acids is generally loose (Hayes and Ma 2003; Yang *et al.* 2005). Thus, a differential control of the presence and function of anion permeases in the plasma membrane of apical and subapical root zones appears to be more likely. In this context it is particularly intriguing that application of Al to the root apex induced mainly the release of oxalate from the adjacent sub-apical root zone (Fig. 5) which is schematically presented in Fig. 9. Despite the large body of evidence linking root architecture with root absorption of nutrients, the effect of root architecture on root exudation has been virtually unexplored (Walker *et al.* 2003).

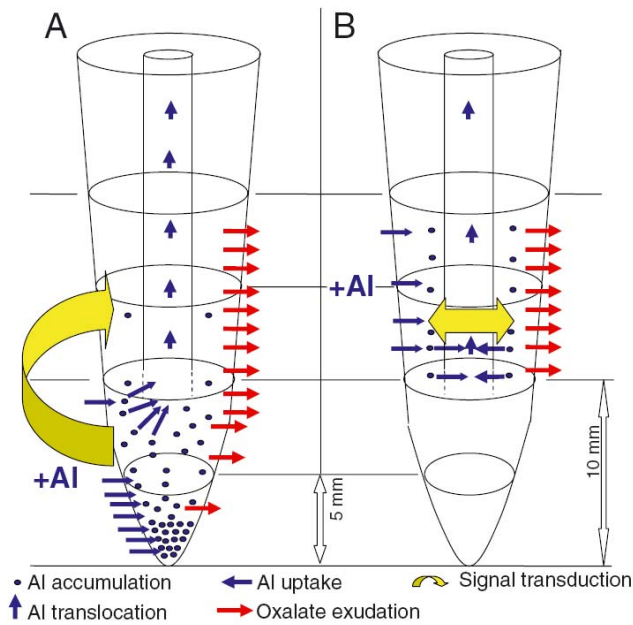


Figure 9. Schematic overview of Al uptake, accumulation, and transport in relation to Al-induced oxalate exudation in adventitious root tips of buckwheat. Aluminium application to the apical 10 mm (a) leads to high Al uptake, accumulation at the root apex, basipetal translocation of Al symplastically in the root cortex and particularly in the xylem. Oxalate release is triggered by Al more in the 11-20 mm zone than in the 0-10 mm treatment zone requiring signal transduction (yellow arrow). Aluminium applied to the 11-20 mm root section (b) is taken up and transported only basipetally at a lower rate while oxalate exudation from the Al-treated zone is triggered at the same zone (yellow arrow).

In most Al excluders the exudation of organic acid anions is confined to the root apex (Ryan *et al.* 1995, Mariano and Kjeltens 2003, Liao *et al.* 2006) thus protecting the most Al-sensitive sites of the root (Sivaguru and Horst 1998, Horst *et al.* 1999, Sivaguru *et al.* 1999). Also in buckwheat the main oxalate-releasing root zone was reported to be the first 10 mm (Zheng *et al.* 1998) or more exactly the first 5 mm (Zheng *et al.* 2005) of the root tip. In the present work it could be shown that particularly the sub-apical root zone 6-20 mm behind the root apex was the main oxalate-exuding root zone (Figs. 5, 6). This difference is caused by the analysis of adventitious roots in contrast to seminal roots analysed by Zheng *et al.* which could be confirmed by own comparative studies with seminal roots (unpublished data).

The induction of the release of oxalate from sub-apical root zones not in contact with Al through Al application to the root apex requires a basipetal signal transduction (Fig. 9). There is no apical signal transduction because Al applied to sub-apical root zones did not induce oxalate exudation from the apex (Figs. 5, 9). The most likely signal is Al itself which is rapidly taken up into the symplast (own unpublished work) where it is bound to oxalate (Ma *et al.* 1997) at the site of Al application, and transported symplastically to sub-apical root

zones (Fig. 4, for a more extensive discussion on Al transport see below). How Al triggers organic acid anion permeases is not understood so far (Ryan 2001). The present results suggest that not only apoplastic Al but rather symplastic Al is involved in the activation of an oxalate permease in buckwheat.

The specific experimental approach also allowed the calculation of Al transport out of the root zone to which Al was applied. Principally, three transport pathways have to be considered: apoplastic transport in the cortical cell walls, symplastic transport, and xylem transport which requires the transport into the central cylinder and the presence of differentiated xylem vessels. Based on the diffusion coefficients for apoplastic flow of ions provided by Pitman (1977) of less than 1 mm in 6 hours and the Al contents shown in Fig. 4, apoplastic transfer of Al from the Al-treated root zone to the adjacent root zones (5 or 10 mm apart) or even into the xylem sap collection compartment (45 mm away) was expected to be negligible. Also, diffusion in the apoplast is undirected and thus cannot explain that Al applied to the 11-20 mm zone only moved basipetally. Since Al is rapidly taken up into the symplast (own unpublished work) symplastic transport is more likely and could explain transfer of Al from the site of uptake to the next root zone 5, 10 or even 20 mm away (Fig. 4). Symplastic transport may also explain basipetally targeted transport of Al driven by unloading of Al into the xylem. Aluminium taken up by the 10 mm root apex was particularly rapidly loaded into the xylem (Fig. 4). Increasing xylem-Al transport could be shown as early as 1h after Al application (data not shown; Ma and Hiradate, 2000). When Al was applied to the 11-20 mm zone, xylem loading was less. This could be explained by an impeded symplastic Al transport from the epidermis to the central cylinder and thus to the xylem in differentiated root tissue. It has been shown that proceeding root differentiation in *Arabidopsis* affects the distribution of plasmodesmata. Epidermal cells of developing roots became progressively more isolated, suggesting that plasmodesmata in these cells were either less prevalent or effective (Duckett *et al.* 1994). The described scenario is in agreement with the morphology of the buckwheat adventitious root shown in Fig. 8. Whereas the apical 10 mm were largely undifferentiated tissue, the 11-15 and even more clearly the 16-20 mm zones showed clear differentiation between root cortex and central cylinder, suberinization of the endodermis, and formation of lignified xylem vessels.

The transfer of Al into the xylem involves a ligand exchange from oxalate to citrate (Shen *et al.* 2004), because hardly any oxalate but large concentration of citrate are found in the xylem sap of buckwheat (Ma and Hiradate 2000; Fig 7). The exact localization of this ligand exchange is still unknown, although the xylem companion cells in the central cylinder are the

most probable candidates. Ma and Hiradate (2000) showed that the xylem citrate-concentration is constitutively high and not affected by Al application and thus loading of Al into the xylem. In contrast to these results, a significant positive correlation between Al and citrate transport-rates in the xylem sap independent of the root zone of Al application was found (Fig. 7). The reason for this discrepancy might be the site of xylem-sap collection. Xylem sap was sampled from the excised root 45 mm behind the root apex which may well reflect the effect of Al uptake and loading into the xylem on xylem-sap composition. Sampling the xylem sap at the stem level might lead to shifts in the citrate/Al ratio because of xylem loading and unloading along the xylem pathway. In hortensia (*Hydrangea macrophylla*), another Al accumulator plant species, a close 1:1 correlation between citrate and Al could be found in xylem exudates sampled at the stem level (Naumann and Horst, 2003). In buckwheat the Al transport rate in the xylem sap was strongly affected by the kind and length of the apical root zone exposed to Al (Fig. 4, Fig. 7). Application of Al to zones including the root apex, and 10 mm zones compared to 5 mm zones led to higher Al transport rates. The different regressions for the relationships between xylem-Al and citrate transport-rates for the Al application to 5 or 10 mm zones (Fig. 7) is difficult to explain on the basis of the available data. It is evident that not the Al transport rate determines the citrate transport rate in the xylem sap which did not differ between the two applications. In both cases, Al supply enhanced the citrate transport rates from about 2 to 5 nmol root tip⁻¹ 6h⁻¹. It may thus be speculated that the Al concentration in the apical 5 mm root apex determines the citrate release to the xylem. More detailed studies on the synthesis and transport of citrate in the root apex differentiating between the root cortex and the central cylinder are urgently needed.

In conclusion, the data presented show that the Al-induced release of oxalate (Al exclusion mechanism protecting the cell wall from Al injury) and Al uptake and accumulation (Al tolerance) are spatially not separated in the root apex. The further characterization of Al uptake at the root apex as affected by oxalate is subject to ongoing studies and will be reported in a subsequent paper.

Oxalate exudation into the root-tip water free space confers protection from Al toxicity and allows Al accumulation in the symplast in buckwheat (*Fagopyrum esculentum* Moench)

Benjamin Klug, Walter J. Horst

Published in: *New Phytologist* (2010) doi: 10.1111/j.1469-8137.2010.03288.x

Abstract

A better understanding of aluminium (Al) uptake and transport is expected to contribute to unravel the apparent contradiction between Al exclusion and Al accumulation in buckwheat.

We studied the effect of Al supply on the root-tip Al and oxalate concentrations of the apoplastic water free space fluid (WFSF) and the symplast as affected by temperature, oxalate supply and the anion-channel blocker phenylglyoxal (PG).

Aluminium supply rapidly activated the release of oxalate to the WFSF to establish a 1:1 Al:oxalate ratio. In the symplast, the Al concentration was 100 times higher than in the external solution, and the Al to oxalate ratio was 1:2. Loading and unloading of Al, but not of oxalate, into and from the symplast were reduced at low temperature and are thus under metabolic control. Application of PG reduced the constitutive and the Al-enhanced WFSF oxalate concentrations and enhanced Al-induced root-growth inhibition. Different from a 1:3 Al:oxalate ratio, a 1:1 ratio ameliorated only partly Al-induced root-growth inhibition without affecting root-tip Al contents or WFSF Al concentrations.

We present a hypothesis with an Al(Ox)^+ plasma-membrane transporter in the root cortex and a xylem-loading Al(Cit)^{n-} transporter in the xylem parenchyma cells as key elements of Al accumulation in buckwheat.

Introduction

Aluminum toxicity is a major factor limiting crop productivity on acid mineral soils which comprise 40 % of the world's arable land (Conner & Meredith, 1985). Aluminium toxicity is characterized by a rapid inhibition of root growth leading to reduced water and nutrient uptake and finally to limited growth and yield of Al-sensitive crops. However, great intra- and interspecific differences in Al resistance exist (Kochian *et al.*, 2005; Ma & Furukawa, 2003). Aluminium resistance, a term which is used here in its general sense as a plant characteristic which allows a plant to grow without growth inhibition at elevated Al supply, rely on the exclusion of Al from binding and uptake of Al by the roots and thus low Al concentrations in the leaves ($< 100 \mu\text{g (g dry matter)}^{-1}$) in most crops. However, some of the most Al-resistant plant species are Al accumulators and have evolved Al tolerance. Among these plant species are tea (*Camellia sinensis* var. *sinensis*), hortensia (*Hydrangea macrophylla*) and buckwheat (*Fagopyrum esculentum* Moench) which accumulate Al in leaves up to several mg (g dry matter)⁻¹ (Matsumoto *et al.*, 1976, Naumann & Horst, 2003, Ma *et al.*, 1997a.). The mechanism underlying the internal tolerance mechanisms of the Al accumulator buckwheat are rather well understood. Once taken up, Al is bound as an Al-oxalate complex and is transported radially to the central cylinder where a ligand exchange to citrate is proposed to occur (Ma & Hiradate, 2000). In the xylem Al is transported as Al-citrate complex into above-ground plant parts where again Al changes the ligand back to oxalate (Ma *et al.*, 1998). When the Al import into the leaf exceeds a certain limit, especially at the leaf margins, an Al-citrate complex will be additionally formed (Shen *et al.*, 2004). Aluminium is transported exclusively into transpiring organs and does not accumulate in the seeds (Shen *et al.*, 2006) suggesting that Al is not phloem-mobile. In contrast to Al tolerance, Al uptake in buckwheat is not well understood yet. In response to Al treatment buckwheat releases oxalate from the root tips without a lag phase (Ma *et al.*, 1998; Zheng *et al.*, 1998) which is a typical feature of Pattern I Al excluders according to Ma *et al.*, 2001. Thus, it appears that the anion permease facilitating the oxalate exudation is constitutively expressed in buckwheat (Ma *et al.*, 2001; Yang *et al.*, 2005) such as the malate permease TaALMT1 in wheat (Delhaize *et al.*, 2007). However, a molecular and physiological characterization of this anion permease is still missing in buckwheat. The Al-activated release of oxalate suggests that Al is bound to oxalate in the root apoplast thus protecting Al-sensitive binding sites. Applying oxalate in different Al:oxalate ratios to buckwheat roots, Ma & Hiradate (2000) showed a strong reduction of Al uptake and translocation in the xylem sap even at a 1:1 ratio thus confirming the role of Al

complexation in Al exclusion. They conclude from their results that the Al accumulation of buckwheat requires the uptake of Al as Al^{3+} and a stratification along the root apex of oxalate release and Al^{3+} uptake. However, using mini-rhizotrons which allowed differentiating between spatial responses to Al with regard to Al uptake and organic acid-anion exudation and to measure simultaneously Al and organic acid transport in the xylem, we recently provided evidence that Al-induced release of oxalate, Al uptake and Al accumulation are spatially co-localized in the root apex (Klug & Horst, 2010).

On the one hand the uptake process of Al was suggested to be an active process, because xylem-sap Al concentrations exceeded by far the concentration in the external solution (Ma & Hiradate, 2000). But on the other hand, the lack of a response of Al uptake and translocation in the xylem sap to the respiration-inhibitor hydroxylamine rather indicated a passive process (Ma & Hiradate, 2000). Thus, the nature of the Al-uptake process in buckwheat is not yet unequivocally clarified.

The present study is focused on a characterisation of the transport of Al from the root apoplast into the root symplast of buckwheat. Special emphasis is placed on the characterisation of the Al and organic acid composition of the apoplastic water free space fluid (WFSF) in relation to Al uptake. It is expected that the better understanding of the Al uptake will contribute to unravel the apparent contradiction between Al exclusion and Al accumulation in the Al-resistant Al accumulator buckwheat.

Material and Methods

Plant Material

Buckwheat (*Fagopyrum esculentum* Moench) cultivar “Lifago” (Deutsche Saatveredelung AG, Lippstadt, Germany) was germinated in peat substrate with 30% clay (Balster Einheitserdewerk GmbH, Fröndenberg, Germany). Plants were grown for 4 weeks in a green house at 25/20 °C day/night temperature. After this period of growth the shoots were cut 1 cm below the first node with adventitious root initials and additionally above the primary leaf to reduce transpiration. These shoot cuttings were transferred to low ionic strength nutrient solution with the following composition [μM]: 500 KNO_3 , 162 MgSO_4 , 30 KH_2PO_4 , 250 $\text{Ca}(\text{NO}_3)_2$, 8 H_3BO_3 , 0.2 CuSO_4 , 0.2 ZnSO_4 , 5 MnSO_4 , 0.2 $(\text{NH}_4)_6\text{Mo}_7\text{O}_{24}$, 50 NaCl , and 30 Fe-EDDHA for 4 days keeping the shoots at 100 % relative humidity (rH) until adventitious

roots had emerged. The following day the plants were adapted to lower rH by reducing air humidity. Another day later, the pH of the nutrient solution was reduced in three steps to 4.3 resulting in at least 12 h for adaptation to the low pH before the beginning of the Al treatment.

Aluminium loading of intact adventitiously rooted cuttings

With onset of the treatment, rooted and pH-adapted cuttings were transferred to either 0 μM or 75 μM AlCl_3 in simplified nutrient solution containing 500 μM CaCl_2 , 8 μM H_3BO_3 ; 100 μM K_2SO_4 at pH 4.3. A concentration of 75 μM AlCl_3 was shown to be an Al concentration, leading to a root growth inhibition between 50 and 60 % (data not shown). The pH was controlled and readjusted when necessary to 4.3 using 0.1 M HCl or 0.1 KOH added drop wise under continuous stirring. The nutrient solution was aerated permanently.

Aluminium loading and unloading of excised adventitious roots

Roots of pH-adapted cuttings were excised 10 mm behind the root tip. 30 root tips per sample were collected in net trays in ice cold minimal nutrient solution at pH 4.3. This nutrient solution was replaced 3 times to remove cellular contamination due to wounded tissues at the cutting surface. All root tips, but not the control treatment, were transferred in their net trays to either a warm or cold solution containing 75 μM AlCl_3 , pH 4.3. Only warm loaded root tips were transferred (after blotting to remove adhering solution) to either warm or cold unloading minimal nutrient solution without Al for 10 or 30 min. The net trays in the respective treatment solution were constantly shaken on a wave platform shaker (Heidolph polymax 2040, Heidolph Instruments GmbH & Co. KG, Schwabach, Germany).

Aluminium loading in presence of oxalate and phenylglyoxal

pH-adapted buckwheat cuttings with adventitious roots were transferred to simplified nutrient solution. All treatments containing Al were pre-treated for 15 min with 75 μM AlCl_3 at pH 4.3 as an initial Al stimulus. After this pre-treatment the cuttings were transferred to the treatment solutions containing +/- 75 or 200 μM AlCl_3 , +/- 10 μM PG (Phenylglyoxal, Merck KGaA, Darmstadt, Germany) as anion-channel inhibitor, and +/- 75 or 200 μM oxalate. The

pH was monitored and adjusted if necessary during the treatment duration of 24 h. For measuring root growth, root tips were marked with Plaka colour (Pelikan, Feusisberg, Switzerland) using a fine paint brush 1 cm behind the tip and measured after 24 h using a ruler. Xylem sap was extracted from 2 cm stem segments by centrifugation at 6,000 g for 5 min. Prior to centrifugation the cut ends were rinsed in double deionised water and gently blotted dry. The sap of two stem segments was combined to one composite sample. In the recovered xylem sap Al was analyzed by GF-AAS after appropriate dilution, and organic acids (OAs) were analysed by HPLC (see below). The Al fractionation in the root tips was performed as specified below.

Fractionation of Al and organic acids in the root tissue

In order to characterize the binding stage and compartmentation of Al and OAs in the roots a fractionated extraction procedure was applied following the procedure suggested by Yu *et al.* (1999) modified and described by Wang *et al.* (2004) and Rangel *et al.* (2009). Briefly, 30 10-mm root tips were excised from adventitious roots on an ice-cooled graduated glass cutting plate. The root tips were then placed upright with the cutting surface facing down in a filter unit with a pore size of 0.45 μm (GHP Nanosep[®]; MF Centrifugal device; Pall Life Sciences; Ann Arbor; MI, USA). Until the extraction begun the filter units were stored on ice never exceeding 5 min. The nutrient solution adhering to the surface of the roots was removed by centrifugation at 60 g for two min. The water free space fluid (WFSF) was then extracted at 4,000 g for 15 min. The cytoplasmic contamination of the WFSF was low. The activity of the cytoplasmic marker enzyme malate dehydrogenase (MDH) in the WFSF never exceeded 0.5 % of the root-tip homogenate. Subsequently the root tips were frozen at -20 °C, defrozen, and again centrifuged at 4000 g for 15 min yielding the symplastic fraction. The volume of each fraction and sample was determined by micropipetting. To obtain pure cell-wall material, which is defined as ethanol-insoluble residue of the homogenate (Fry, 1988), the root tips were transferred to an Eppendorf vial and homogenised in 500 μL ethanol (96 % w/v) in a swing mill (MM200; Retsch; Haan; Germany) at 30 strokes min^{-1} for 3 min. The homogenate was pelleted by centrifugation at 23,000 g for 15 min. The pellet was resolubilized and centrifuged again. This procedure was repeated 3 times. The collected supernatants from each washing step were evaporated in a centrifugal evaporator (RCT 10-22T; Jouan; Saint-Herblain, France), and the residue was digested in concentrated ultra pure nitric acid and its

Al content determined. Since the Al content of the ethanol fraction was very low and did not respond to Al treatment time and Al supply it was neglected in the calculation of the symplastic Al. The pellet contained the purified cell-wall fraction and was digested as performed for bulk root-tip Al analysis. In addition to Al OAs in the WFSF and the symplastic sap were analysed in sub-samples.

Aluminium determination

Aluminium was determined by GF-AAS (Unicam 939 QZ; Analytical Technologies Inc.; Cambridge; UK) at a wavelength of 308.2 nm, an ashing phase of 20 sec at 1,500 °C and an atomisation phase of 3 sec at 2,300 °C. Each sample was measured twice. Root tips were digested over night in 500 µL double-distilled ultra-pure nitric acid under continuous shaking at room temperature. After digestion the samples were diluted as necessary with double deionised water.

Determination of organic acids

Organic acids in the root exudates as well as in the extracts of root tissue were measured by isocratic High Pressure Liquid Chromatography (HPLC, Kroma System 3000, Kontron Instruments, Munich, Germany). The OAs were injected through a 20 µl loop-injector (Auto-sampler 360) of the HPLC, separating different OAs on an Animex HPX-87H (300 x 7.8 mm) column (BioRad, Laboratories, Richmond, CA, USA), supplemented with a cation H⁺ micro-guard cartridge, using 10 mM perchloric acid as eluant at a flow rate of 0.5 ml per minute, constant temperature of 35 °C (Oven 480), and 74 hPa of atmospheric pressure. Measurements were performed at a wavelength $\lambda = 214$ nm (UV Detector 320). Prior to the analysis of exuded organic acid anions the nutrient solution samples were run through a cation-exchange column (hydrochloric form) (AG® 50W-X8; Biorad; Life science group; Hercules; CA, USA) followed by concentration to dryness via centrifugal evaporation (RCT 10-22T; Jouan; Saint-Herblain, France).

Results

The bulk Al contents of the apical 10 mm root tip rapidly increased within the first four hours of Al treatment (Fig. 1). Then the Al contents levelled off and after 8 h remained stable up to 24 h Al treatment. After a lag phase of about 1 h the Al concentration in the xylem sap increased linearly up to 24 h Al treatment (Fig. 1). The xylem sap Al concentration reached the concentration of the external solution (75 μ M) after 8 h and about twice this concentration after 24 h Al treatment. The contents of the OAs present in the aqueous extract of the 10-mm root tip were succinate = oxalate > malate. Whereas succinate (12.9) and malate (12.4) did not change during the Al treatment, the oxalate content (13.8) decreased with Al treatment duration to 5.0 (nmol (cm root tip)⁻¹).

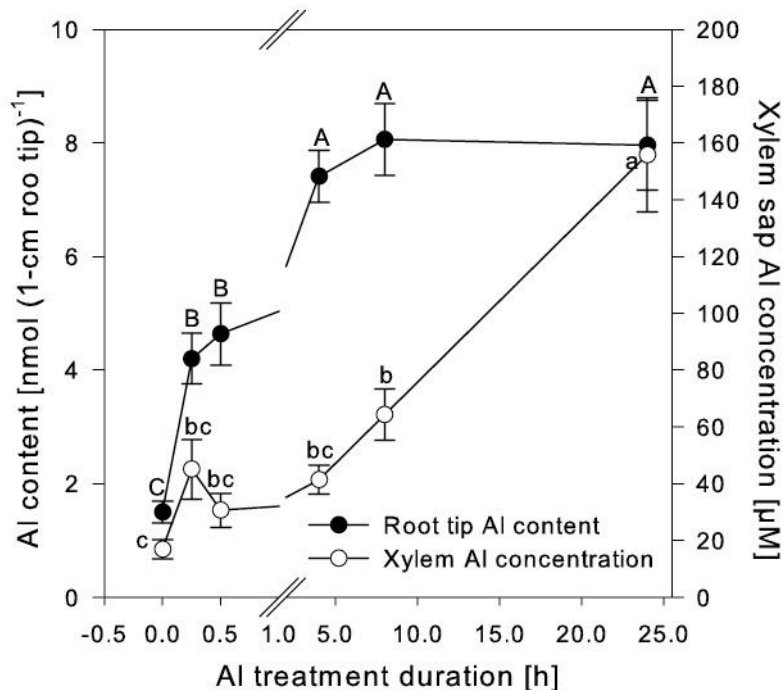


Figure 1. Effect of Al treatment duration on the Al contents of 10-mm root tips and xylem-sap Al concentrations of adventitiously rooted buckwheat plants grown in simplified nutrient solution (500 μ M CaCl₂, 8 μ M H₃BO₃; 100 μ M K₂SO₄) without and with 75 μ M AlCl₃ at pH 4.3. Points represent means \pm SE, n = 5. Different letters denote significant differences between treatment durations at $P = 0.05$. Succinate and malate contents were not significantly affected by treatment duration.

The Al content of the 10-mm root apices was operationally fractionated into the water free-space fluid (WFSF), symplast, and cell-wall fraction. After Al treatment, the Al concentration in the WFSF quickly reached 250-600 μ M, thus a 5-8 times higher concentrations than in the external solution supplied, and remained stable over the 24 h Al treatment period (Fig. 2a).

The symplastic Al concentration increased to about 5 mM and 11 mM after 0.5 h and 4 h Al treatment, respectively (Fig. 2b). Compared to the external Al concentration Al accumulated in the symplast by a factor of more than 100. After 24 h the symplastic Al concentration decreased to 7 mM. The Al content of the cell walls increased steadily over the Al treatment period (Fig. 2c). The relative quantitative contribution of each root-tip Al fraction to the sum over all fractions revealed that up to 4 h Al treatment, the symplastic fraction showed the greatest share of the total Al content (Fig. 3).

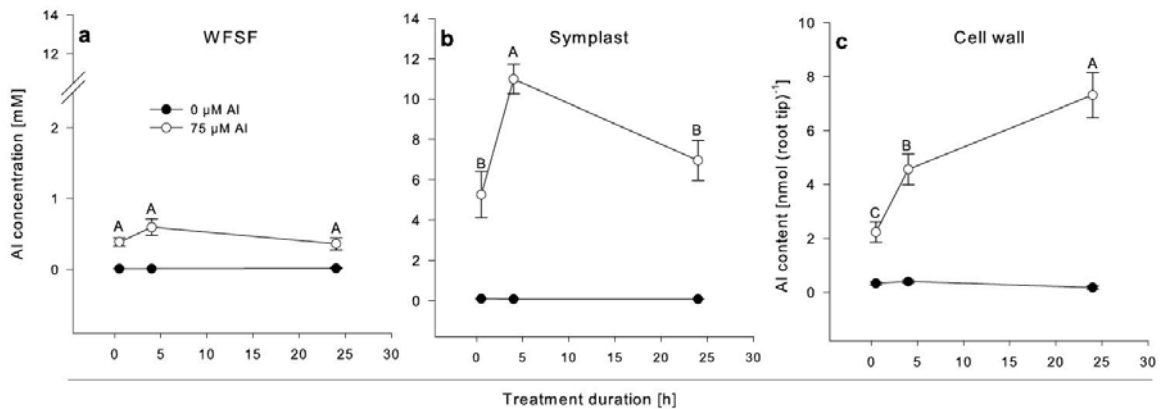


Figure 2. Aluminium concentrations in (a) the water free-space fluid (WFSF), (b) the symplastic sap, and the cell wall Al content (c) of 10-mm adventitious root tips of buckwheat plants not treated or treated with 75 μM AlCl_3 for 0.5, 4 and 24 h in simplified nutrient solution (500 μM CaCl_2 , 8 μM H_3BO_3 ; 100 μM K_2SO_4 , pH 4.3). For the description of the fractionated extraction technique see Materials and Methods. Plants were rooted for 4 days followed by 1 day pH adjustment. Two independent experiments were conducted. ANOVA did not reveal a treatment x experiment interaction. Thus points represent means of two independent experiments \pm SE, $n = 6$. Means with different letters denote significant differences between treatment durations within the +Al treatment at $P = 0.05$.

After longer Al treatment the cell-wall fraction became more important. The increasing share of the cell-wall fraction may have been due to both an internal redistribution of Al and decrease in symplastic Al, because the total Al content of the root tip did not increase between 4 and 24 h Al treatment duration (compare Fig. 1). The relative contribution of the WFSF Al fraction was small and decreased with Al treatment duration because of increasing bulk-tissue Al contents.

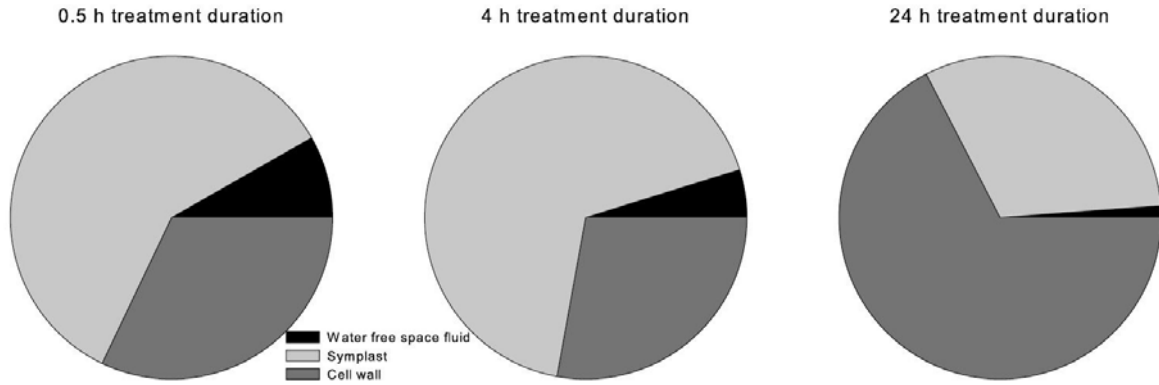


Figure 3. Relative contributions of cellular Al fractions to the total Al content of 10-mm apices of adventitious buckwheat roots after 0.5, 4 and 24 h of Al treatment ($75 \mu\text{M}$) in simplified nutrient solution ($500 \mu\text{M CaCl}_2$, $8 \mu\text{M H}_3\text{BO}_3$; $100 \mu\text{M K}_2\text{SO}_4$ pH 4,3).

In the WFSF as well as in the symplast, oxalate was the most abundant organic acid anion which responded to the Al supply. The oxalate concentration in the symplast was higher by a factor of about 25 than in the WFSF (Fig. 4). The oxalate concentrations were significantly correlated with the Al concentrations in the WFSF as well as in the symplast. The slope of the regression line for the WFSF is not significantly different from the 1:1 line and suggests an Al oxalate complex formation in a ratio of 1:1 in the WFSF (Fig. 4a).

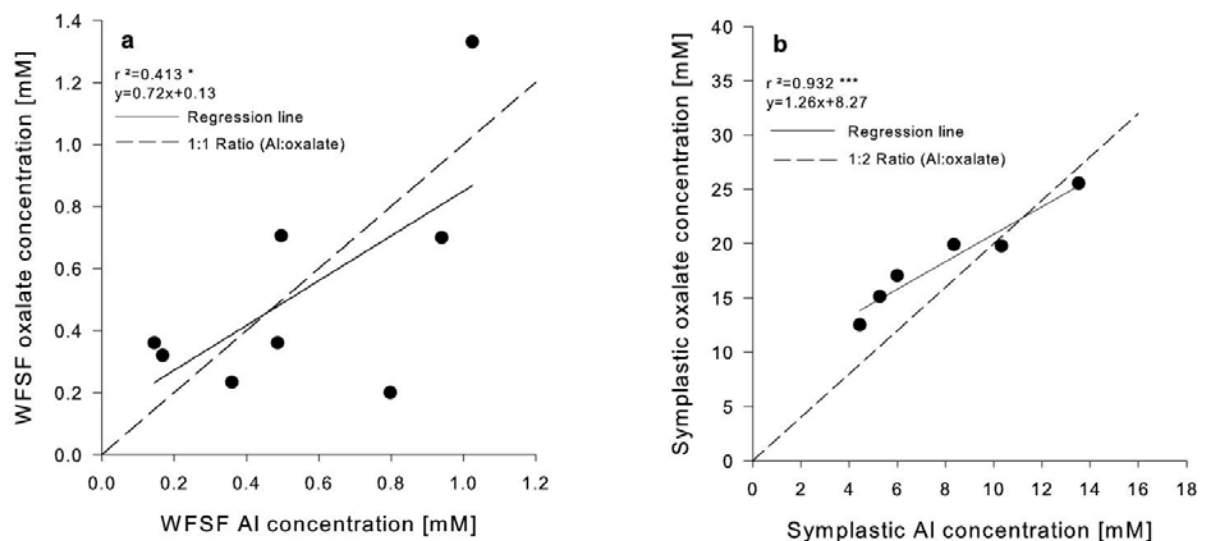


Figure 4. Correlations between Al and oxalate concentrations in the water free-space fluid (a) and the symplastic fraction (b) of adventitious 10-mm buckwheat root tips. Fractionated extraction of the 1-cm root tips after 0.5, 4 and 24 h of Al treatment ($75 \mu\text{M}$) in simplified nutrient solution ($500 \mu\text{M CaCl}_2$, $8 \mu\text{M H}_3\text{BO}_3$; $100 \mu\text{M K}_2\text{SO}_4$ pH 4,3). Points represent single values. For comparison the 1:1 (a) and 1:2 (b) Al:oxalate ratios are shown. For the ANOVA, * and *** denote levels of significance at $P < 0.05$ and 0.001 , respectively.

The ratio of the Al and oxalate concentration was close to two and the regression line for the symplastic fraction was close to the 1:2 line indicating a 1:2 Al oxalate complex in the symplast (Fig. 4b). The intercepts with the y-axis suggest a constitutive oxalate concentration of 0.1 and 10 mM in the WFSF and the symplast, respectively.

For further unravelling the Al accumulation and transport into the central cylinder we used excised adventitious root tips. In a first approach we studied the metabolic control of the initial steps of Al accumulation (loading) and unloading in the apoplast and symplast (Fig. 5). Within 30 min Al loading the Al concentration of the WFSF reached the Al concentration of the external solution of 75 μM independent of the temperature (Fig. 5a). After transfer of the roots to Al-free solution the WFSF Al concentration quickly decreased to the control level, again independent of the temperature. The Al concentration of the symplast, which after 30 min of Al treatment reached more than one mM at 25°C, was decreased to 600 μM at 4°C (Fig. 5b). During the unloading period the symplastic Al concentration decreased only at 20°C but not at 4°C.

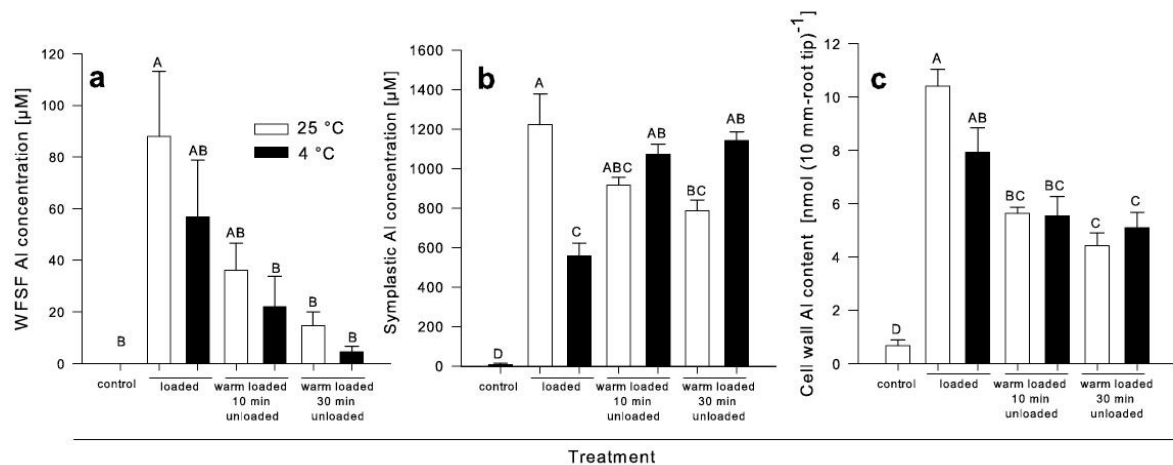


Figure 5. Concentrations of Al in the water free space fluid (WFSF) (a) the symplast (b), and cell-wall Al content (c) of excised 10-mm apices of adventitious buckwheat roots. Fractionated extraction of the root tips after 30 min treatment with 75 μM Al (loading) in minimal nutrient solution (500 μM CaCl_2 , 8 μM H_3BO_3 ; 100 μM K_2SO_4 , pH 4.3) and subsequent unloading for 10 and 30 min in minimal solution without Al supply at 25°C (white bars) or 4°C (black bars). Different letters denote significant differences at $P < 0.05$ between treatment durations; $n = 5$.

Exposing the root apices for 30 min to Al rapidly enhanced the Al content of the cell walls independent of the temperature (Fig. 5c). The Al content was higher than in intact roots (compare Fig. 2c). After transferring the Al-loaded roots to Al-free solution the Al content of the cell walls rapidly decreased to about 50 % without a temperature effect.

Among the organic acids analysed in the WFSF and symplastic sap of the excised root tips, oxalate was again the most abundant and the only organic acid which responded to Al supply. Aluminium supply increased the oxalate concentration in the WFSF to 250 μM within 30 min without temperature effect (Fig. 6a). Transferring the root tips to Al-free solution initiated a rapid temperature-independent loss of oxalate. The symplastic oxalate concentration was higher than in the WFSF by a factor of 100 (Fig. 6b). It was not significantly affected by Al, temperature and unloading period. However, there was a consistent trend of enhanced oxalate concentrations at higher temperature and during Al unloading.

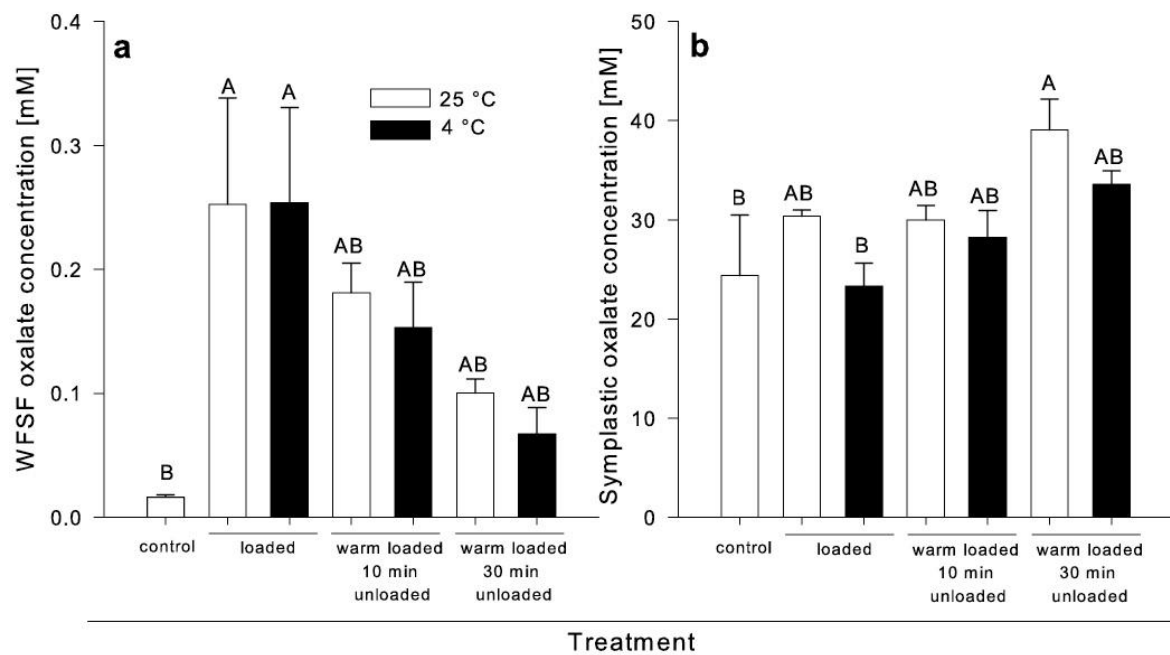


Figure 6. Water free space fluid (a) and symplastic (b) oxalate concentrations of excised 10-mm apices of adventitious buckwheat roots. Fractionated extraction of the root tips after 30 min treatment with 75 μM Al (loading) in minimal nutrient solution (500 μM CaCl_2 , 8 μM H_3BO_3 ; 100 μM K_2SO_4 , pH 4.3) and subsequent unloading for 10 and 30 min in minimal solution without Al supply at 25°C (white bars) or 4°C (black bars). Different letters denote significant differences at $P < 0.05$ between treatment durations; $n = 5$.

To further explore the role of apoplastic oxalate on Al uptake we used the anion channel blocker PG and varied the apoplastic oxalate concentration by external application of oxalate. In order to induce oxalate exudation and a possible Al uptake system all Al-treated plants were exposed to 75 μM Al at pH 4.3 in a minimal nutrient solution for 15 minutes irrespective of the subsequent treatment. Application of PG reduced the constitutive and the Al-enhanced WFSF oxalate concentrations (Fig. 7a). External supply of oxalate (75 > 200 μM) increased the WFSF oxalate concentrations further compared to Al supply alone (Fig. 7b). The WFSF

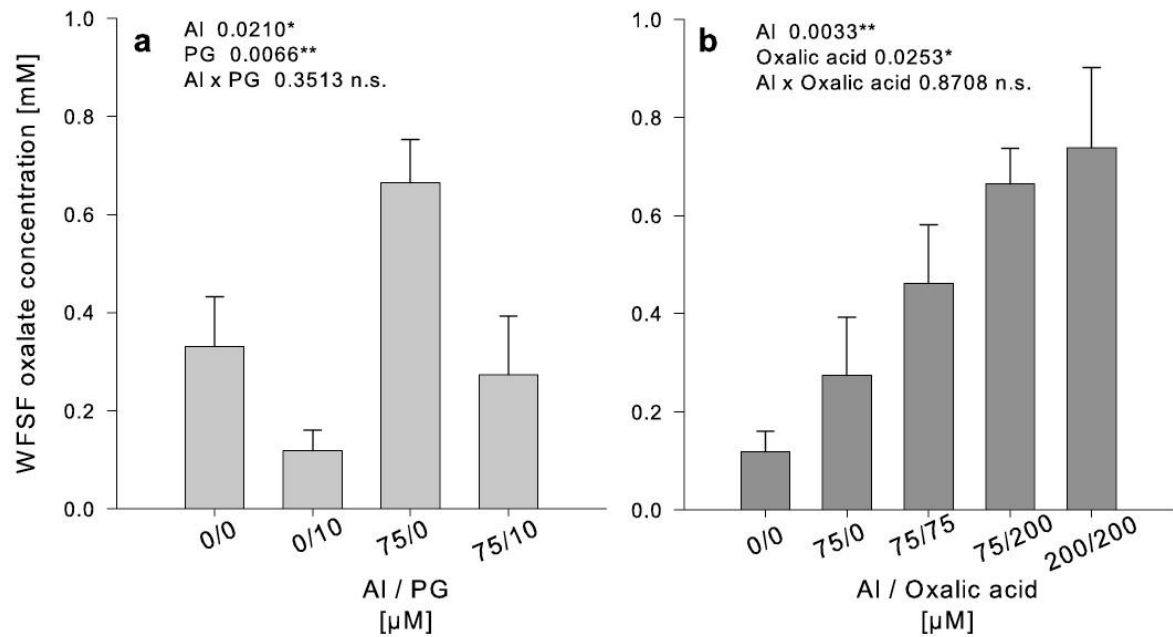


Figure 7. Oxalate concentrations in the water free space fluid (WFSF) as affected by Al and PG treatment (a) and the oxalate supply (b) in the nutrient solution. Adventitious roots of buckwheat plants were grown in simplified nutrient solution of 500 μM CaCl_2 , 8 μM H_3BO_3 , 100 μM K_2SO_4 at pH 4.3. They were exposed or not exposed to 75 or 200 μM AlCl_3 , 10 μM PG and 75 or 200 μM oxalate for 24 hours. Only Al-treated plants were pre-treated with 75 μM Al for 15 min prior to the PG and oxalate addition. The WFSF was recovered by centrifugal extraction. For the ANOVA, * and ** denote significant effects at $P < 0.05$ and 0.01, respectively, ns non significant. Data represent means \pm SE, $n = 4$.

oxalate concentration was higher by a factor of about 3 than the oxalate concentration of the external solution. The root growth-rate was not affected by PG application alone (Fig. 8a). However, when combined with Al treatment, the Al-induced inhibition of root elongation was further enhanced (significant Al*PG interaction). Aluminium treatment increased the Al content (Fig. 8c) and the Al concentration of the WFSF (Fig. 8e). Application of PG slightly reduced the WFSF Al concentration but did not affect the root-tip Al content.

Oxalate application in a ratio Al/oxalate of 1:1 ameliorated Al-induced root-growth inhibition compared to Al application alone to 50% compared to 80% without oxalate supply independent of the Al supply (75 or 200 μM) (Fig. 8b). This amelioration could not be related to lower root-tip Al contents (Fig. 8d) or WFSF concentrations (Fig. 8f). Application of 200 μM oxalate to 75 μM Al restored root growth nearly to the control (- Al) level (Fig. 8b). This can be explained by greatly reduced root-tip Al contents (Fig. 8d) and WFSF Al concentrations (Fig. 8f).

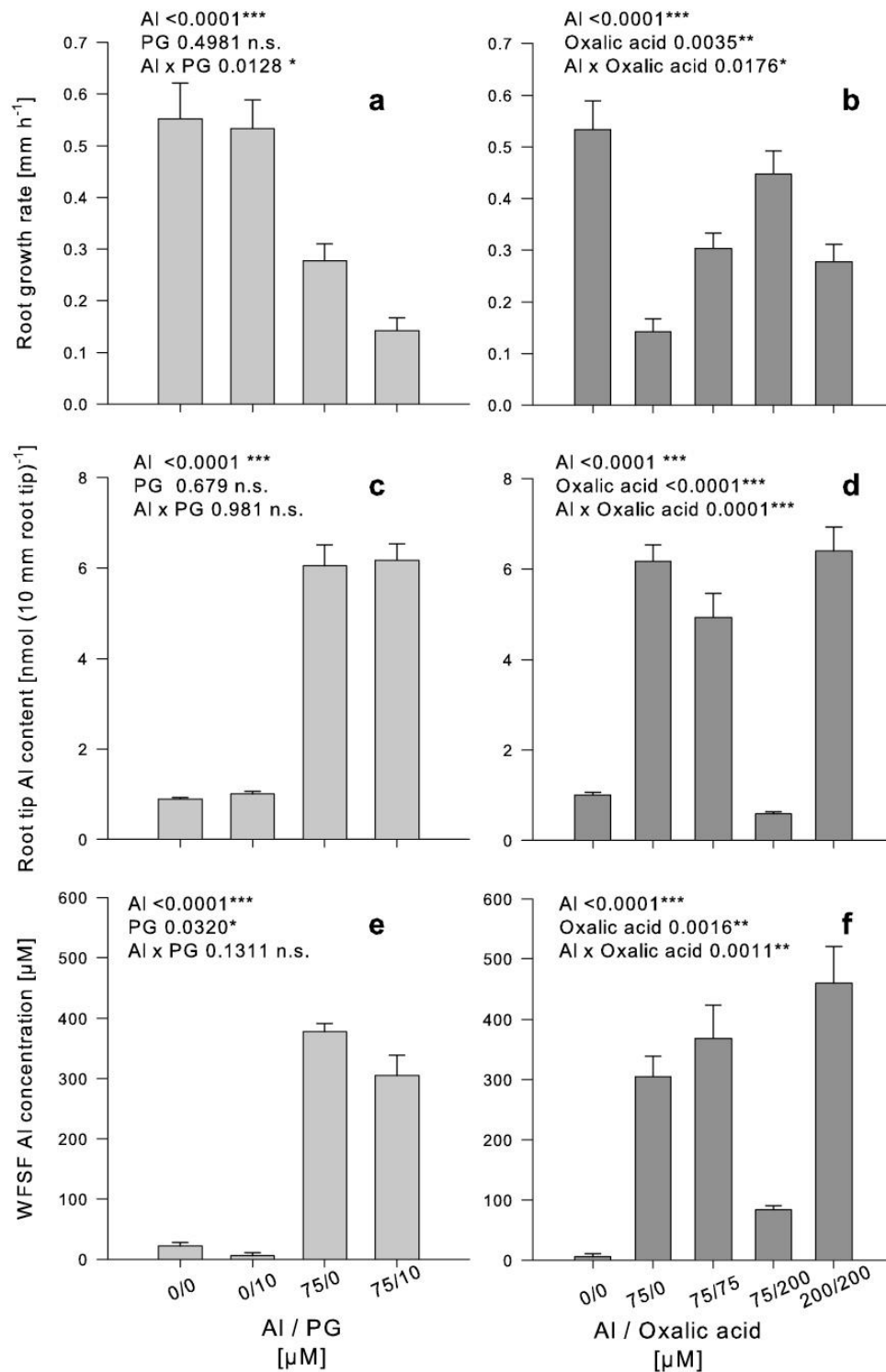


Figure 8. Root-growth rate, bulk Al root-tip content and Al concentration in the water free space fluid (WFSF) after centrifugal extraction as affected by Al and PG (a, c, e) or the oxalate supply (b, d, f) in the nutrient solution. Adventitious roots of buckwheat plants were grown in simplified nutrient solutions of 500 μM CaCl₂, 8 μM H₃BO₃, 100 μM K₂SO₄ at pH 4.3. They were exposed or not exposed to 75 or 200 μM AlCl₃, 10 μM PG and 75 or 200 μM oxalate for 24 hours. Only Al-treated plants were pre-treated with 75 μM Al for 15 min prior to the PG and oxalate addition. The WFSF was recovered by centrifugal extraction. For the ANOVA, *, **, and *** denote significant effects at $P < 0.05$, 0.01, and 0.001, respectively, ns nonsignificant. Data represent means +/- SE, n = 4.

Discussion

The methodology established by Yu *et al.* (1999) and refined by Wang *et al.* (2004) and Rangel *et al.* (2009) allowed to separate operationally defined apoplastic and symplastic Al fractions (Fig. 2). Among the 3 fractions, the WFSF Al is expected to best represent *in vivo* localization of Al because it is recovered by centrifugation from the root tips without destroying the compartmentation. It is difficult to decide whether the symplastic and the cell-wall Al fraction under or overestimate the *in vivo* compartmentation. During the extraction process particularly during the recovery of the cell sap, organic ligands may mobilize labile-bound CW Al or symplastic Al which is bound by CW due to a higher Al-binding strength of CW compared to symplastic ligands (Rengel, 1996). In spite of these uncertainties the fractionated extraction procedure has proven to contribute to the understanding of Si amelioration of Al toxicity (Wang *et al.* 2004), Si-accumulating and Si-excluding plant species in relation to their resistance against plant pathogens (Heine *et al.* 2005, 2007). It also clearly differentiates between Al excluders such as *Phaseolus vulgaris* (common bean) and Al accumulators such as buckwheat which after 4h Al treatment accumulated about 10% (Rangel *et al.*, 2009) and 67.4 % (Fig. 3) in the symplast of root apices, respectively.

Aluminium activates the release of oxalate from root tips of buckwheat without a lag phase (Ma *et al.*, 1997b, Klug & Horst, 2010) confirming its classification as Pattern I Al responder (Ma *et al.*, 2001). The oxalate exudation leads to an oxalate concentration in the WFSF of 250 μM after 0.5 h Al treatment (Figs. 4a, 6a). We also determined the oxalate concentration at the rhizoplane using a slow centrifugation (60 g) step preceding the extraction of the WFSF. The oxalate concentration in the rhizoplane water-film was below the detection limit (data not shown). This confirms the biphasic diffusion hypothesis elaborated by Kinraide *et al.* (2005). Using computational and experimental approaches these authors proposed that the epidermis acts as a barrier for both organic acid anion-release and Al uptake by roots. They proposed that this allows, with rather low exudation rates, to establish high organic acid-anion concentrations in the root-cortex WFSF necessary to reduce the Al^{3+} activity and thus protecting the root from Al injury (\rightarrow Al resistance). Our data confirm this hypothesis for buckwheat: An Al:oxalate ratio of 1:1 in the WFSF of root tips (Fig. 4) suggest that the Al^{3+} concentration in the WFSF is rather low. Computation of the Al speciation in the WFSF using GEOCHEM-EZ (Shaff *et al.*, 2009) revealed that at the measured Al and oxalate concentrations (ratio 1:1), 99 % of the Al was present Al:oxalate complex in the presence of

500 μM Ca (simplified nutrient solution). Increasing the Ca concentration to 6000 μM decreased the Al-oxalate formation only to less than 90 %.

The Al-activated release of oxalate from the root tip was not significantly affected by the loading or unloading temperature regime (Fig. 6a), which may indicate that this efflux is not directly coupled to a metabolic energy-requiring process. If the Al-activated oxalate efflux is controlled in the same way as malate and citrate release in other plant species we may assume that the release of organic acid anions from the symplast is mediated by an organic acid-anion permease activated by Al^{3+} (Delhaize *et al.*, 2007) along the membrane potential gradient. Thus, once the potential gradient has been established and is maintained, the release of oxalate is a passive process.

Since we assumed that the triggering of the oxalate exudation and the uptake of $\text{Al}(\text{Ox})^+$ (see below) require an Al^{3+} stimulus we exposed the buckwheat roots to a brief Al treatment (15 min) prior to the combined application of Al and oxalate in this study. This triggering was not performed by Ma & Hiradate (2000). We suggest that this is the reason why in their study, also the supply of Al and oxalate in a 1:1 ratio greatly reduced Al uptake and the Al concentration of the xylem sap.

The role of the WFSF oxalate-concentration in Al resistance of buckwheat is supported by the application of the anion-permease inhibitor PG and the supply of oxalate to the external solution. PG application reduced the WFSF oxalate concentration (Fig. 7a) leading to enhanced Al-induced inhibition of root growth (Fig. 8a). Increasing the external oxalate supply increased the WFSF oxalate concentration (Fig. 7b) alleviating root-growth inhibition by Al (Fig. 8b). However, not the absolute WFSF oxalate concentration, but the Al:oxalate ratio determines the extent of the root-growth inhibition: with increasing ratio Al-induced inhibition of root elongation is ameliorated and finally prevented at a 1:3 ratio (Fig. 9).

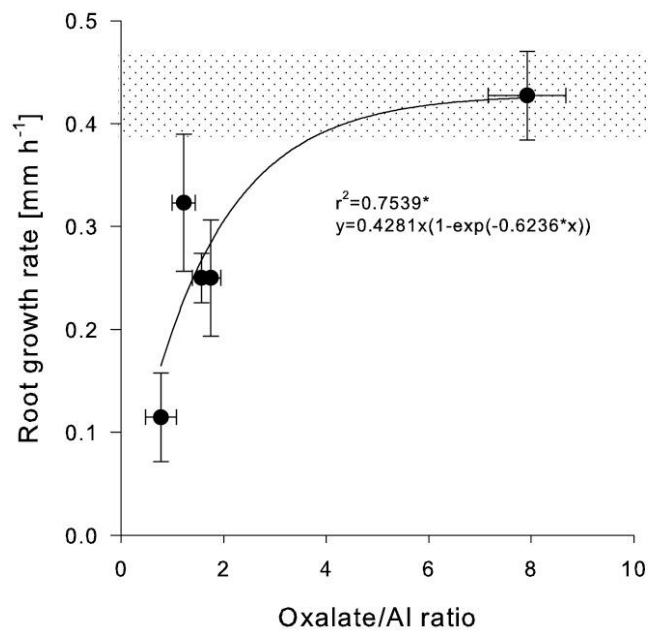


Figure 9. Root growth rate of adventitious roots of buckwheat as affected by the ratio of oxalate to Al in the water free space fluid after centrifugal extraction. Plants were grown in simplified nutrient solutions of 500 μM CaCl_2 , 8 μM H_3BO_3 , 100 μM K_2SO_4 at pH 4.3. They were exposed to 75 or 200 μM AlCl_3 , 10 μM PG and 75 or 200 μM oxalate for 24 hours. Plants were pre-treated with 75 μM Al for 15 min prior to the PG and oxalate addition. Data represent means \pm SE, $n = 4$. The root growth rate (\pm SE) of controls (-Al) are shown as shaded area. For the ANOVA, * denote levels of significance at $P < 0.05$.

Such an oxalate versus Al excess in the external solution not only reduced Al toxicity but also the accumulation of Al in the WFSF (Fig. 8c) and in the entire root tissue (Fig. 8b). Similar results have previously been shown by Ma & Hiradate (2000). The 1:1 oxalate:Al complex still carries a positive charge (Happel, 2007) and thus is expected to slow down the accumulation of Al^{3+} but still to accumulate in the negatively charged root Donnan Free Space (DFS, Briggs & Robertson, 1957). However, the 1:2 and 1:3 Al-oxalate complexes carry negative charges (Happel, 2007) which prevent accumulation in the DFS (Pitman, 1964).

The unmethylated carboxyl groups of the pectic matrix are mainly responsible for the cation-binding properties of the cell walls in the root apoplast (Glass, 2007). These negative charges are primary binding sites of Al^{3+} (Blamey *et al.*, 1990, Chang *et al.*, 1999). The rapid short-term Al accumulation by roots is closely related to the negativity of the root apoplast (Horst *et al.*, 2010 and references therein). This seems to also apply to buckwheat and explain the Al accumulation within 30 min of Al supply (Fig. 1). Binding of Al to the cell wall has been related to Al injury expressing as inhibition of root elongation and induction of callose formation in maize and common bean (Eticha *et al.*, 2005c; Rangel *et al.*, 2005) which is also

true for buckwheat (results not shown). Eticha *et al.* (2005b) and Yang *et al.* (2008) provided evidence for a role of the cell-wall negativity for genotypic differences in Al resistance in maize and rice, respectively. Using similar experimental approaches Zheng (SJ Zheng, Zhejiang University, Hangzhou, China, pers. comm. 2009) showed that the differential Al resistance of two buckwheat genotypes could also be related to differences in the Al binding capacity of root-tip cell-walls.

From the discussion above we conclude that Al is present in the WFSF of the root tip as Al(Ox)^+ which reduces but not prevents Al toxicity and little affects Al accumulation. Al(Ox)^+ will be bound by the negatively charged cell wall (see above), but in addition and increasingly over time (Fig. 3) Al will bind to the pectic matrix because the stability constant of Al(Ox)^+ is 6.1 (logK; Vance *et al.*, 1996) whereas the stability constant of Al-pectin is expected to be significantly higher (Eticha *et al.*, 2005b). This is supported by the fact that, although the stability constant of Al-citrate (1:1) and Al-EDTA is reported to be 8.32 and 16.5 (Martell & Smith, 1982), respectively, the addition of citrate (Rangel *et al.* 2009) and even EDTA added in surplus (Orvig, 1993) did not fully remove Al from the cell walls.

Temperature did not significantly affect the binding of Al by the cell walls (Fig. 5) indicating the passive nature of this process. In contrast to the loading and unloading of Al in the root-tip apoplast, the Al uptake and release of Al from the symplast proved to be affected by temperature (Fig. 5). The membrane transport of Al is not well understood either in Al excluders or in Al accumulators such as buckwheat (Ma & Hiradate, 2000). Ma & Hiradate (2000) showed that Al uptake in buckwheat was not affected by the respiration inhibitor hydroxylamine which suggested a passive uptake process. However, the reduction of Al accumulation in the symplast by 50% at 4 °C suggests an active process. This could be expected because Al is quickly accumulated in the symplast: after 30 min Al supply (75 μM) the symplastic Al concentration reached 5 mM and after 4 h 11 mM, a 10-30 times higher concentration than in the WFSF (Fig. 2). Since Al in the WFSF is expected to be present as Al(Ox)^+ (see above) it appears justified to assume that Al is transported through the membrane in this form by a cation transporter under metabolic control. In addition, the transport could be facilitated by the negative potential difference between the apoplast and the symplast and a steep concentration gradient, since in the cytosol Al(Ox)^+ is expected to immediately change to $\text{Al(Ox}_2\text{)}^-$ because of the higher oxalate concentration in the cell sap (Fig. 4).

Not only Al influx (loading) into the symplast but also the efflux from the symplast (unloading) appears to be temperature-dependent and thus under metabolic control (Fig. 5).

The unloading from the excised root tips may be indicative of the efflux from the symplast to the apoplast which is a prerequisite for xylem loading. The results and the conclusions drawn are similar to studies on Cd and Zn hyperaccumulation in *Thlaspi caerulescens* and *Arabidopsis halleri* (Verbruggen *et al.*, 2009). Klein *et al.* (2008) used cell cultures of *Arabidopsis thaliana* and *T. caerulescens* and concluded from their studies that the Zn/Cd transport pathway between root uptake and transport to the shoot could be elucidated on a cell-culture level. A lower accumulation of Zn and Cd in the cells was primarily due to a greater metal efflux in the accumulating plant species *T. caerulescens* compared to the non-accumulator *A. thaliana* (Klein *et al.*, 2008). This view offers an explanation of the results shown in Figs. 1 and 2: Al is accumulated particularly in the symplast until the loading of the xylem is fully functional leading to a steeply increasing xylem sap Al concentration.

The xylem loading of heavy metals in metal hyperaccumulators has been related to metal transporters such as heavy metal transporting ATPases (HMAs), oligopeptide transporters (OPTs) including the yellow-stripe 1-like (YSL) subfamily, and multi-drug and toxic compound extrusion (or efflux) membrane proteins (MATEs) such as FRD3 which is primarily a citrate permease involved in citrate loading into the xylem implicated in the xylem loading of Fe and possibly also Zn (Verbruggen *et al.* 2009 and references therein). Whether related or different transport proteins are involved in Al loading of the xylem is unknown. Aluminium is expected to be present as an anionic $\text{Al}(\text{Ox}_2)^-$ complex in the cytosol of root cortical cells as suggested by the 1:2 ratio of Al:oxalate in the symplast (Fig. 4). This suggestion is in agreement with data by Ma *et al.* (1998) who concluded from their ^{13}C -NMR analysis of roots and root cell-sap that Al is present in the root as 1:2 and 1:3 Al:oxalate complexes. A higher proportion of $\text{Al}(\text{Ox}_3)^{3-}$ in comparison to our study can be explained by the analysis of total roots with an expected higher vacuolation compared to the more cytoplasmic root apices in our study. Since citrate instead of oxalate is the only Al ligand in the xylem sap (Ma & Hiradate, 2000) it may be expected that ligand exchange from $\text{Al}(\text{Ox}_2)^-$ to $\text{Al}(\text{Cit})^n$ is taking place in the xylem parenchyma cells. This assumption is supported by own unpublished data on the oxalate and citrate contents in surgically partitioned cortical and stele tissues: In the cortical tissue, $40 \mu\text{mol} (\text{cm tissue length})^{-1}$ oxalate and no citrate, in the stele tissue including the xylem, only $0.8 \mu\text{mol} (\text{cm tissue length})^{-1}$ oxalate and $3.5 \mu\text{mol} (\text{cm tissue length})^{-1}$ of citrate were found. Given the high cytosolic pH, it may be expected that a rather stable anionic $\text{Al}(\text{Cit})^n$ complex will form (Borrmann and Seubert, 1999, Happel and Seubert, 2006). Given the high stability of the $\text{Al}(\text{Cit})^n$ complex it appears likely that the metal complex and not citrate and Al^{3+} are transported separately into the xylem sap.

Based on the results and the discussion we present a hypothesis on the transport of Al from the external solution to the xylem in buckwheat (Fig. 10). Initially (minutes), binding of Al^{3+} in the apoplast triggers the release of oxalate through a not yet identified anion permease. Oxalate complexes Al to form the 1:1 complex $\text{Al}(\text{Ox})^+$ which reduces Al binding to Al-sensitive apoplastic binding sites thus increasing Al resistance. However, this complex is not stable enough to fully protect the root tip from Al injury (inhibition of root elongation, callose formation). $\text{Al}(\text{Ox})^+$ is readily transported and accumulated in the symplast via a cation transporter (unknown) under metabolic control. Since the oxalate in the cytosol is constitutively high and increasing with Al accumulation, Al is present in the cytosol as $\text{Al}(\text{Ox}_2)^-$ and may be stored in the vacuoles even as $\text{Al}(\text{Ox}_3)^{3-}$. In the cytosol $\text{Al}(\text{Ox}_2)^-$ is transported through the endodermis into the central cylinder where a ligand exchange to citrate, leading a rather stable $\text{Al}(\text{Cit})^{2-}$ anionic complex, is taking place in the xylem parenchyma cells. This complex is loaded into the xylem through a metal-chelate transporter (unknown) again under metabolic control.

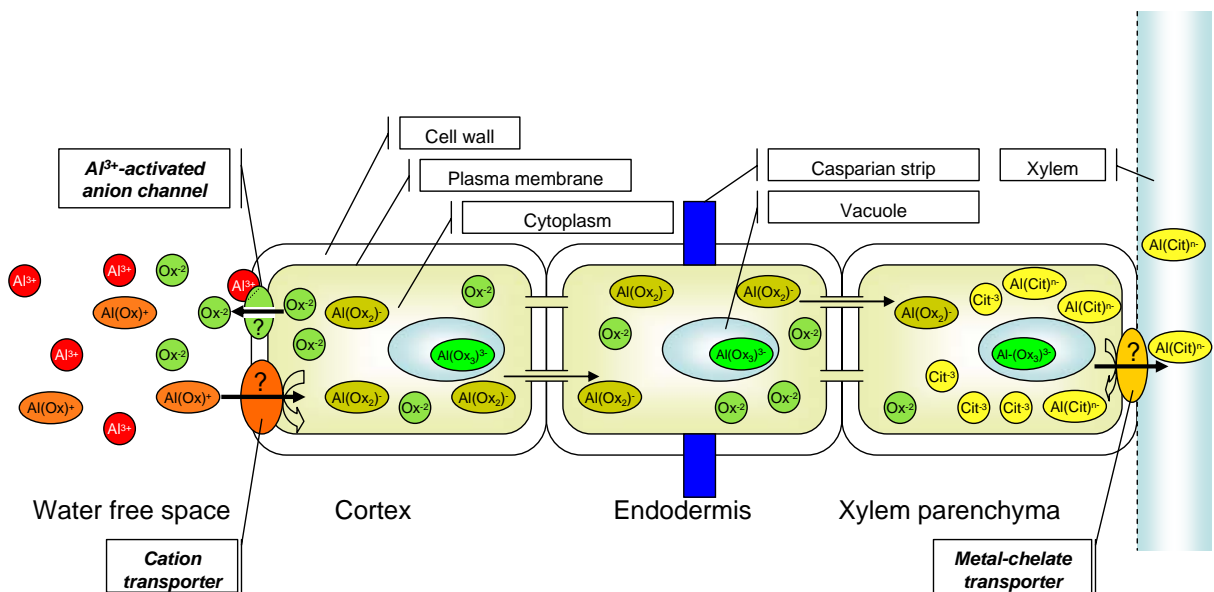


Figure 10. Hypothetical scheme for the transport of Al from the external solution to the xylem. For the explanation of the scheme refer to the discussion. The ? denotes unknown transporters/permeases.

We are aware of the fact that this hypothesis is still speculative. However, it appears to us important to clearly pinpoint the knowledge gaps at this point in order to better focus the physiological and molecular studies necessary to finally decipher Al accumulation in buckwheat and possibly other Al accumulators.

**Aluminium localisation in root tips of the aluminium-
accumulating plant species buckwheat (*Fagopyrum esculentum*
Moench)**

Benjamin Klug, André Specht and Walter J. Horst
(to be submitted)

Abstract

Aluminium (Al) toxicity is the main pedogenic factor limiting crop productivity world wide. Some crop species show high Al resistance either by exclusion of Al from uptake or tolerance of Al in the plant tissue. Buckwheat is known as Al-resistant and Al-accumulating plant species. The Al uptake process in the root tip in Al-accumulating plant species is not completely understood. For visualisation of Al uptake and accumulation fluorescent dyes are usually applied, but the specific staining conditions are not known. Results presented here reveal that these dyes are indeed able to track Al under Al accumulator-specific *in-situ* conditions. Morin allows staining of Al under presence of organic acid ligands. Morin showed higher sensitivity and competitiveness than lumogallion. LA-ICP-MS analysis of Al concentrations was an appropriate method for analysis of element distribution within cross sections of fresh root-tip material, particularly when compared with the Al staining method. Results clearly indicate that Al is highly mobile in radial direction from epidermal to stelar tissues. The root tip predominantly accumulates Al and the following root tip zone show a homogenous Al distribution within the whole root tip cross section. Hereafter follows a zone with enhanced xylem parenchyma Al contents. Distal root tip regions only fluoresce within single xylem vessels. Both, the fluorescent staining and LA-ICP-MS measurements revealed the same root Al accumulation pattern and the used calibration method for LA-ICP-MS allowed a precise quantitative Al determination.

Introduction

Organic acids play a major role in detoxifying aluminium (Al) in the root-tip apoplast (Al resistance by Al exclusion) or within the symplast and moreover in the Al accumulation processes in shoots (Al tolerance) (Ma *et al.*, 1998; Chapter I and II). This symplastic detoxification, compartmentation, and translocation are the most important tolerance-mediating processes. However, these processes require the Al transport through at least one membrane. Currently our knowledge concerning this membrane passage of Al through biological membranes is limited and not completely understood. These shortcomings may be primarily ascribed to the complex aqueous coordination chemistry of Al, its high affinity to O₂ donor compounds and the lack of affordable and appropriate stable isotopes (Taylor *et al.*, 2000). Therefore, Al was often detected by fluorescence microscopy and spectrometry. The fluorochromes morin and lumogallion form stable complexes with Al. The fluorescence emission of the chromophore-Al complexes have been used frequently for the determination and quantification of Al in freshwater, generally in biological samples, and extensively for the localization of Al in plant tissues, particularly in root tips (Ščančar and Milačič, 2006; Levesque *et al.*, 2000; Tanoi *et al.*, 2001; Ahn *et al.*, 2002; Gutierrez and Gehlen, 2002; Eticha *et al.*, 2005a; Jones *et al.*, 2006).

The formation of the morin-Al complex is strongly influenced by the binding stage of Al. Also the precise binding conditions of lumogallion are currently unknown. The correct assessment of the specific conditions underlying Al-dye complex formation is of particular importance, especially in the case of Al-accumulating plant species like buckwheat, where Al is supposed to be bound to organic acids.

The targeted staining of Al within roots of buckwheat could give further information about the uptake processes for Al. However, this requires information on specific dye-ligand interactions and subsequent responses in fluorescence emission. Browne *et al.* (1990b) stated that morin is a reagent with minimized disturbance. In that study the fluorescence of the Al-morin complex was directly related to Al³⁺ and Al-hydroxy complexes indicating that morin forms complexes only with inorganic monomeric Al species but not with organic acids (Lian *et al.*, 2003). The precise Al-morin complex formation and underlying stability constants remained unclear for a long time. It was reported that morin detects cell wall-bound Al (Ahn *et al.*, 2002), but Eticha *et al.* (2005a) unequivocally showed that morin could not stain cell wall-bound Al. The results of Eticha *et al.* support the conclusion that morin is not able to stain Al in high stability complexes (Lian *et al.*, 2003).

The aim of this study was to in-depth investigate the limitations and prospects of morin and lumogallion for staining Al. For this purpose the Al-accumulating plant species buckwheat was chosen which utilizes oxalate and citrate as main Al complexors in the plant tissue. The established staining method for Al gives further insights into the proposed radial symplastic pathway of Al within the buckwheat root-tip symplast (Chapter I and II). Furthermore, the method comparison of staining soluble Al species with the determination of total Al concentrations by LA- ICP-MS substantially contributed to unravelling Al-binding stages and ligand exchange processes during radial Al transport in the root tip.

Material and Methods

Plant Material

Buckwheat (*Fagopyrum esculentum* Moench) cultivar “Lifago” (Deutsche Saatveredelung AG, Lippstadt, Germany) was germinated in peat substrate containing 30% clay (Balster Einheitserdewerk GmbH, Fröndenberg, Germany). Plants were grown for 4 weeks in a green house at 25/20 °C day/night temperature. After this period of growth the shoots were cut 1 cm below the first node with adventitious root initials and additionally above the primary leaf to reduce transpiration. These shoot cuttings were transferred to low ionic strength nutrient solution with the following composition [μM]: 500 KNO_3 , 162 MgSO_4 , 30 KH_2PO_4 , 250 $\text{Ca}(\text{NO}_3)_2$, 8 H_3BO_3 , 0.2 CuSO_4 , 0.2 ZnSO_4 , 5 MnSO_4 , 0.2 $(\text{NH}_4)_6\text{Mo}_7\text{O}_{24}$, 50 NaCl , and 30 Fe-EDDHA for 4 days keeping the shoots at 100 % relative humidity (rH) until adventitious roots had emerged. The following day the plants were adapted to lower rH by reducing air humidification. Another day later the pH of the nutrient solution was reduced in three steps to 4.3 resulting in at least 12 h for adaptation to the low pH before the beginning of the Al treatment. Afterwards, the plants were transferred to a simplified nutrient solution (500 μM CaCl_2 , 8 μM H_3BO_3 ; 100 μM K_2SO_4 , pH 4.3) supplemented either with 0 μM or 75 μM AlCl_3 . A concentration of 75 μM AlCl_3 was verified to inhibit root-growth between 50 and 60% (Chapter II) and to activate Al exclusion and tolerance mechanisms (Chapter I and II). The pH was controlled frequently and, when necessary, re-adjusted to 4.3 using 0.1 M HCl or 0.1 KOH added drop wise under vigorous stirring. The nutrient solution was aerated continuously.

Fluorometry

To systematically clarify the complex formation of Al with lumogallion and morin either the Al concentration at a given dye concentration or the dye concentration at a given Al concentration was varied (Fig. 2, Fig. 3). The aim of this experiment was to identify the effect of different Al: organic ligand ratios (e.g. 1:1 and 1:3; Al/ligand) on the fluorescence yield. The Al:organic ligand solutions were incubated at 25 °C for 0.5 h. Morin (33 mM in DMSO) was added to a final concentration of 30 µM at pH 4.8. The Al-morin complex formation was done at 25 °C for 1 h under continuous shaking. Lumogallion (1 mM in 0.1 M sodium acetate buffer, pH 5.2) was added to a final concentration of 30 µM lumogallion in the sample. After 1 h incubation at 60 °C on an incubation shaker the fluorescence was measured with a Hitachi spectrofluorometer (F2000, Hitachi Ltd., Tokyo, Japan)

Microscopy

Adventitious root tips of buckwheat plants treated with 75 µM Al for 24 h were excised 10 mm behind the root tip and immediately placed in chilled (4°C), Al-free simplified nutrient (see above) solution for 10 minutes. The tips were then fixed with the distal end facing down in an upright position on a Tissue-tek® (OCT Compound for Cryostat Sectioning, Sakura Finetek Europe B.V., Zoeterwoude, Netherlands) base, frozen at -20 °C, and then completely embedded in Tissue-tek®. These root-tip preparations were sectioned by means of a cryo microtome (Leica 2800 E Frigocut, Microtome Cryostat, Leica Microsystems GmbH, Wetzlar, Germany) at a chamber temperature of -20 °C and object temperature of -16 °C. Cross sections (16 µm) were positioned in a drop of morin and placed under a Zeiss Axioscope microscope (Zeiss, Axioscope, Jena, Germany), equipped with epifluorescence illumination (Mercury lamp, HBO 50W). The filter settings were: Band pass filter BP 395–440 nm (exciter), beam splitter FT 510 nm, and long-wave pass filter LP 515 nm (emitter) (Browne *et al.*, 1990b). Pictures were taken with digital camera (Axio Vison, Zeiss, Jena, Germany)

In a second approach, apical 0 - 5, 6 – 10, 11 – 15, 16 – 20, 21 – 25 and 26 – 30 mm adventitious root sections from plants treated with 75 µM Al for 0,5, 4 or 24 h were embedded in 5 % (w/v) low-gelling point agarose (Fluka, Buchs, Switzerland) at 35 °C. These embedded root tips were free-hand sectioned using a razor blade. Slices of agarose-embedded root tips were placed on microscopy glass slides, and a drop of morin solution was placed on the agarose-embedded free-hand root-tip sections. After an incubation time of 5 min, samples

were examined as described before. Photographs were taken from each root tip zone from at least 12 replications derived from individual root tips. A representative picture was selected and depicted in Figure 5.

Laser-ablation ICP-MS

For LA-ICP-MS an additional experiment was carried out. Plants were treated for 24 h with 75 μM AlCl_3 in 18 L simplified nutrient solution (500 μM CaCl_2 , 8 μM H_3BO_3 ; 100 μM K_2SO_4 , pH 4.3). Root tips were excised and sectioned in 5 mm segments (0-5, 6-10, 11-15, 16-20, 21-25 and 26-30 mm behind the tip). These segments were embedded into 5 % (w/v) low-gelling point agarose (Fluka, Buchs, Switzerland) at 35 °C. These embedded root tips were free-hand sectioned using a razor blade. Slices of agarose and embedded root tips were placed on microscopy glass slides. The embedding of root tips in agarose served as protection against desiccation in the argon flow and, furthermore, represented an adequate physical fixation with regard to occurring forces during the laser ablation process. Tissues were ablated using a solid state NYAG-laser (UP193 SS, New Wave Research Co. Ltd., Cambridge, England). The laser beam was adjusted to a diameter of 20 μm and 50 % energy (1.82 J cm^{-1}). The ablation chamber, coupled to the ICP-MS torch via a polyethylene tube, was filled with argon as carrier gas at a flow rate of 0.3 L min^{-1} . After passing the chamber the flow rate was accelerated to 1.15 L min^{-1} . The ^{13}C signal served as internal standard. ^{13}C and ^{27}Al signals were detected using the quadrupole ICP-MS (7500 CX, Agilent Technologies, Santa Clara, USA). Table 1 summarizes further specifications of ICP-MS settings.

Table 1: ICP-MS tuning parameters

Plasma conditions:	
RF power	1300 W
RF matching	1.7 V
Sample depth	5.8 mm
Torch-H	0.2 mm
Torch-V	0.7 mm
Carrier gas	0.3 L min^{-1}
Make-up gas	1.15 L min^{-1}

For the calibration of the Al signal a mixture of pectin and agar was used. The C content in the dry matter of 46 % and a dry matter content of 2.9% were adjusted to finally match the conditions of freshly harvested adventitious buckwheat root tip cuttings. Aluminium was added to the calibration mixture (0, 5 and 10 nmol (10 mm-root tip)⁻¹) to simulate Al concentrations typically observed in root tips. After polymerization slices were cut and placed on microscopy glass slides. Calibration was performed as described for the samples (see above). Every cross section was visually captured by microscopy so that the individual diameter of each replicate could be determined by the laser ablation system software (Version 11) (New Wave Research Inc., Fremont, CA, USA). The diameter was sectored into 4 circular regions and one central region (Fig. 1). These regions are termed in the following as: I - central cylinder, II - endodermal, III - inner cortical, IV - outer cortical, V - epidermal tissues.

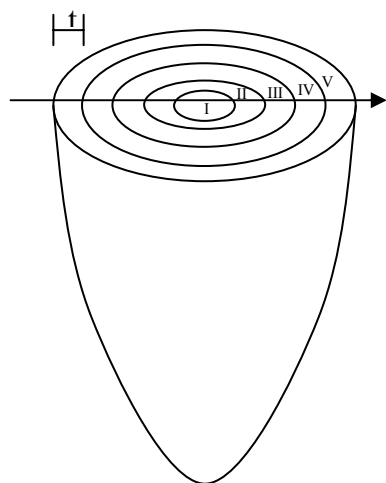


Figure 1. Schematic overview over the laser-ablation path across the root-tip cross-section. The arrow represents the diametric ablation path. I-V represent tissue areas with the same radial share (t) of the whole radius.

Results

Morin and lumogallion showed increasing fluorescence intensity with increasing Al concentrations when recommended dye concentrations (30 μM Morin; 60 μM Lumogallion) were applied (data not shown). Both dyes highly effectively stained Al in the 1-10 μM concentration range. However, variation of the dye concentrations at a given Al concentration, which yielded approximately the same fluorescence intensity for both dyes, showed an optimum curve for morin (Fig. 2a) with an optimum of 30 μM . The highest lumogallion fluorescence intensity was already measured at 10 μM dye application. Further increasing the lumogallion concentrations (10-40 μM) did not significantly change in fluorescence.

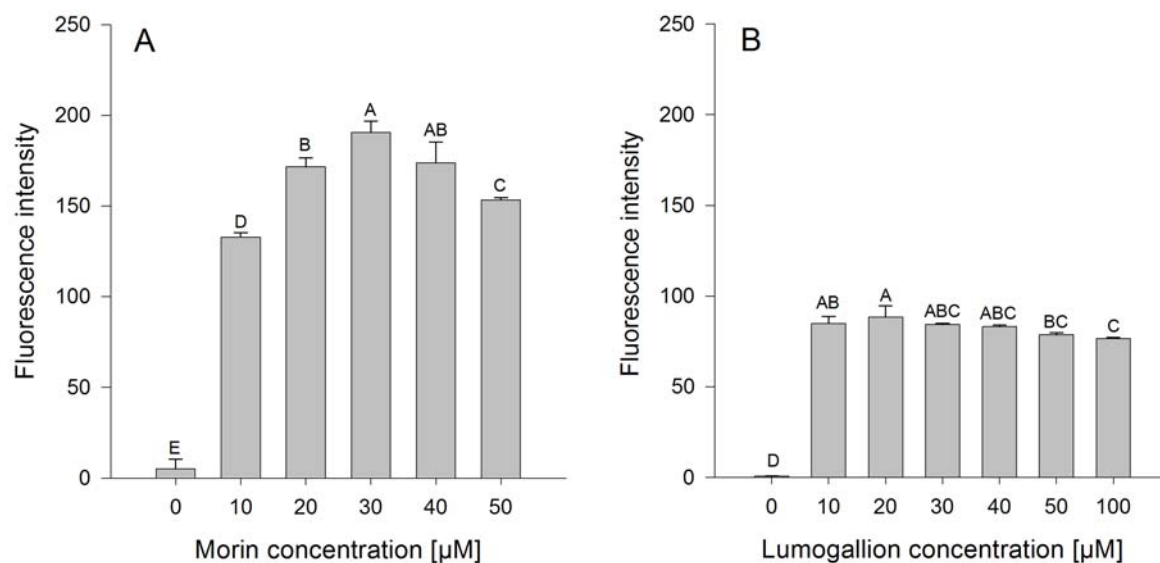


Figure 2. Effect of morin and lumogallion concentrations on the fluorescence intensity at given Al concentrations. For morin (A) 6 μM and for lumogallion (B) 3 μM AlCl_3 were added. Morin was measured at pH 4.8 at excitation and emission wavelengths of 418 nm and 502 nm. Lumogallion was measured at pH 5.2 in 0.1 M acetate buffer at excitation and emission wavelengths of 507 nm and 567 nm. Bars represent means \pm SD, $n = 4$. Different letters denote a significant difference (Tukey test $P < 0.05$).

The effectiveness of both dyes to stain Al was tested by using a dye concentration of 30 μM (Fig. 3). Increasing the Al concentration increased the fluorescence intensity steeper for morin than for lumogallion. Moreover, the fluorescence of the Al: morin complex responded to increasing Al concentrations up to 120 μM whereas the maximum of the Al: lumogallion fluorescence was already reached at 50 μM Al. Therefore, morin showed higher fluorescence intensities than lumogallion irrespective of the Al concentration. The Al-morin fluorescence-intensity significantly increased throughout the tested concentration range. However, lower Al than dye concentrations (3-10 μM) did not significantly differ in the case of morin but had significantly higher fluorescence intensities compared to lumogallion.

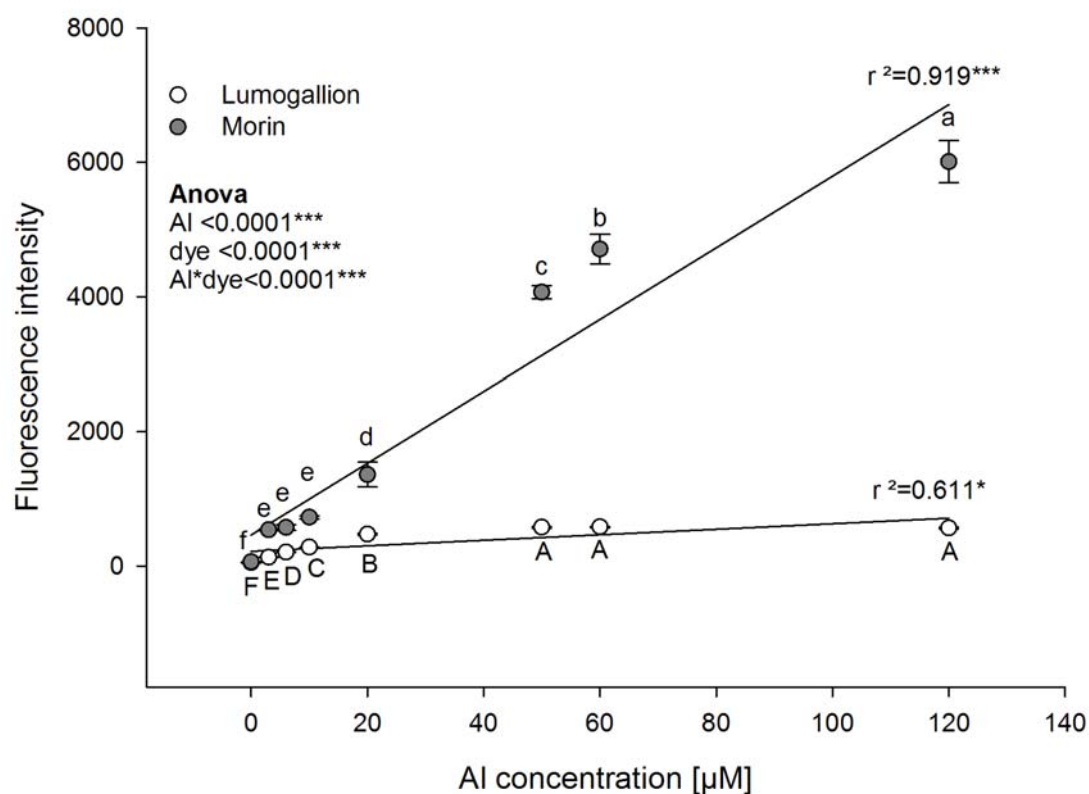


Figure 3. Regression analysis of fluorescence intensities of Al-lumogallion and Al-morin complexes at given dye concentration (30 μM) at varied Al concentrations. Lumogallion measurements were done at pH 5.2 in 0.1 M acetate buffer at excitation and emission wavelengths of 507 nm and 567 nm, respectively. Morin measurements were done at pH 4.8 at excitation and emission wavelengths of 418 nm and 502 nm, respectively. Symbols represent means \pm SD, $n = 4$. Morin samples at 50, 60 and 120 μM Al were diluted appropriately to remain in the effective measuring range. Different letters denote a significant statistical difference (Tukey test $P < 0.05$). Capital letters denote the comparison between different Al-lumogallion fluorescence-intensities. Lower case letters denote the comparison between different Al-morin fluorescence-intensities.

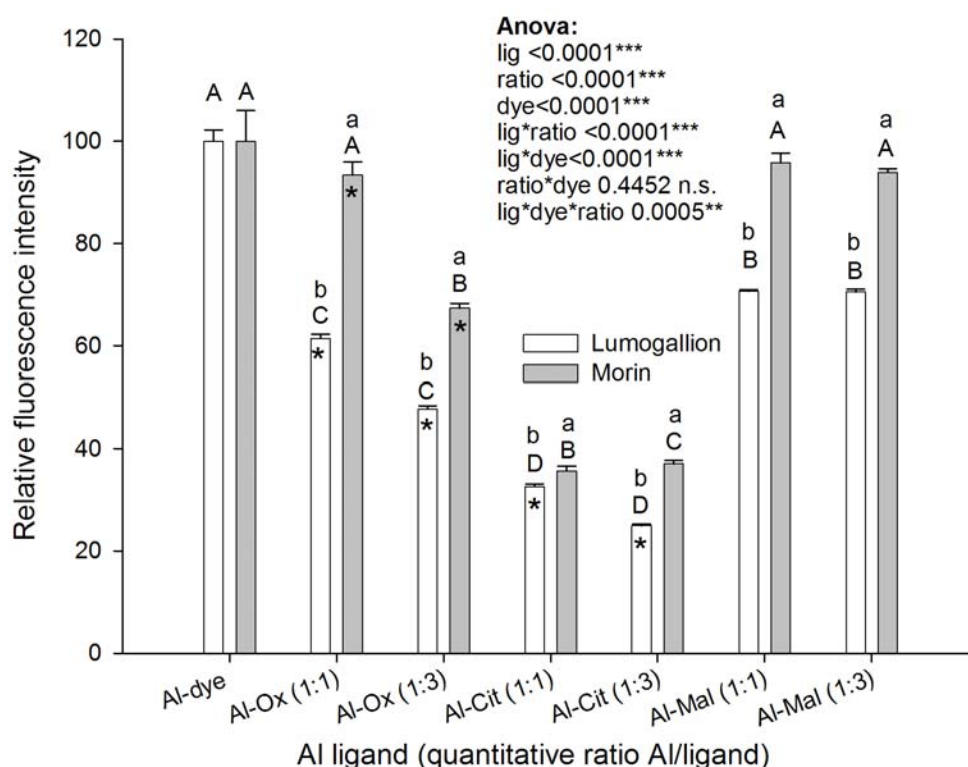


Figure 4: Relative fluorescence intensity of lumogallion and morin as affected by the presence of the Al-chelating ligands oxalate, citrate, and malate in different ratios. Morin: AlCl_3 6 μM , morin 30 μM , organic acids 6 or 18 μM , pH 4.8; detection at excitation and emission wave lengths 418 nm and 502 nm, respectively. Lumogallion: AlCl_3 20 μM , lumogallion 60 μM , organic acids 20 or 60 μM , buffered by sodium acetate buffer pH 5.2; detection at excitation and emission wavelengths of 507 nm and 567 nm, respectively. Bars represent means \pm SD; $n = 4$. Different letters denote significant statistical differences (Tukey test $P < 0.05$). Capital letters denote the comparison between different ligands within one dye and one ratio. Lower case letters denote the comparison between lumogallion and morin within one ligand and one ratio. The asterisks mark significant differences between different ratios within one dye and one ligand.

Aluminium is known to be detoxified in Al-resistant and accumulating plant species by organic acids, but the effectiveness of Al staining dyes in the presence of organic acids was not systematically analysed, yet. Therefore, we studied the Al dye fluorescence in the presence of citrate, malate and oxalate (Fig. 4). Thereby, the effect of different Al:ligand ratios was analyzed, too. The fluorescence intensity of the Al-dye complex without any competing ligand was set to 100 %. Oxalate in a ratio of 1:1 and particularly of 1:3 (Al:oxalate) reduced the fluorescence intensity of the Al-lumogallion complex stronger than that of the Al-morin complex (Fig. 4). The presence of citrate greatly reduced the fluorescence intensity of both Al-dye complexes even at the 1:1 ratio. The presence of malate

only reduced the fluorescence intensity of the Al-lumogallion but not of the Al-morin complex.

The results indicate that morin is more sensitive and competitive than lumogallion particularly in the presence of competing ligands such as oxalate and citrate. Therefore, we used morin for further Al *in-situ* localisation experiments in buckwheat root-tip cross-sections. Morin staining of buckwheat root cross-sections after treatment with 75 μM Al from 0.5 – 24 h revealed that significant concentrations of Al were present across the whole cross section as early as 0.5 h of Al treatment (Fig. 5A). Only a very low autofluorescence was detected in the cross sections not treated with Al (Fig. 5C).

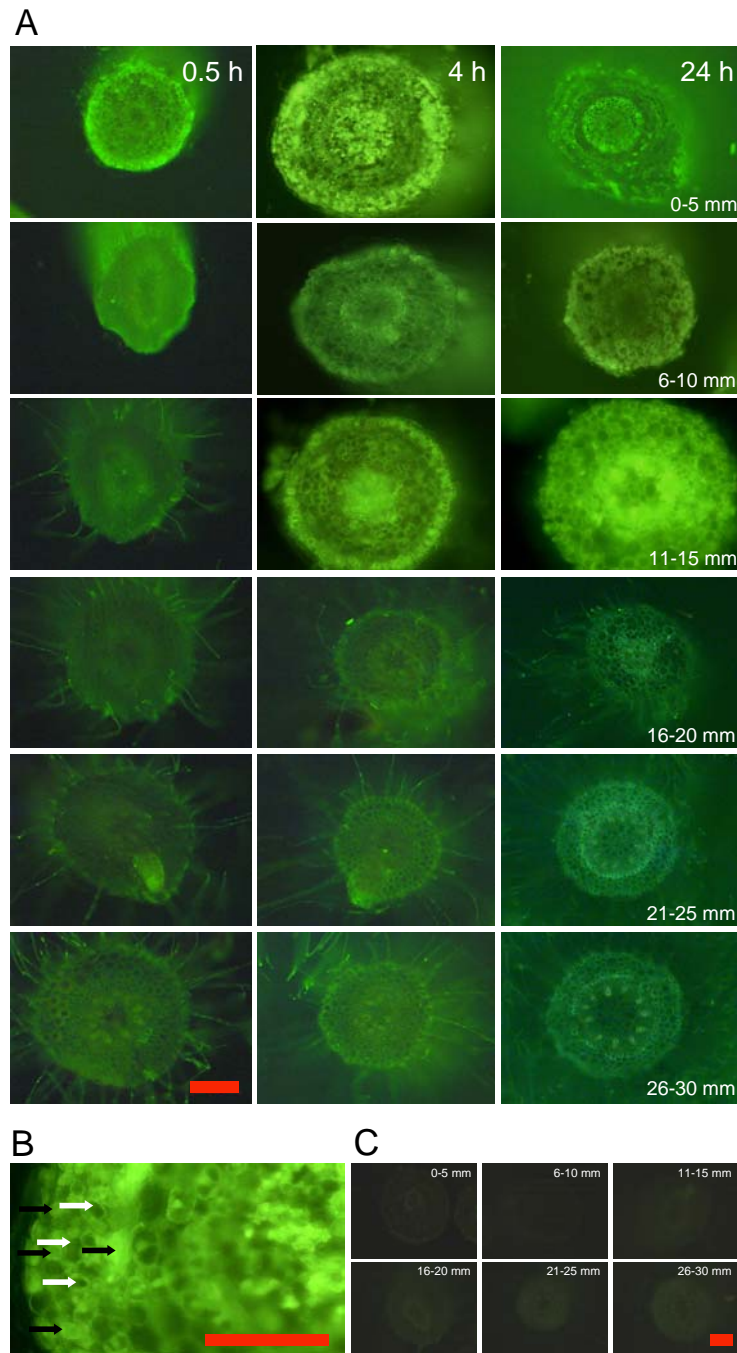


Figure 5. (A) Fluorescence images of the Al-morin complex in buckwheat root-tip cross-sections obtained from increasing distance from the root tip (columns) and with increasing Al treatment duration (rows) ($75 \mu\text{M AlCl}_3$ for 0.5, 4, and 24 h). Samples were intact root tips in simplified nutrient solution ($500 \mu\text{M CaCl}_2$, $100 \mu\text{M K}_2\text{SO}_4$, $8 \mu\text{M H}_3\text{BO}_3$, pH 4.3). Scale bar represents $200 \mu\text{m}$ at 100-fold magnification. (B) Close up of the 0-5 mm cross section. Black arrows indicate cells with intact cytoplasm showing high symplastic fluorescence intensities, white arrows indicate during preparation damaged and empty cells. Scale bars represents $100 \mu\text{m}$ at 200 fold magnification. (C) Cross sections of the control treatment (24 h) with increasing distance from the root tip stained by morin. Scale bar represents $200 \mu\text{m}$ at 100 fold magnification.

The typical and characteristic distribution of Al within the 0-5 mm zone, which is considered to be symplastic due to the fluorescence localisation, was already obtained after 0.5 h of Al treatment (Fig. 5B). Thereby, the highest symplastic Al concentrations were found in the outer cortical cell layers (Fig. 5A). Also the 6-10 mm zone exhibited high symplastic Al contents. However, the fluorescence contribution of the epidermal layers relative to the total fluorescence of the cross section decreased with increasing distance from the root tip. The 11-15 mm root zone showed lower symplastic Al concentrations compared with more apical zones. The most pronounced Al-morin fluorescence-intensity was located in the stelar and endodermal root-tip tissues. In this zone the first root-hairs developed. This Al distribution pattern also remained in the 16-20 mm zone, where root hairs were still present. The following 21-30 mm root zones showed both a low fluorescence intensity, where only single xylem vessels exhibited a marked Al-morin fluorescence. In the 21-25 mm zone first lateral roots emerged in the majority of the samples. Compared to the primary root these lateral root tips were stained more intensively. The areas surrounding the lateral roots, particularly where the endodermal cell layer is penetrated, the fluorescence exhibited no enhanced intensity.

With increasing Al-treatment duration (4 h) the distribution pattern of Al within the first root section remained principally unchanged compared to 0.5 h Al treatment; the epidermal zones again showed the highest fluorescence. Furthermore, the 11 – 15 mm zone exhibited enhanced endodermal and stelar Al contents not only in xylem vessels but also in xylem parenchyma cells. The Al-morin fluorescence in a distance of 16-20 mm after 4 h Al treatment showed a comparable distribution pattern as found after 0.5 h of treatment duration, too. The same is true for the sections from zone 5 and 6 (21 - 30 mm). Lateral root formation and long root hairs existed in both zones. In this section a homogenous and low fluorescence intensity throughout the whole cross section was obtained with increased fluorescence intensities only in single xylem vessels.

The pattern of fluorescence was principally also not changed under prolonged Al supply (24 h): (1) the sections from 11-15 mm from the root tip showed higher endodermal fluorescence, (2) cross sections from the 16-20 mm zone had higher stelar Al contents, whereas the outer cell layer showed almost no Al-morin fluorescence, (3) sections from both distal zones (21-25 and 26-30 mm) exhibited bright Al-morin fluorescence only in single vessels.

After extended Al treatment durations for 24 h the root morphology and the Al distribution in the apical 0-5 mm zone was studied more detailed. Sections were prepared from more precisely defined distances from the tip by using a cryo-microtom. Al treatment led to severe

morphological distortions at the root apex. Epidermal and outer cortical layers seem to be detached from the root (Fig. 4).

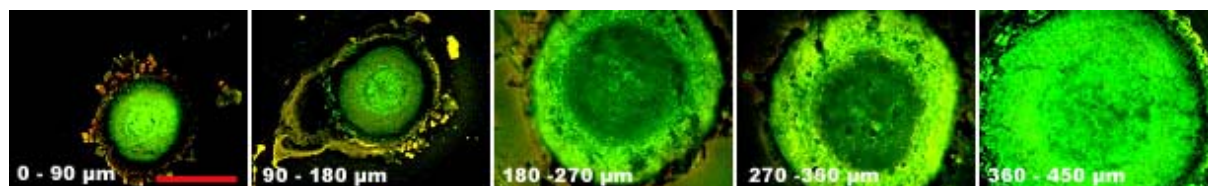


Figure 6. Root tip cross section in a distance of 0-450 μm from the root tip after 24 h treatment duration in simplified nutrient solution (500 μM CaCl_2 , 100 μM K_2SO_4 , 8 μM H_3BO_3 , 75 μM AlCl_3 , pH 4.3).

In a distance of 0-180 μm the Al-morin fluorescence was homogeneously distributed throughout the cross sections with higher fluorescence yields in the 0 – 90 μm zone compared to the 90 – 180 μm section. Microscopy of the subsequent regions from 180 to 360 μm revealed that Al accumulated predominantly in the outer cortical cell layers. The homogenous Al distribution obtained by free hand sectioning in a distance of 6-10 mm (see above) here already appeared in a distance of >360 μm .

The qualitative information about the Al distribution in distinct root tip sections as obtained by morin staining was further substantiated by LA-ICP-MS measurements. Figure 7 shows a representative Al quantification pattern expressed as Al-signal intensity in distances of 0-5 (Fig. 7A) and 11-15 mm (Fig. 7B) from the root tip. This signal intensity was calibrated (see “Materials and Methods” section) and either calculated as Al concentration (Fig. 8) or as Al contents (Fig. 9). The latter was extrapolated by the geometric volume of 4 hollow cylinders and one central cylinder (see Fig 1). To do so, the root diameter of each root cross-section was divided by 9 resulting in 4 circular zones (two times) and one central zone (see Fig. 1) which are in the following termed as epidermal layer, outer and inner cortical layer, endodermal layer and stelar tissue. By including a ^{13}C signal as internal calibrator it was possible to determine that the ^{27}Al signal was obtained at constant ^{13}C intensities. This is important to ensure because the amount of material ablated by the laser beam has to be constant and should not be affected by different cell-layer integrities or other artefacts, e.g. different absorptions of laser energy due to variable colours of tissues along the ablation path. Cross sections prepared from the apical root tip (0-5 mm) showed high ^{27}Al peaks in the epidermal and outer cortical cell layer and lower intensities in the inner root-tip tissues. Despite comparable carbon contents in the 11-15 mm root tip zone compared to the remaining

root zones the Al distribution followed a different pattern, e.g. compared to the apical root tip. Here, the highest Al concentrations were found in the inner root-tip tissues, whereas the outer cell layers exhibited rather low fluorescence intensities.

Using the described calibration method the LA-ICP-MS results (Fig. 8 & 9), which were assigned to the individual root tissue layers, have been statistically evaluated. Indeed, there were statistically significant differences between the individual tissue layers and root-tip zones. Beginning at the root tip the cross section was characterized by enhanced Al concentrations in the epidermal and outer cortical cell layers (Fig. 8). This Al distribution pattern completely changed in the adjacent 5 mm zone to a homogenous Al distribution. In the next 5 mm section the highest Al concentration was found in the stelar tissue and, at least in tendency, also in the endodermal layer. This trend was also found in the 16-20 mm zone, where the elevated Al concentration in the endodermis became more pronounced. Both following zones were characterized by low and more homogenously distributed Al with slightly lower Al concentrations in outer than inner root tip tissue layers.

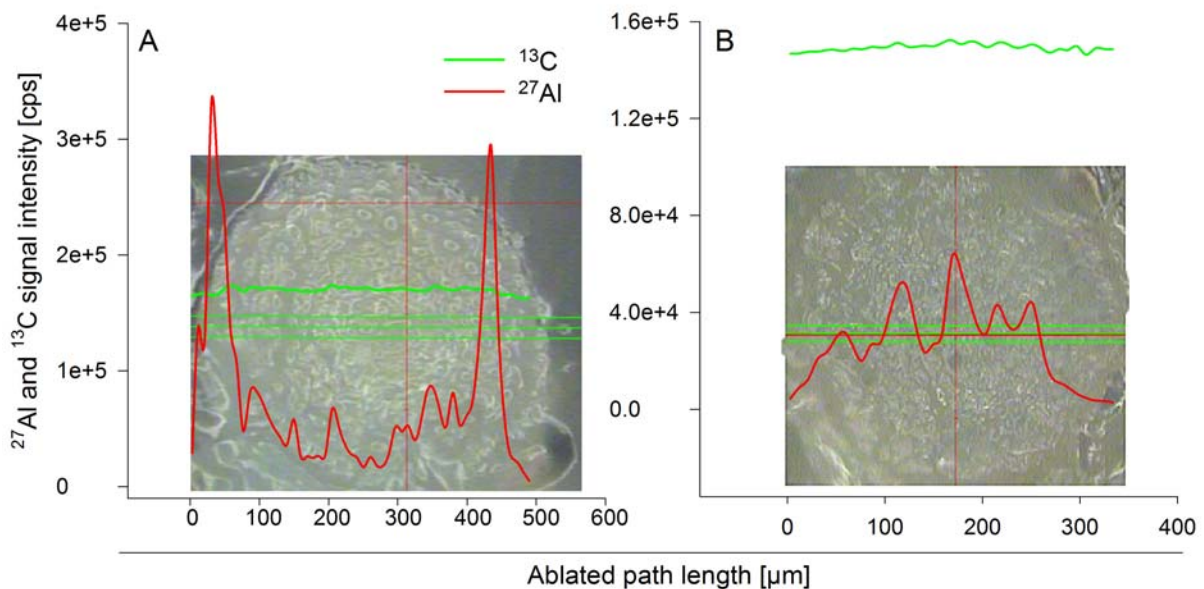


Figure 7. ^{27}Al and ^{13}C signal intensities of a representative cross section prepared from the 0-5 mm (A) and 11-15 mm (B) zone after 24 h treatment with $75\ \mu\text{M}$ Al in minimal nutrient solution ($500\ \mu\text{M}$ CaCl_2 , $100\ \mu\text{M}$ K_2SO_4 , $8\ \mu\text{M}$ H_3BO_3 , pH 4.3). The red line represents the ^{27}Al the green line the ^{13}C (internal standard) signal intensities. The triple green line represents the ablated path. The Al signal intensity was normalized by calculating means over the ablated path length of $10\ \mu\text{m}$ and 1 sec ablation time. The laser beam was adjusted to a diameter of $20\ \mu\text{m}$ and 50 % energy resulting in $1.82\ \text{J cm}^{-1}$.

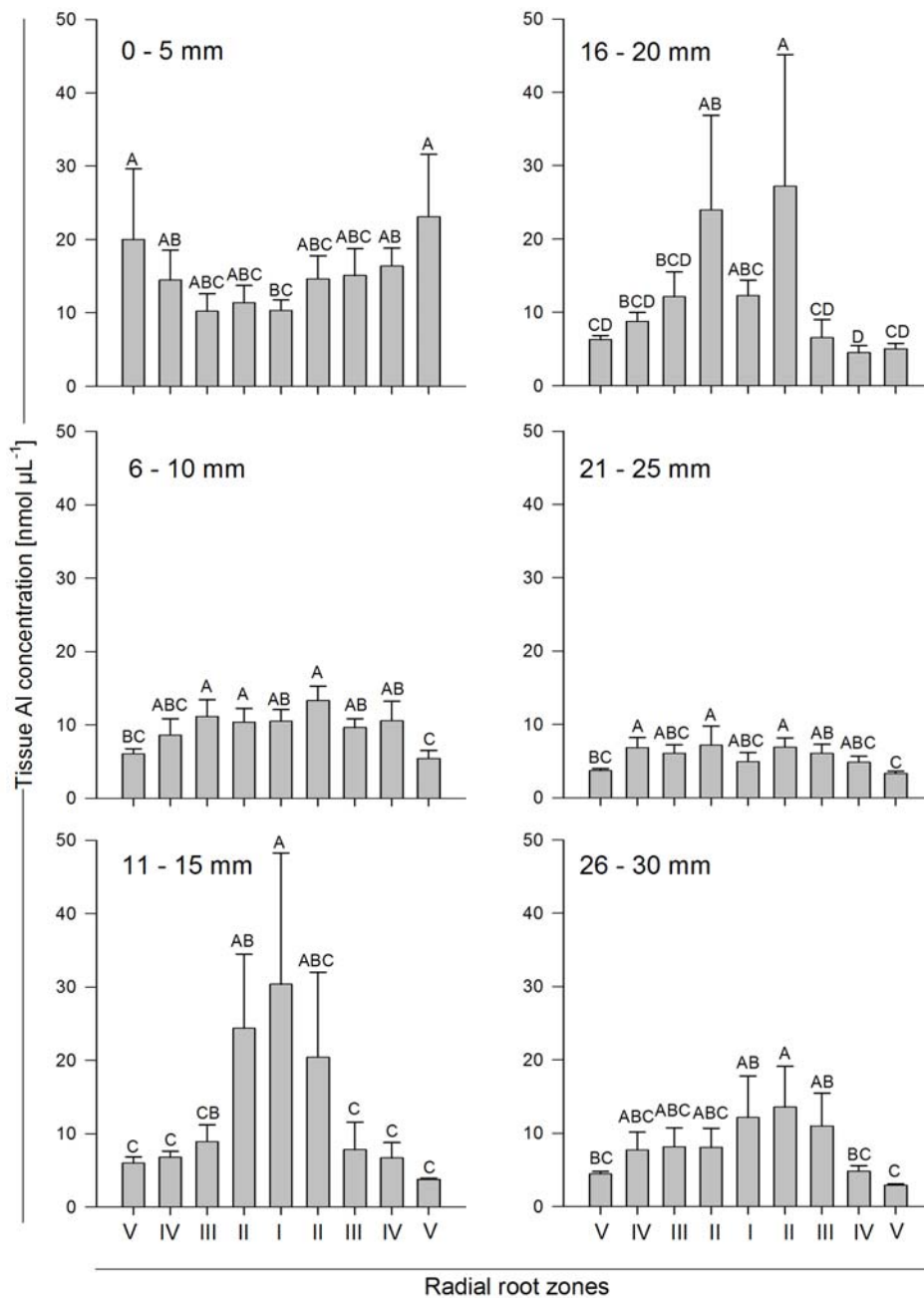


Figure 8. Aluminium concentrations in different root tip tissue layers (bars) and different distances from the root tip (graphs) after 24 h treatment with 75 μM Al in simplified nutrient solution (500 μM CaCl_2 , 100 μM K_2SO_4 , 8 μM H_3BO_3 , pH 4.3). Root tip tissue layers were defined by dividing the root diameter into nine even regions. Data were calibrated by ablation of agarose/pectin mixture with the same carbon and water contents than buckwheat root tips and defined Al contents. The Al signal intensity was normalized by calculation means over ablated path length of 10 μm and 1 sec ablation time. Bars represent means of 6 ablated cross-section diameters of 6 different root tips per 5 mm zone. Different letters denote significant statistical differences (Tukey test $P < 0.05$).

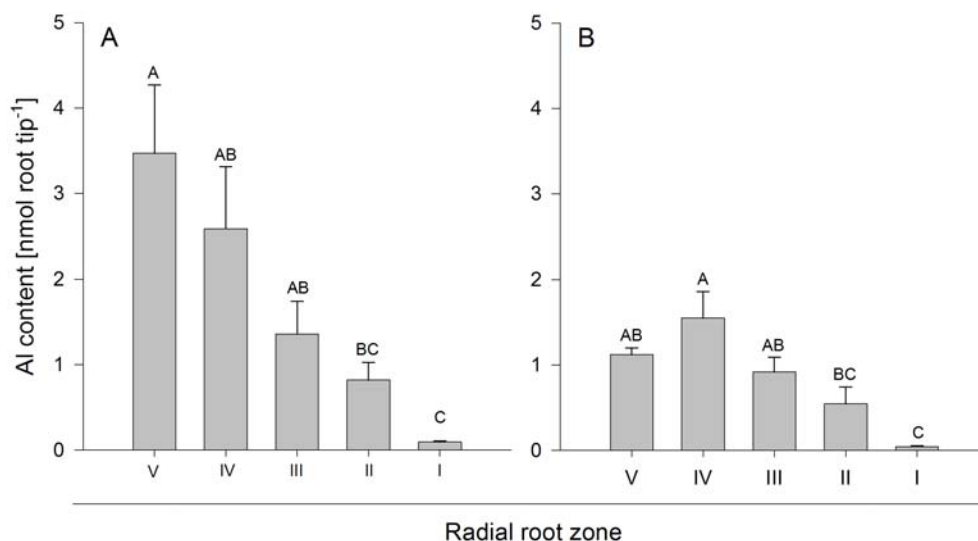


Figure 9. Aluminium contents of different hollow cylinders and one central cylinder of a buckwheat adventitious root tip calculated by the volume in distances of 0-5 (A) and 6-10 (B) mm from the tip after 24 h of 75 μM Al treatment in minimal nutrient solution (500 μM CaCl_2 , 100 μM K_2SO_4 , 8 μM H_3BO_3 , pH 4.3). Root tip hollow cylinders (II to V) and central cylinder (I) were calculated by previously defined nine even regions in the root diameter (see Figure 1). Data were calibrated by ablation of agarose/pectin mixture with the same carbon and water content than buckwheat root tips and defined Al contents. The Al signal intensity was normalized by calculating means over ablated path length of 10 μm and 1 sec ablation time. Bars represent means of 6 ablated cross section diameters of 6 different root tips per root tip zone. Different letters denote significant statistical differences (Tukey test $P < 0.05$).

The analysed Al concentrations from Figure 8 were multiplied with specifically calculated volumes of the previously defined nine sections (Figure 1) forming four artificial hollow cylinders and one central cylinder (in Figure 9 depicted as I-V). By doing so it, was possible to calculate Al contents of specific root zones. When compared to the 5 – 10 mm root zone the 0-5 mm zone had higher Al contents in the cortical root zones systematically decreasing in the inner parts of the cross section (Fig. 9A and B). Segments from more distal root tip zones exhibited a comparable Al distribution as obtained from the 5-10 mm root zone (data not shown). Thus, the total Al contents decrease at least in tendency with increasing distance from the root tip. This Al distribution is a consequence of specific volumes of the individual root cylinders from zone V to zone I. The outer cell layers (V) represent already 40% and, therefore, the greatest part of the total root tip volume whereas the central stelar cylinder comprises only about 1.2 % of the total root tip volume. Results presented here clearly show that the Al analysis by the LA-ICP-MS technology is a useful tool for the evaluation of conventional total root-tip Al analyses. Taken together, the apical 5 mm root tip zone

accumulated 8 nmol (root tip)⁻¹ whereas the subapical root tip zone (6-10 mm) showed lower Al contents of about 3.5 nmol (root tip)⁻¹. These calculated values range within the same magnitude as compared to the bulk root tip analysis (about 10 nmol (10 mm root tip)⁻¹).

Discussion

The use of dyes for mineral element-specific in-situ staining allows qualitative but not quantitative statements on the element distribution within tissues. However, knowledge of binding-stages and stability constants of dye-complexes facilitate both relative quantification and qualitative statements. One example may illustrate this: if an Al measurement revealed high amounts of Al in a specific tissue, but the same tissue exhibits only low levels of fluorescence, the conclusion can be drawn that Al is very stably complexed in complexes which are characterised by higher stability constants than the Al-dye complex. A spectrofluorometric clarification of specific Al species by a complex-specific shift of emitted wavelength spectra failed to provide further information about Al-ligand interactions (Brauer, 2001). Both morin and lumogallion are known to detect Al with high sensitivity, but information on their specific efficiencies is currently inconsistent. The lumogallion staining method was reported to be more sensitive for Al detection than the use of morin at least in confocal microscope applications (Kataoka *et al.*, 1997). In contrast, in this study the morin staining method showed a higher sensitivity. However, lumogallion was reported to have a high stability constant, a measure of the stability of complex, ($\log k$ 7.76) over pH ranges from 2 to 5.7 (Shuman, 1992), whereas the stability constant of the Al-morin complex was reported to be slightly lower ($\log k$ of 6.47). Unfortunately, in that study the effect of pH was not further specified (Katyral and Prakash, 1977). Later, Saarl and Steltz (1983) showed a clear pH dependency of Al-morin complex formation and fluorescence intensity, which might explain the discrepancy in stability constants and underestimation of the Al-morin stability. Differences in the sensitivity of both dyes may result from the coordination chemistry of the dye-Al complex formation. Lian *et al.* (2003) reported that morin is able to form complexes in 1:1 and 2:1 ratios. Results about the stoichiometric relations were also not unequivocally clarified. The data of Saarl and Seltz (1983) suggest a 1:1 morin-Al complex formation. However, the ratio was determined using an immobilization method leaving some questions about the reagent: morin binding properties. Furthermore, complexes with a 1:1 and 1:2 and/or 1:3 (Al/morin) stoichiometry were reported (Brown *et al.*, 1990; Sawada *et al.*, 1978). The specific complex formation was concentration-dependent where low total morin concentrations (near 1 μ M) yielded 1:1 species.

Al-lumogallion complexes at a ratio of 1:1 were frequently reported (Kataoka *et al.*, 1997; Hoshino and Yotsuyanagi, 1985). Results presented in Figure 2 revealed that the fluorescence intensity of a 1:1 Al-dye ratio increases with increasing proportion of morin, whereas the fluorescence decreases when the lumogallion concentration is increased. Indeed, the Al-morin complex had increased fluorescence emission when the morin:Al ratio was switched to 1:3. Thus, one Al ion can be complexed by one, two or even three molecules of morin thereby gradually increasing fluorescence intensity of the complex. However, when the 1:3 ratio is exceeded, the fluorescence intensity decreases. In contrast, lumogallion exhibited the maximal fluorescence intensity at a 1:1 concentration ratio indicating that lumogallion indeed binds Al exclusively in a ratio of 1:1.

Lumogallion has been shown to detect Al even in the presence of organic ligands (Shuman, 1992; Sutheimer and Cabaniss, 1995). However, the chemical form of Al, which is detected by morin, remains unknown so far, although water quality analyses suggest that the morin complex is weak in comparison to other typical ligands like oxalate (Lian *et al.*, 2003). The authors concluded that morin can only detect Al in its inorganic forms (e.g. Al^{3+} , $\text{Al}(\text{OH})_2^+$) (Lian *et al.*, 2003). These contradictory results (on the one hand morin stains Al more efficiently than lumogallion, on the other hand morin is not able to form a complex with Al in the presence of organic acid anions) led us to conduct a test series to clarify the competitiveness of each dye to stain Al in the presence of Al-complexing carboxylic acid anions. Compared to lumogallion morin emitted higher fluorescence intensities than lumogallion. Furthermore, the presence of oxalic, malic or citric acid anions reduced the fluorescence intensity less pronounced, e.g. malate hardly affected the fluorescence intensity of the Al-morin complex, but significantly reduced the one of the Al-lumogallion complex. Oxalate only slightly reduced the fluorescence intensity of the Al morin but more of the Al lumogallion complex. Nevertheless, the presence of citrate greatly reduced the fluorescence of both Al-dye complexes. The autofluorescence of Al and the individual dyes alone was negligible (less than 5 %). Therefore, we conclude from these results that the use of morin is an appropriate method to track Al on its symplastic way in Al accumulating plant species. This is a prerequisite particularly for investigations in buckwheat, where Al is symplastically detoxified by oxalate (Ma and Hiradate, 2001; Chapter I and II).

In this study a LA-ICP-MS based method was developed for the tissue-specific *in-situ* measurement and calibration of Al concentrations and contents. The method was successfully evaluated by comparing the results of the new method with the conventional bulk-root tip Al

determination, since, indeed, the extrapolation of tissue-specific Al contents to whole bulk root tip levels yielded comparable Al contents as analysed directly in total root tips.

Al uptake in Al accumulating plant species like buckwheat showed that Al is translocated in substantial amounts in above ground plant organs (Ma and Hiradate, 2000 Shen *et al.*, 2006). As a prerequisite, Al needs to be predominantly symplastically transferred in the root tip in radial direction towards the stelar tissues; the apoplast appears to play only a minor role in Al diffusion (Chapter I). However, the exact transport route of Al radial direction was not analysed so far.

Therefore, in this study special emphasis was put on the localization of Al within the root and the characterisation of Al tolerance-mediating processes, which primary take place in the root. To do so, morin was chosen as appropriate Al staining dye owning the necessary capabilities (1) to stain Al within the root tip tissue and (2) to track Al and its transport in the roots. Preliminary results on buckwheat revealed that Al is primarily accumulated in the apical region of the root tip, while the subapical region was characterized by the highest Al translocation efficiency (Chapter I). Further analyses substantiated that Al is highly mobile in the radial direction in buckwheat root tips. Different root tip zones showed different radial Al localisation patterns in the individual root-tip tissues (Fig. 1).

Al primarily accumulates in the outer cortical layers of the apical root tip (0-5 mm) (see Fig. 5, 7 and 9). Additionally, the apical region but not the remaining regions visually showed the highest symplastic Al-morin fluorescence contribution in relation to the total Al distribution (Fig. 5b) irrespective of the treatment duration, which suggests that this Al content is either not transported by induced-translocation processes or this distribution represents an equilibrium concentration of accumulation and translocation. Our data suggest that Al is in this root zone not exclusively bound to fixed charges in the pectic cell wall matrix but is also present in a soluble, morin detectable binding stage (Eticha *et al.*, 2005a), which is in buckwheat mostly detoxified by oxalate (Chapter II). This may be further underlined by morin-Al staining experiments since this zone also exhibited the highest fluorescence indicating a high accumulation of soluble Al. The root cell-wall has a high capacity for Al sorption (Zhang and Taylor, 1990). Jones *et al.* (2006) suggested that one origin of apoplastic fluorescence development, apart from pectic bound Al and symplastically located Al, correlates with the saturation of binding sites of the cell wall. Hence, in buckwheat either the fixed negative charges appear to be saturated already after very short (<0.5 h) Al treatment durations or the concentration of soluble, oxalate-detoxified Al is rather high. The latter

possibility requires the activation of oxalate exudation without delay after starting the Al treatment.

In contrast to the apical root zone the 6 -10 mm zone showed a homogenous Al distribution (Fig. 5a) especially after 0.5 and 4 h of Al treatment. The 24 h treatment additionally showed a pronounced Al-morin fluorescence in the outer cortical cell layers. This predominant Al accumulation in these cell layers is not in accordance with the Al distribution pattern obtained by LA-ICP-MS radial ablation of the cross sections. This discrepancy indicates a difference in total Al contents analysed by ICP-MS and the soluble Al concentration within the morin-stained root tissue. It is possible that Al in outer cell layers is less stable detoxified as Al-(Ox)₁⁺ complex. This would be in line with analysis on water free space fluid, where Al and oxalate were found primarily in a 1:1 ratio (Chapter II). This Al-(Ox)₁⁺ complex reduces the Al-morin fluorescence only slightly (Fig. 4). While the Al is translocated to the central cylinder the complex shifts to a Al:Ox ratio of 1:2. This complex form showed a pronounced reduction in fluorescence (Fig. 4). Indeed, a 1:2 Al-Oxalate complex was found in the root tip symplast of adventitious buckwheat root tips (Chapter II). It appears that the WFSF of the outer cortical cell layers is infiltrated by Al, which is detoxified by oxalate in a 1:1 ratio. Then, changing the complex ratio to Al-(Ox)₂⁻ while moving to the central cylinder leads to decreased fluorescence intensities. Therefore, we propose that the outer cortical cell layers, particularly in the 6 -10 mm distance from the root tip, are the primary zone of Al entrance into the symplast. At the same time it appears to be the location of most pronounced Al uptake (Chapter I), because the uptake promoting Al:Oxalate gradients are present in the same zone (Chapter II).

Zone 3 (11-15 mm) and zone 4 (16-20 mm) were characterized by enhanced fluorescence (Fig. 5) as well as by increased total Al contents (Fig. 8) in the central cylinder region. Here, Al was primarily localized in the outer layers of the central cylinder suggesting that xylem parenchyma cells accumulate the majority of Al in this distance from the root tip. Surgically dissected cortical and stele tissues from distal root tip zones revealed that substantial Al concentrations of 2 nmol (mg fresh matter)⁻¹ were found in the stele tissue as compared to 4 nmol (mg fresh matter)⁻¹ of cortical tissues. However, the analysis of bulk Al contents in the cortical tissue represents a mixture of apoplastic and symplastic Al, whereas the stele tissue represents Al contents only representing symplastic Al, because these tissues are disconnected from Al located in the cortical apoplast by the endodermis. It is known that the xylem parenchyma cells are primarily responsible for xylem loading of ions for long distance transport (Köhler and Raschke, 2007). Furthermore, it was shown that specific transporters,

for example the boron transporter BOR1, are restricted to pericycle cells (Takano *et al.*, 2002). Pericycle cells comprise the outermost part of the stele, which showed the brightest Al-induced fluorescence in our study. Obviously, these cells play a key role in xylem loading of Al in buckwheat roots. The unloading of parenchymal cells in a distance of 10-20 mm is characterized by fluorescence of single xylem vessels in distal regions (20-30 mm) of the root tip. These zones seem to transport Al so that their Al accumulation and contribution to xylem-Al loading is rather low.

The entrance of metals (e.g. Al) into the central cylinder and subsequent xylem loading points to the capability of cells to unload metals from the cytoplasm. This capability primarily determines the difference between metal non-accumulating and tolerant accumulator plant species (Klein *et al.*, 2008). Currently the majority of the plant species characterized in terms of Al uptake was investigated by Al-specific dye fluorescence, which was observed in the outer cortex and epidermal regions (Kataoka *et al.*, 1997; Jones *et al.*, 2006). Thus, root radial Al transport processes into the stele do not take place in Al non-accumulating plant species. Usually, mineral transport processes are controlled by transporters, channels or plasmodesmata. In the case of K⁺ cortical cells are dominated by a K⁺ channel particularly facilitating K⁺ influx into the root cell, whereas in stelar cells K⁺ channels are prevalent, which enable the K⁺ efflux into the apoplast / xylem (Roberts and Tester 1995). However, such clear differences were not obtained in *Arabidopsis* cortical and stelar tissues (Maathuis *et al.*, 1998). Some authors questioned the role of K⁺ efflux channels in xylem sap K⁺ loading (Kochian & Lucas 1988, Lacombe *et al.*, 2000). They preferred a process mediated by active transport systems (Kochian & Lucas 1988) or a combination of active and passive xylem loading processes (Lacombe *et al.*, 2000). However, not only the orientation of transporter could be decisive for translocation processes but also tissue specific expression patterns. A promoter::GUS localization study on a Zn transporter of *Arabidopsis* (AtZIP4::Gus) revealed that the transporter expressed in the stele indicating that this Zn transporter is associated with uptake into the root cell symplast rather than with xylem loading (Milner and Kochian 2008). The process of Al translocation needs further clarification including investigations on molecular mechanisms specifically e.g. proteins involved Al transport. To do so, this study clearly showed that future analyses should take tissue-specific longitudinal & radial local differences into account.

Differences in aluminium accumulation and resistance between genotypes of the genus *Fagopyrum*

Benjamin Klug; Thomas Kirchner; Walter J. Horst
(To be submitted)

Abstract

Aluminum (Al) toxicity is a major factor reducing crop productivity worldwide. There is a broad variation of inter- and intra-specific Al resistance. Whereas the Al resistance mechanism are generally well explored in Al-excluding plant species, Al resistance through Al accumulation and Al tolerance is not yet well understood. Therefore, we screened a set of 94 genotypes of the Al accumulator genus *Fagopyrum* with special emphasis on *Fagopyrum esculentum* Moench, with the objective to identify genotypes with greatly differing Al accumulation capacity. The genotypes were grown in Al-enriched peat-based substrate for 30 days. Based on the Al concentration of the xylem sap which varied by a factor of 5, only quantitative but no qualitative genotypic differences in Al accumulation could be identified. Aluminium and the citrate concentrations and Al and Fe concentrations in the xylem sap were positively correlated suggesting that Fe and Al are loaded into and transported in the xylem by related mechanisms. In a nutrient solution experiment using selected genotypes differing in Al and citrate concentrations in the xylem sap, inhibition of root elongation by Al, root oxalate-exudation and Al accumulation proved to be highly significantly correlated. This confirms that Al activated oxalate exudation is a prerequisite for both, protection of the root apoplast from Al injury (Al exclusion) and Al accumulation (Al tolerance).

Introduction

Aluminium toxicity is one of the major constraints for crop production on acid soils (Kochian *et al.*, 2004). The area of acid soils is further increasing and represents significant percentages of the world's arable lands. There is evidence that long-term acidification induced by changes in widespread not sustainable land use and consequent vegetative succession is one reason for further acidification (Krug and Frink, 1983). Therefore, the physiological understanding of mechanisms participating in the adaptation of plants to acid soils and concomitant mineral toxicities is of major importance. However, the knowledge in external resistance mechanisms is far advanced, but the understanding of internal tolerance mechanisms in this context still lacks a fast progress. It has been often screened and bred for Al resistance of important crop plants (Horst *et al.*, 1997; Yang *et al.*, 2000; Zhou *et al.*, 2007), including Al-excluding and Al-accumulating plant species. However in buckwheat the result revealed that the exudation of chelating ligands, particularly oxalate, is not directly associated with genotypic differences in Al resistance (Peng *et al.*, 2003). This might indicate, especially in Al-accumulating and highly resistant plant species that not only Al-exclusion mechanisms were exclusively responsible for the high resistance, but also tolerance mechanisms are significantly participating. However, the analysis of the contribution and the incorporation of internal Al-tolerance mechanism-analysis in screening experiments was up to now completely omitted.

The mechanisms restricting Al uptake and translocation in non-Al accumulators are proposed by Ma and Hiradate (2000) which emphasize the role of cell wall composition (Martin, 1986), the Al chemistry and the development of hydrophobic bands, which may restrict apoplastic transport pathways. It is known for Al accumulating buckwheat that Al is transported symplastically, which circumvents the physical apoplastic barrier, the casparian strip (Ma *et al.*, 1998; Chapter I and II). Furthermore, it is known that Al is complexed symplastically by oxalate anions which allows soluble binding stages of Al and thus the precipitation of Al-hydroxides in the near neutral pH of the cytoplasm is avoided. Therefore, Al could be actively transported into root cell vacuoles as well as by long-distance transport via xylem flow into the vacuoles of leaf cells.

Therefore, the aim of the study was to screen a set of buckwheat (*Fagopyrum esculentum*, *Fagopyrum tartaricum* and *Fagopyrum acutatum*) genotypes and species for differences in the above ground Al accumulation. Furthermore, this study will facilitate an evaluation of the interrelation of resistance and internal tolerance. The analysis of the ionome in the xylem sap of buckwheat will give first hints for the association of other ions to the transport of Al and

provides indications for related transport mechanisms. However, the identification of either qualitatively or quantitatively differing genotypes and the restriction of tolerance and accumulation mediating mechanisms to a number of possibly related genes will provide the opportunity for first genotype related transcriptomic insights in the Al accumulation of buckwheat and the understanding of Al-tolerance and translocation in buckwheat.

Material and Methods

Plant material

The experiments were conducted using the reference cultivar of buckwheat *Fagopyrum esculentum* “Lifago” known from former experiments (Chapter I and II) which was provided by Deutsche Saatveredelung AG (Lippstadt, Germany). Additionally, a set of 94 *Fagopyrum* accessions was kindly provided by the gene bank of the Leibniz Institute of Plant Genetics and Crop Plant Research (IPK, Gatersleben, Germany). These *Fagopyrum* accessions included various genotypes of *Fagopyrum esculentum* Moench var. *Esculentum*; *Fagopyrum esculentum* Moench var. *Emarginatum* (Roth) Alef.; *Fagopyrum tataricum* (L.) Gaertn. and *Fagopyrum acutatum* (Lehm.) Mansf. ex Hammer. The overall genetic origin of these genotypes includes Europe and Asia (see S1). For the analysis of Al resistance mechanisms in a nutrient solution experimental approach genotypes from the species *Fagopyrum esculentum* Moench with differing Al translocation patterns were chosen.

Plant cultivation

Plants were sown into peat-based substrate containing 30 % clay without the addition of Al, because Al toxicity should not interfere during the process of germination. In the following 4 weeks of cultivation Al was added in 4 steps each consisting 2 g $\text{Al}_2(\text{SO}_4)_3 \cdot 18\text{H}_2\text{O}$ resulting in 8 g of $\text{Al}_2(\text{SO}_4)_3 \cdot 18\text{H}_2\text{O}$ per L substrate. This amount was determined based on a substrate-specific Al-buffer curve, as usually performed for the production of blue coloured *Hydrangea macrophylla* (Naumann and Horst, 2003), with a target pH of the aqueous substrate extract of 4.3. The reference cultivar “Lifago” was additionally exposed to various Al concentrations (0; 2; 4; 6 and 8 g of $\text{Al}_2(\text{SO}_4)_3 \cdot 18\text{H}_2\text{O}$ per L substrate) to evaluate the response of the plant to increasing Al supply. Three plants were grown in each pot, containing 1 L of substrate for four weeks. Samples of these three plants were generally combined to one composite sample.

The experimental design was a randomized block design with three replicates. Plants were grown in a greenhouse at 20 °C at daytime and 18 °C during the night.

Substrate analysis

The pH, the concentration of soluble total and monomeric Al and mineral nutrients in the substrate were determined in a 1:3 water extract after 1 day incubation of the substrate at room temperature. The extracts were passed through a filter with a pore size of 0.45 µm. Al and mineral nutrients were determined by optical inductively coupled plasma-emission spectroscopy (Spectro Analytical Instruments GmbH, Kleve, Germany). Monomeric Al concentration was determined following the method of Kerven *et al.* (1989) using aluminon as dye for Al and spectrophotometric measurement of the Al-aluminon complex extinction at 532 nm.

Genotypic comparison in nutrient solution

Genotypes with differential Al accumulation capabilities were chosen for further investigations in a nutrient solution experiment. Plants were grown for 4 weeks in a green house at 25/20 °C day/night temperature. After this period of growth the shoots were cut 1 cm below the first node with adventitious root initials and additionally above the primary leaf to reduce transpiration. These shoot cuttings were transferred to low ionic strength nutrient solution with the following composition [µM]: 500 KNO₃, 162 MgSO₄, 30 KH₂PO₄, 250 Ca(NO₃)₂, 8 H₃BO₃, 0.2 CuSO₄, 0.2 ZnSO₄, 5 MnSO₄, 0.2 (NH₄)₆Mo₇O₂₄, 50 NaCl, and 30 Fe-EDDHA for 4 days keeping the shoots at 100 % relative humidity (rH) until adventitious roots had emerged. The following day the plants were adapted to lower rH by reducing air humidity. Plants were then grown for 2 weeks in nutrient solution. Afterwards, the pH of the nutrient solution was reduced in three steps to 4.3 resulting in at least 12 h for adaptation to the low pH before the beginning of the Al treatment (+/- 75 µM AlCl₃ at pH 4.3). The Al treatment was performed in simplified nutrient solution, containing 500 µM CaCl₂, 100 µM K₂SO₄ and 8 µM H₃BO₃ to avoid mineral interactions during that short-term Al treatment.

Sampling of xylem sap

Sampling of xylem sap was performed following the method described by Ma and Hiradate (2000) with some modifications. The stem was severed 2 cm above the root. The cut surface

was rinsed with ddH₂O and blotted off. The xylem sap was collected for not more than 0.5 h to yield reliable data on concentrations of solutes in the xylem sap. The xylem sap was collected in 1 mL micro-pipette tips which were trimmed to fit the cut stem. The volumes of the exudates were determined by 1000 µL micropipettes. Exudates were directly frozen in liquid N₂.

Mineral element analysis

Mineral element contents in the bulk-leaf tissue were determined in the primary leaf after dry ashing at 480 °C for 8 h, dissolving the ash in concentrated 1:3 diluted HNO₃, and then diluting (1:10 v/v) with ddH₂O. Measurements were carried out by optical inductively coupled plasma-emission spectroscopy (Spectro Analytical Instruments GmbH, Kleve, Germany). The Al concentration in the xylem sap was determined after appropriate dilution with ddH₂O by graphite furnace atomic absorption spectrometry (GF-AAS). The composition of other minerals in the xylem sap was performed after dilution by applying inductively coupled plasma-emission mass spectrometry (7500 CX, Agilent Technologies, Santa Clara, USA).

Determination of organic acids

The organic acid (OA) concentrations in the root exudates as well as in the xylem sap were measured by isocratic High Pressure Liquid Chromatography (HPLC, Kroma System 3000, Kontron Instruments, Munich, Germany). The OAs were injected through a 20 µl loop-injector (Auto-sampler 360) of the HPLC, separating different OAs on an Aminex HPX-87H (300 x 7.8 mm) column (BioRad, Laboratories, Richmond, California, USA), supplemented with a cation H⁺ micro-guard cartridge, using 10 mM perchloric acid as eluant at a flow rate of 0.5 ml per minute, at a constant temperature of 35 °C (Oven 480), and 74 hPa of atmospheric pressure. Measurements were performed at a wavelength $\lambda = 214$ nm (UV Detector 320). Prior to the analysis of exuded OA the nutrient solution samples were exchanged using a cation exchange column (Hydrochloric form) (AG® 50W-X8; BioRad; Life science group; Hercules; CA) followed by concentration to dryness via centrifugal evaporation.

Results

Supplementation of the substrate with $\text{Al}_2(\text{SO}_4)_3 \cdot 18\text{H}_2\text{O}$ significantly decreased the pH of the substrate due to its acidic hydrolysis (Fig. 1). An Al supply of 8 g lead to pH values of 4.2-4.0. Increasing total soluble and monomeric Al concentrations were found after exceeding an Al application of 6 g. Neither the pH reduction, nor the Al supplementation to the substrate lead to reduced growth of the reference buckwheat cultivar “Lifago” (Fig. 2)

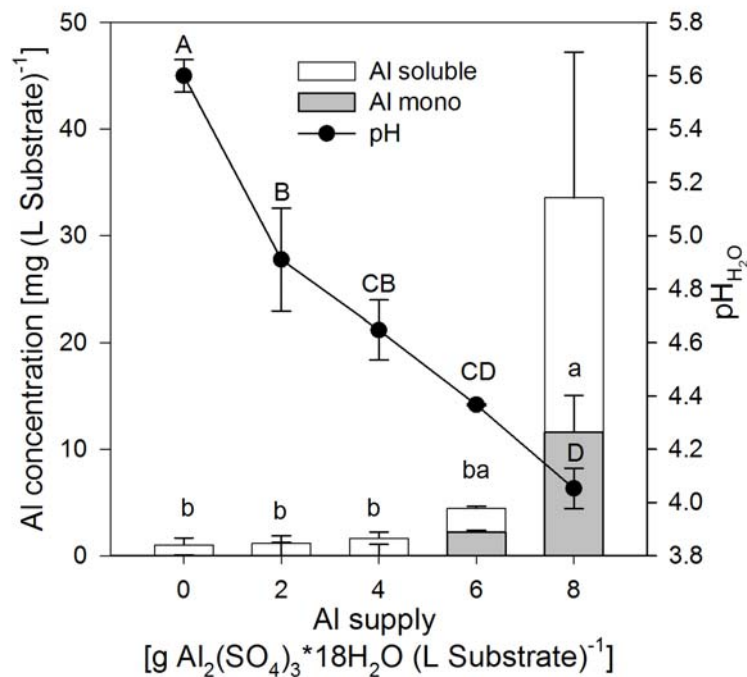


Figure 1. Total soluble, monomeric Al concentrations and substrate pH in the aqueous substrate extract as affected by increasing supply of $\text{Al}_2(\text{SO}_4)_3 \cdot 18\text{H}_2\text{O}$. Bars represent means \pm SE, $n = 3$. Different letters denote significant differences between treatment durations at $P < 0.05$. Capital letters denote the comparison between different pH values. Lower-case characters represent the comparison between different monomeric Al concentrations.

The vegetative shoot growth of the buckwheat cultivar “Lifago” (Fig. 2) was not affected and showed an equivalent height irrespective of the applied Al amount. Increasing amounts of Al, especially the 8 g treatment did not induce obvious mineral deficiency symptoms. Furthermore, a ranking of root growth in the substrate showed most pronounced root growth at 4 g Al (data not shown). This might indicate optimum growth conditions under the presence of small amounts of Al. These conditions are also indicated, albeit not significantly in the shoot fresh matter production of the reference cultivar (Fig. 3).



Figure 2. Vegetative shoot growth of buckwheat cv. “Lifago” as affected by increasing $\text{Al}_2(\text{SO}_4)_3 \cdot 18 \text{H}_2\text{O}$ supply in 1 L substrate, four weeks after germination.

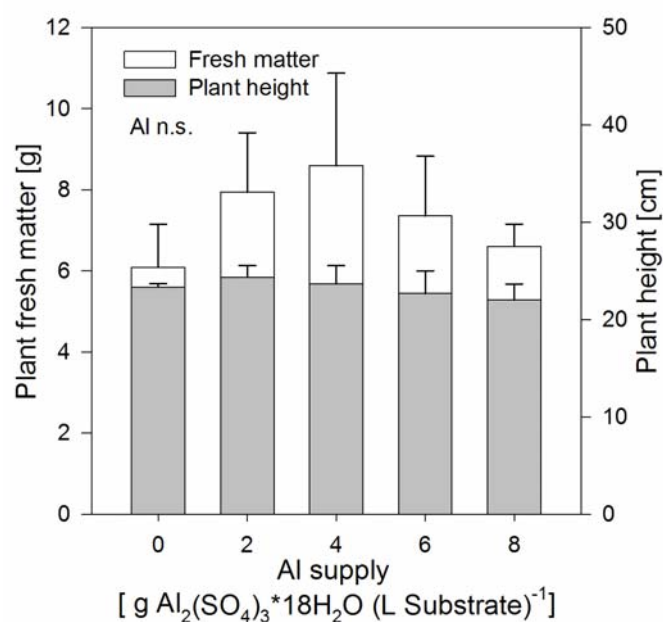


Figure 3. Plant fresh matter production and height of buckwheat cv. “Lifago” as affected by increasing $\text{Al}_2(\text{SO}_4)_3 \cdot 18 \text{H}_2\text{O}$ supply in 1 L substrate three weeks after germination. Bars represent means \pm SE, $n = 3$. For the ANOVA ns denotes nonsignificance at $P=0.05$.

The soil analysis revealed that monomeric Al species (Al^{3+}) are present at an Al supply of 8 g. However, the above ground Al accumulation, analyzed in the primary leaf, showed enhanced Al contents at an Al application of 2 g compared to the control (0 g) (Fig. 4A). The Al accumulation increased with increasing Al supply. The phosphorus concentration in the primary leaf was not affected by increasing Al supply (data not shown), but decreased significantly in the soil solution. The Al concentration in the xylem sap exceeded 200 μM at Al applications of 4 g and reached values of about 400 μM at an Al application of 6 g. The Al concentration did not further increase beyond an Al supply exceeding 6 g. The citrate and Al

concentrations in the xylem sap are significantly correlated (Fig. 4B) and the citrate concentration increased with increasing Al concentrations.

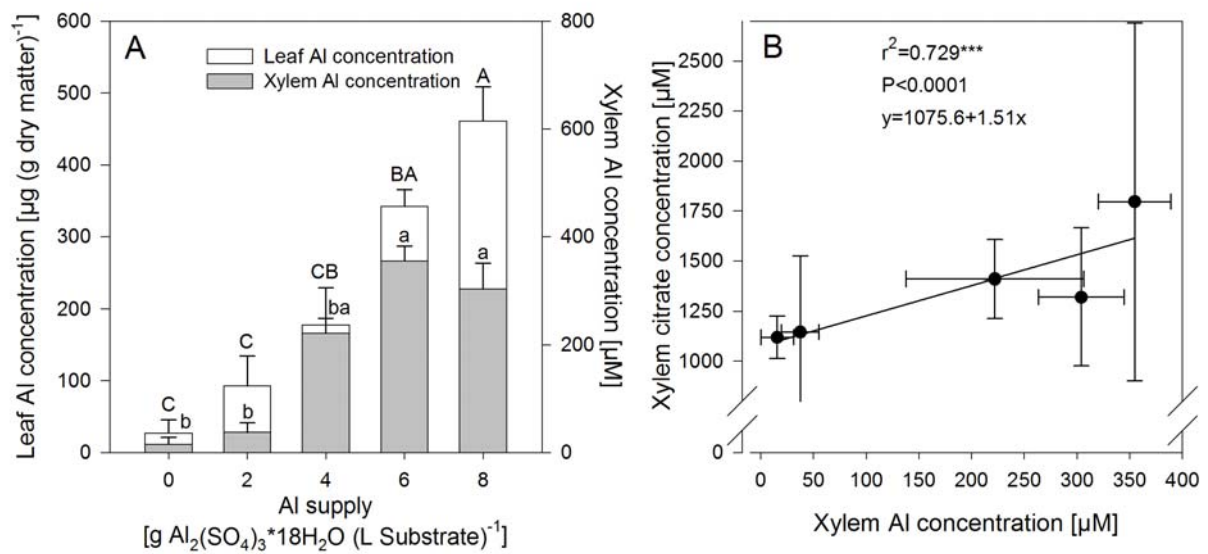


Figure 4. A: Leaf Al concentration and xylem sap Al concentration of buckwheat cv. “Lifago” as affected by increasing Al₂(SO₄)₃*18 H₂O supply in 1 L substrate three weeks after germination. Bars represent means +/- SE, n = 3. Different letters denote significant differences between treatment durations at $P = 0.05$. Capital letters denote the comparison between different leaf Al concentrations. Lower-case characters represent the comparison between different xylem Al concentrations. B: Correlation of Al and citrate concentrations in the xylem sap as affected by increasing Al₂(SO₄)₃*18 H₂O supply in 1 L substrate three weeks after germination. For the ANOVA *** denote levels of significance at $P = 0.001$.

The xylem-sap Al concentrations responded to the applied Al concentration. Therefore, we chose the xylem sap concentration and an Al supply of 8 g Al₂(SO₄)₃*18 H₂O for the comparison of different buckwheat genotypes with different growth habits. The fresh matter production of the 94 genotypes varied between 5 and 10 g per plant. The number of leafs per plant was particularly highly variable. Some genotypes showed about 5 times more leaves than others. The analysis of Al accumulation in the primary leaf might have been affected by different numbers of leafs for different genotypes (data not shown) which could have led to dilution or concentration effects in the analysed leaf tissue, thus the xylem Al concentration appeared to be a more suitable parameter for the characterization of the Al accumulation capacity.

The comparison of the xylem Al concentration revealed a broad genotypic variation of the Al concentration in the xylem sap (Figure 5). However, we were not able to identify one buckwheat genotype that did not translocate Al into the shoot. The Al concentration of genotypes with the most pronounced Al translocation capacity are reaching concentrations of

about 450 μM Al in the xylem sap. The lowest concentrations, which were found in some genotypes, were in the range of 100 μM at the same supply of Al.

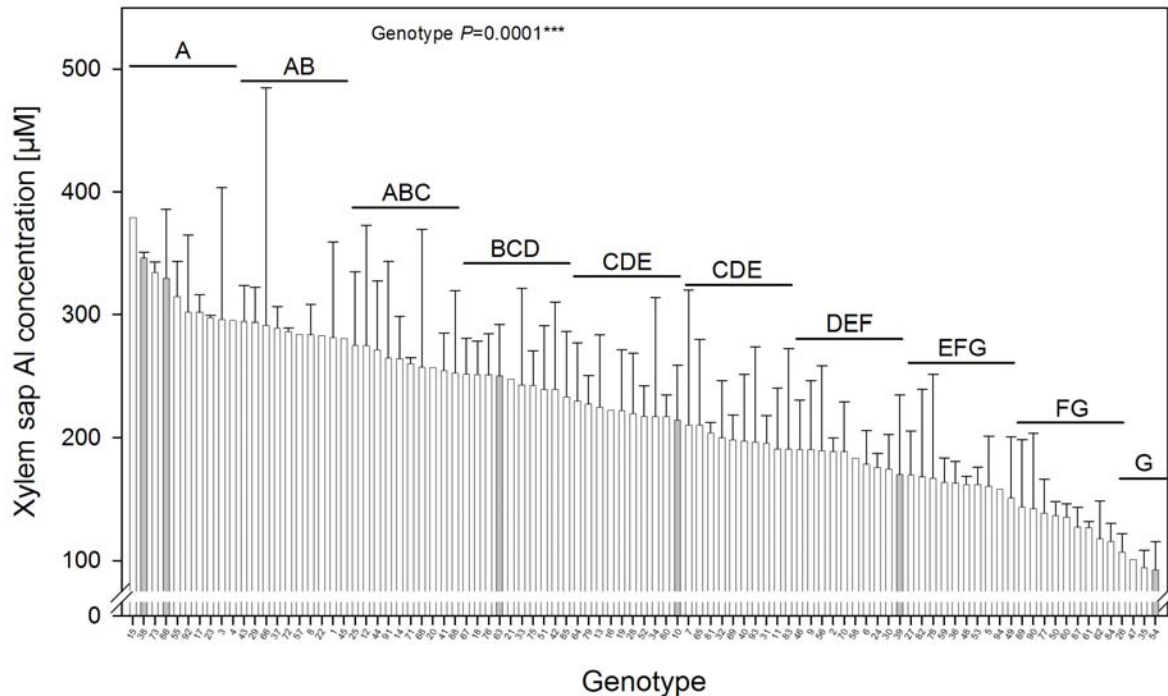


Figure 5. Xylem sap Al concentration of 94 different buckwheat genotypes after 4 weeks of substrate culture with an Al supply of 8 g $\text{Al}_2(\text{SO}_4)_3 \cdot 18 \text{H}_2\text{O}$. Three plants per 1 L pot were combined to one composite sample, bars represent means \pm SE, $n = 3$. Different letters denote significant differences between treatment durations at $P = 0.05$. Genotypes were grouped according to their xylem sap Al concentration.

The genotypes also differed in the Al concentration of the primary leaf (Fig 6). However, the Al concentrations of the leaves were not correlated with the Al concentrations of the xylem sap (Fig. 5).

A correlation analysis with the whole set of genotypes revealed a highly significant correlation of the citrate and Al concentration in the xylem sap (Fig 7A). Generally, citrate in the xylem sap seemed to be available in excess compared to Al. The analysis of the ionic composition of the xylem sap was extended with a sub-set of genotypes. All identified inorganic compounds were analyzed for a correlation with the Al concentration in the xylem sap. These analyses revealed that only the iron concentration was related to the xylem Al concentration (Fig 7B). It was found that about 20 times more citrate than Al in the xylem sap. Ten times more Al than Fe was transported. Also citrate and Fe translocation were significantly correlated ($P < 0.0001$). The slope showed values of 95 which suggested that 95 times more citrate than Fe were loaded into the xylem.

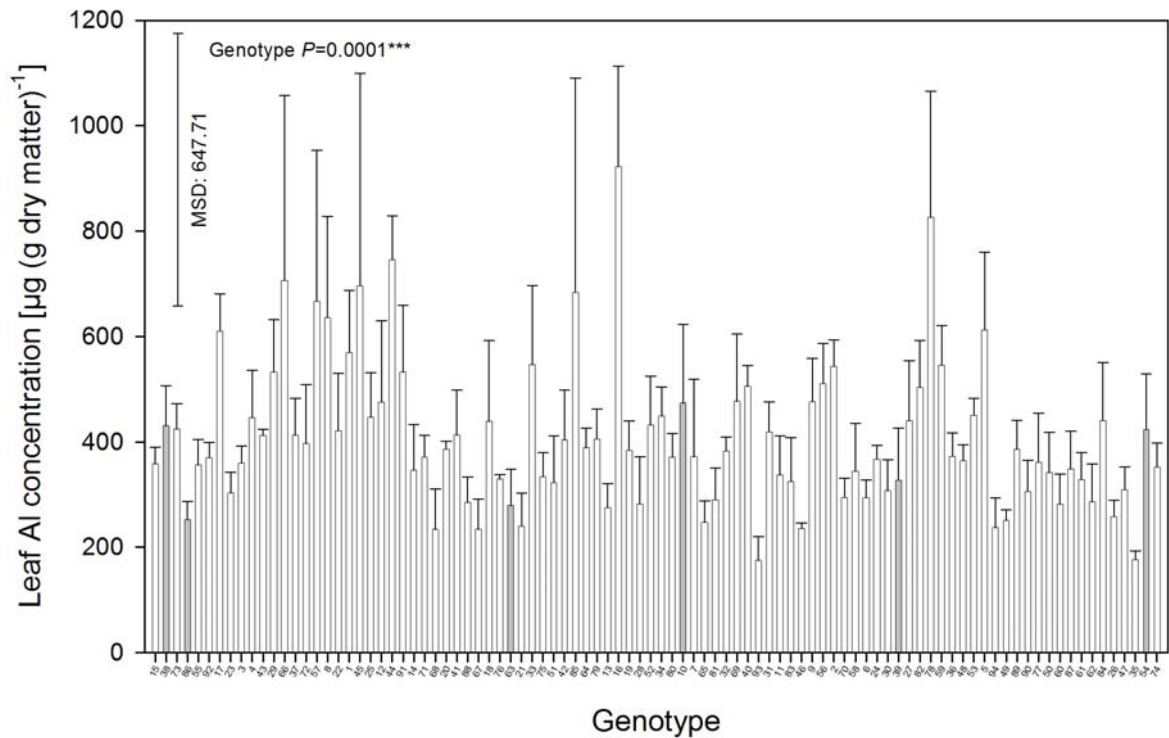


Figure 6. Leaf Al concentration of 94 different buckwheat genotypes after 3 weeks of substrate culture with a Al supply of 8 g $\text{Al}_2(\text{SO}_4)_3 \cdot 18 \text{H}_2\text{O}$. Three plants per 1 L pot were combined to one composite sample, bars represent means \pm SE, $n=3$. The order of genotype arrangement follows descending xylem sap Al concentration (see Fig. 5). MSD was determined at $P = 0.05$.

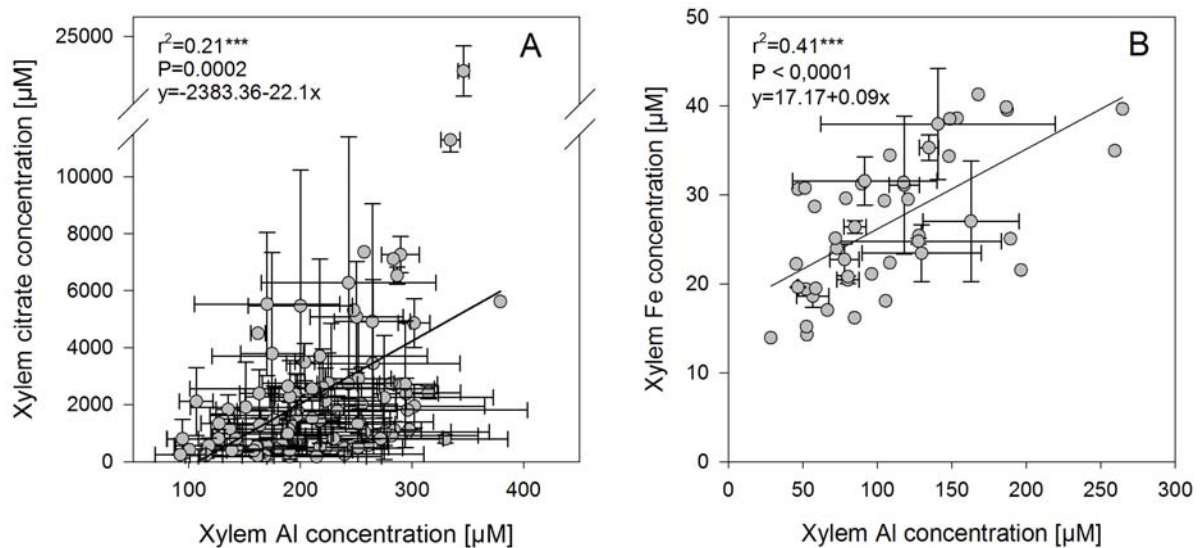


Figure 7. Correlation of xylem sap citrate with xylem sap Al concentrations (A) and correlation of xylem sap Al with xylem sap iron concentrations (B). Samples were obtained as stem bleeding sap after collection for 30 min. Points represent means \pm SE, $n = 3$, For the ANOVA *** denote levels of significance at $P = 0.001$.

For further analysis, six genotypes, spread over the whole xylem Al concentration spectrum, were chosen for an experiment in nutrient solution. These genotypes were significantly different in their Al translocation quantities, and additionally showed different response patterns of the xylem-sap citrate concentration. Each Al concentration in the xylem sap (depicted in dark grey bars in Fig. 5), categorized by high, mid and low Al concentrations in the xylem sap, was represented by a genotype which showed either an Al concentration responding or a non-responding citrate concentration in the xylem sap.

The analysis of the bulk root Fe contents further supported an interaction between Al and Fe. Irrespective of the genotype, Al treatment lead to a reduction of the iron contents in the bulk root system compared to the control treatment (Fig. 8). This can only partly be explained by the omission of Fe supply during the short term (24 h) Al treatment to avoid interactions of the iron-chelate EDDHA and Al, because also the controls without Al did not receive Fe during this period. It thus appears that Al supply enhanced the Fe transport from the roots to the shoots.

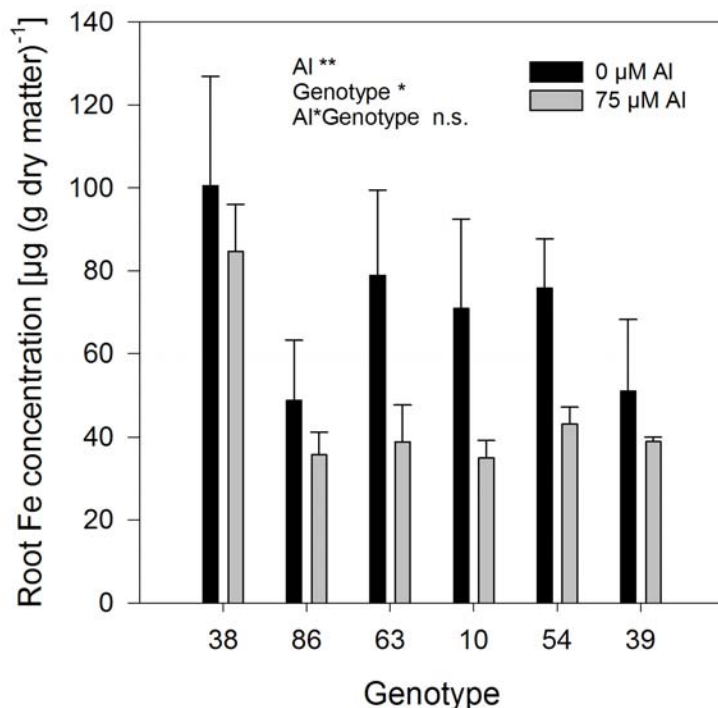


Figure 8. Iron content of the bulk root dry matter of buckwheat cultivars differing in Al translocation after preculture in complete nutrient solution with 60 µM Fe-EDDHA and subsequent +/- Al treatment for 24 h in simplified nutrient solution without Fe addition. Bars represent means +/- SE, n = 3. For the ANOVA, * and ** denote significant effects at $P < 0.05$ and 0.01, respectively, ns nonsignificant.

In contrast to the substrate experiment the plants used in the nutrient solution approach had comparable shoot architectures, because adventitiously rooted cuttings were used. The shoots of these cuttings were reduced to one leaf and the hypocotyl prior the rooting procedure. This facilitated the comparison of *in-planta* Al fluxes between genotypes, because all genotypes had the same number of leaves during the Al treatment. The genotypes 38, 86 and 63 showed in trends higher Al concentrations in the leaf dry matter than the genotypes 10, 39 and 54, even though only the genotypes 38,10 and 54 were significantly different. The decreasing trend of Al accumulated in the leaves from genotype 38 to 54 might be in line with the decreasing xylem sap concentration as determined in the substrate experiment, where also genotype 38 and 86 had the highest Al xylem sap concentration and the latter two genotypes were characterized by lower Al concentrations in the xylem sap.

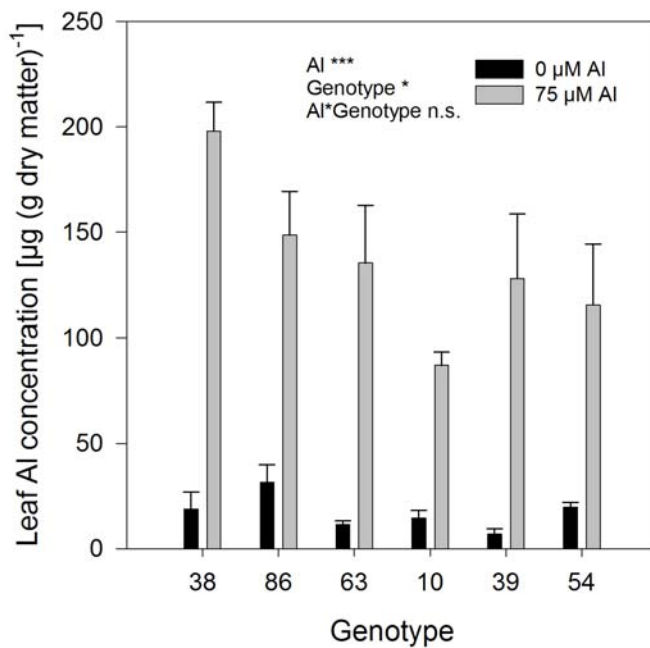


Figure 9. Leaf Al concentration in the dry matter of buckwheat cultivars differing in Al translocation after preculture in complete nutrient solution and subsequent +/- Al treatment for 24 h in simplified nutrient solution. Bars represent means +/- SE, n = 3. For the ANOVA, * and *** denote significant effects at $P < 0.05$ and 0.001, respectively, ns nonsignificant.

Root oxalate exudation was significantly activated by Al application. The genotypes 38 and 86 showed significantly higher exudation rates than the genotypes 39 and 54 (Fig. 10A). Citrate was exuded in minor amounts and showed no Al-activated exudation pattern (Data not shown).

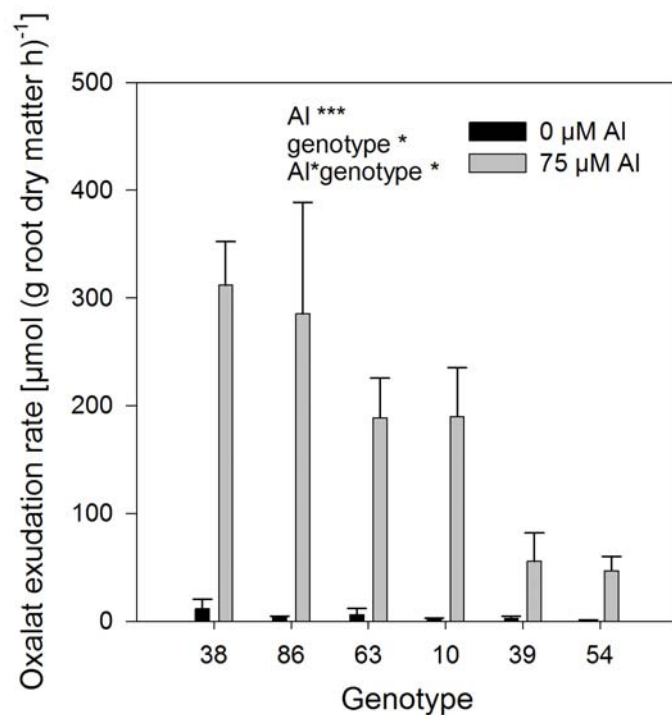


Figure 10. Oxalate anion exudation rate of roots of buckwheat cultivars differing in Al translocation after pre-culture in complete nutrient solution +/- Al treatment for 24 h in simplified nutrient solution without.. Bars represent means +/- SE, n = 3. For the ANOVA, * and *** denote significant effects at $P < 0.05$ and 0.001, respectively.

The root growth-rate of the control treatment was in the range of 0.7-1 mm h⁻¹. Aluminium supply decreased the root growth in some genotypes. The genotypes 38, 86, and 63 showed no root-growth inhibition while the genotypes 10, 39 and 54 were inhibited by 30-50 % due to the 75 µM Al treatment (Fig. 11).

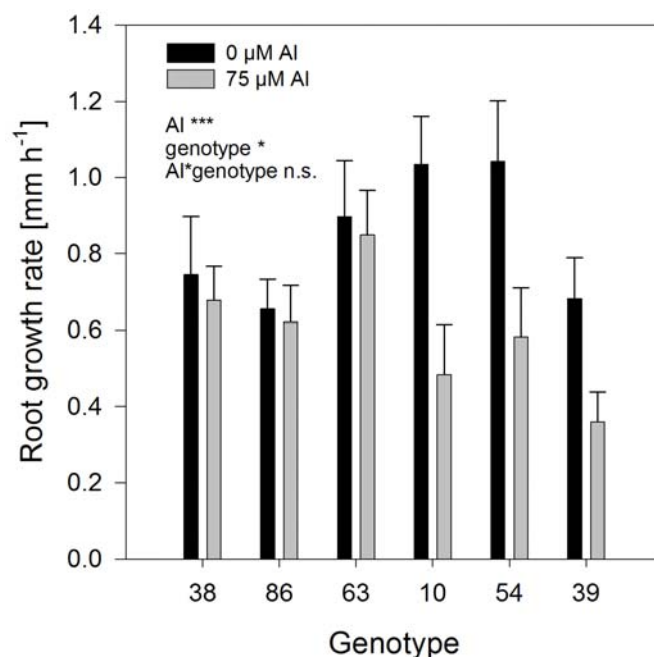


Figure 11. Root growth-rate of buckwheat cultivars differing in Al translocation after preculture in complete nutrient solution and subsequent +/- Al treatment for 24 h in simplified nutrient solution. Root growth rate was analyzed by marking the root tip 1.5 mm behind the tip before the treatment and measuring the distance again after 24 h. Bars represent means +/- SE, n = 3. For the ANOVA, * and *** denote significant effects at $P < 0.05$ and 0.001, respectively, ns nonsignificant.

Discussion

Substrate parameters

As a prerequisite for this study it was confirmed that the application of Al to the substrate led to the presence of Al in a plant-available form (Fig. 1), which is supposed to be Al^{3+} (Ma and Hiradate, 2000). At a substrate pH of about 4.3 a major proportion exists as mononuclear Al species. This general pH dependency is in line with the analysis of Marion *et al.* (1976) who showed that Al^{3+} is the predominant Al species in this pH range. However, the difference between monomeric Al according to Kerven *et al.* (1989) and total soluble Al (ICP-OES) clearly indicates that also polynuclear, most probable Al stably complexed by organic ligands such as humic acids was also present.

The Al concentration in the leaves of the Al accumulator buckwheat increased with increasing Al supply (Fig. 4) even at 2 g $\text{Al}_2(\text{SO}_4)_3 \cdot 18 \text{H}_2\text{O}$ which did not lead to increased monomeric Al in the substrate extract. This indicated that buckwheat may be able to take up/mobilise not only mononuclear Al. Buckwheat is known not only as an Al accumulating plant species but also for its high phosphorus acquisition efficiency (Amann and Amberger, 1989; Zhu *et al.*,

2002). Since P is often fixed to Al and Fe oxides and hydroxides desorption of P requires the solubilization of Al/Fe by root-exuded ligands such as oxalate. This might suggest that the Al uptake efficiency and P efficiency are closely related.

In conclusion, the application of Al in amounts of up to 8 g Al₂(SO₄)₃*18 H₂O L⁻¹ substrate proved to lead to high concentration of mononuclear Al in the substrate solution thus facilitating the comparison of the genotypic Al translocation capabilities irrespective of genotypic differences in P efficiency.

Genotypic aspects

The main focus of this study was the determination of differences in Al accumulation in the shoots among a large number of *Fagopyrum* species and genotypes. The comparison revealed that all tested species and genotypes accumulated Al in the shoot, thus no qualitative differences were found. However, genotypes differed in xylem Al concentration by about a factor of five (Fig. 5). The accumulation trait could not be related to the origin of the genotypes. Genotypes with highest Al concentration in the xylem sap originated from different regions as for example Belarus (genotype 15), Iran (genotype 38), North Korea (genotype 73), and Italy (genotype 86).

The similar range of Al accumulation was also found within the family of *Melastomeaceae* (Jansen *et al.*, 2002b). Species from that family were shown to accumulate Al in huge amounts in the shoots. However, the variation within the family was shown to be in the range of 6-66 mg Al g⁻¹ dry matter. In contrast, a comparison of members from the taxa *Polygonaceae*, the family of buckwheat, showed that some genotypes differing in Al resistance did not accumulate Al in their shoots (You *et al.*, 2005). This might suggest that the trait of Al accumulation is not spread over the whole family of the *Polygonaceae* thus being rather typical for the genus *Fagopyrum*. Based on semi-quantitative tests the Al accumulation trait was mapped onto a recent angiosperm phylogeny. This classification revealed that Al hyperaccumulation is a simple, primitive trait that has not arisen independently several times during evolution but was lost independently in many derived taxa (Jansen *et al.* 2002a; White, 2002). The authors suggested that the trait of Al accumulation shows low incidence in evolutionary advanced groups which appears to be correlated with the herbaceous habit. Therefore, own results rather indicate that the genus *Fagopyrum* might represent an exceptional case where the evolutionary background does not fit into this generalistic proposition and thus needs to be further studied by other mapping approaches. Regardless of

the fact that no qualitative differences in the Al accumulation of the 94 genotypes could be found, which makes comparisons on the transcriptomic or genetic level difficult, we still contribute new information to the not completely understood trait of Al accumulation.

Xylem sap Al concentration the parameter of choice

Aluminium concentrations in leaves showed significant genotypic differences (Fig. 6). Unfortunately this parameter was not suitable for a genotype or even species spanning comparison due to great differences in growth habitus. The number of leaves or the total above-ground biomass confounded the comparison of the concentrations on the dry matter basis. A higher biomass production might have led to a dilution effect. Such a dilution effect was found for Cd accumulation of maize cultivars, where the genotype with the highest biomass production showed lower Cd concentrations (Kurz *et al.*, 1999). Therefore, the xylem sap Al concentration was chosen as the primary parameter for the comparison of the genotypes and their Al accumulation capacity. The xylem sap was sampled only for 0.5 h, because various studies showed that only shortly after cutting off the shoot representative data on the *in vivo* xylem composition can be assessed (Siebrecht & Tischner, 1999). The same technique has been used for the characterization of heavy metal hyperaccumulation. Xylem sap Cd and Zn concentrations were used to show considerable scope for the selection of advanced hyperaccumulation ecotypes with the objective of increasing the phytoextraction efficiencies to remediate metal-contaminated soils (Lombi *et al.*, 2001).

Al transport

The prevailing uptake capability of heavy metals and particularly Al in hyperaccumulating plant species such as buckwheat raises the evolutionary question about specific transport processes for non essential metals. Why do plants take up toxic metals and evolve C-cost intensive internal detoxification mechanisms? One suggestion is that the plant may take some benefit of the toxic metal, either by acting as a defence or deterrence to pathogens and herbivores or simply enabling plants to grow on acid soils (White, 2002). Another suggestion is that proteins involved in the metal homeostasis are unspecific and thus may represent an uptake route for not essential elements. Transporters often exist as a part of a large family with variable functions. However, some proteins are highly specific for particular metals, but some are rather unspecific and can potentially transport a range of related metals (Williams and Salt, 2009). There are indications for the latter suggestion to apply to buckwheat. The

trend obtained in the xylem sap Fe translocation is retrieved in the iron contents of the bulk root dry matter (Figure 8). This indicated, that Al treatment enhances the transport of root Fe to the xylem. The xylem citrate transport may be the connective link between Al and Fe transport rates because Al and citrate transport rates were correlated in the xylem sap (Figure 4B and 7A) as well as the iron and Al transport were significantly correlated.

Using NMR Ma and Hiradate (2000) showed that Al is complexed by citrate in the xylem sap. However, in their study the citrate concentration showed no response to externally applied or internally transported Al. In contrast, in the present study a significant correlation between xylem citrate and Al concentrations existed. Both, the increasing Al supply led to increasing citrate concentrations in the reference cultivar (Fig. 4B) and the genotypes which translocated Al more efficiently were characterized by higher citrate concentrations in the xylem sap as compared to genotypes translocating Al on a lower level (Fig. 7A). Furthermore, we were able to show the same relationship on the xylem sap level of excised single root tips and intact plants (Chapter I and II). These data strongly suggest that the citrate concentrations in the xylem sap of buckwheat respond to the Al supply even though citrate is available in excess especially in the lower Al concentration ranges. The excess of citrate over Al in the xylem sap suggests that the xylem loading of citrate is not exclusively coupled to Al transport processes. But the presence of Al enhances the citrate xylem-loading which also facilitates Fe xylem-loading. Iron is known to be transported in the xylem coupled to citrate which is loaded into the xylem through MATE-proteins (FRD3, Durett *et al.*, 2007); but the particular Fe species transported through the plasma membrane is not yet specified. The data presented in this study might suggest that Al leads to an enhanced citrate synthesis within the xylem parenchyma cells which then could be directly transported into the xylem via FRD3-transporters. Another possibility could be that the Al citrate complex is loaded directly into the xylem as suggested (Chapter II).

A similar close relationship between Al and citrate concentrations in the xylem sap has been described for three cultivars of *Hydrangea macrophylla* which is also known to be an Al accumulating plant species. Geochem PC calculations indicated that citrate plays a dominant role for Al transport in *Hydrangea* (Naumann and Horst, 2003).

Excess citrate in the xylem sap was not found if the xylem sap was sampled shortly behind the root tip (Chapter I) which may indicate that several other processes, like Zn, Ca (Ueno *et al.*, 2008) and Fe (Durett *et al.*, 2007) transport are also closely connected to citrate loading of the xylem getting increasing importance with increasing xylem path length in direction to the shoot. A direct coupling of Al and citrate transport to the xylem sap of excised root tip might

also be related to the fact that Al was the only metal which was supplied in the used simplified nutrient solution. In contrast, in full nutrient solution and in substrate solution used in other experiments a set of different metals was present.

In conclusion the results suggest that in buckwheat roots both, Fe and Al are loaded into and transported in the xylem as citrate complexes. Thus citrate might be an unspecific metal ligand in the xylem sap. However, the specific Al loading process into the xylem which was shown to be a metabolism dependent process (Chapter II), needs to be further analysed.

Association of Al resistance and Al accumulation

Using a subset on genotypes based on differential Al and citrate xylem sap concentrations (Fig.5, Fig.7) it appears that the genotypes which built up high concentrations of Al in the xylem sap and translocated Al most efficiently also showed enhanced Al-activated root oxalate-exudation rates (Fig.10). Therefore, these genotypes exhibited enhanced Al resistance (less inhibition of root elongation, Fig.11) compared to the genotypes translocating lower amounts of Al.

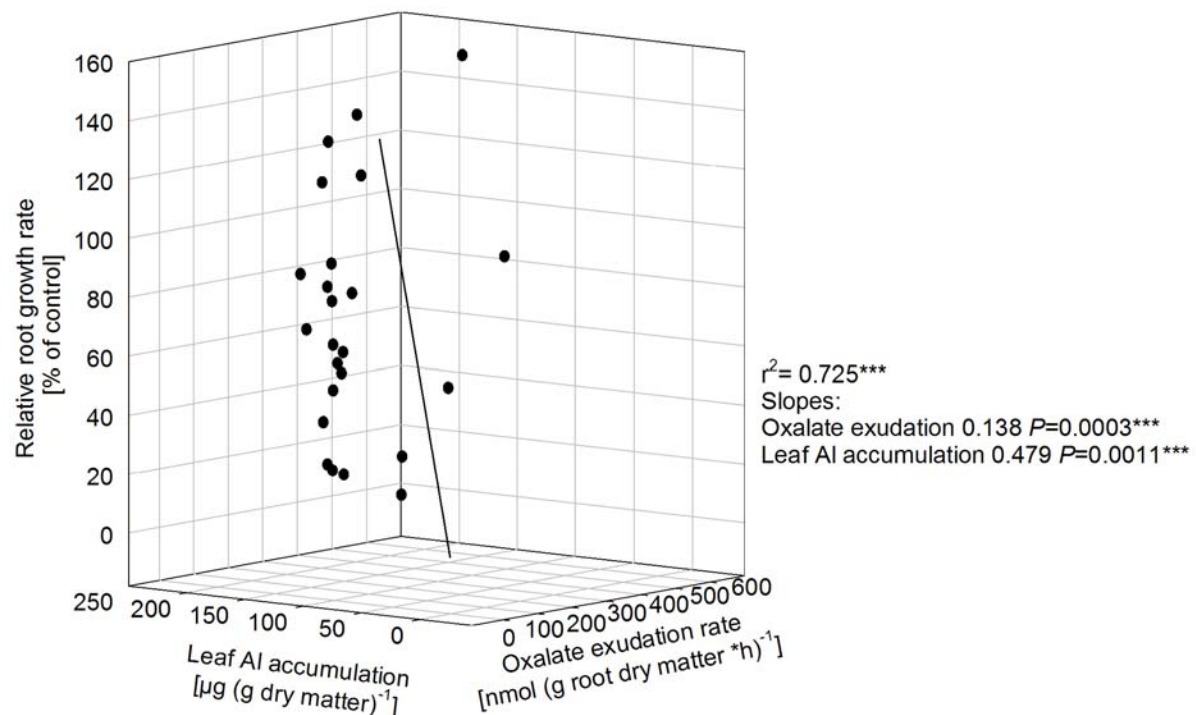


Figure 12. Correlation analysis of resistance and tolerance-mediating processes and their contribution to the maintenance of the relative root growth rate (0 μM Al = 100 %) of 6 buckwheat genotypes under Al toxic conditions (75 μM). Multiple linear regression revealed that all independent variables contribute to the relative root growth-rate at $P < 0.05$.

Consequently, Al resistance mediated by oxalate exudation and Al accumulation appears to be positively correlated in buckwheat. These results further substantiate the conclusions based on our previous studies showing that Al exclusion and Al accumulation are not mutually exclusive but spatiotemporally interrelated (Chapter I). However, it is difficult to quantify the relative importance of oxalate exudation/Al exclusion and Al accumulation/Al tolerance for the performance of buckwheat on acid, Al-toxic soils. The multiple regression analysis (Fig. 12) of inhibition of root elongation by Al, root oxalate-exudation and Al accumulation revealed for the selected set of genotypes grown in hydroponics a highly significant regression coefficient. Thus the dependent variable relative root growth can be predicted from a combination of the independent variables oxalate exudation rate and leaf Al accumulation. Both, oxalate exudation and Al accumulation reduce Al toxicity clearly indicating that the Al-activated exudation of oxalate confers protection of the roots against Al injury and mediates Al accumulation at the same time. This is in agreement with mainly apoplastic lesions of Al toxicity as elaborated by Horst *et al.*, (2010). Oxalate exudation leads to the formation of an Al oxalate complex thus reducing the positive charge of the toxic Al^{3+} and interaction with the negative charges of the cell wall and the plasma membrane. Since the rate of oxalate exudation is not high enough only a 1:1 Al:oxalate complex can form which is still positively charged $(Al-Ox)^+$ (Chapter II). This confers some protection of apoplastic Al-sensitive charges (enhanced Al resistance as expressed as reduced inhibition of root elongation). At the same time $(Al-Ox)^+$ is accumulation in the apoplast which facilitates its uptake into the symplast as $(Al-Ox)^+$ as suggested (Chapter II).

In conclusion, also the comparison of the Al resistance in relation to Al-induced oxalate exudation and Al accumulation of *Fagopyrum* genotypes support the previously postulated interrelationship between Al exclusion and Al accumulation (Chapter II).

The contribution of the above ground Al accumulation to the inhibition of Al sensitivity is not negligible: If 250 μM are estimated as a mean xylem sap Al concentration at an average xylem sap exudation rate of 200 μL per h (Ma and Hiradate, 2000; and own unpublished data) the amount of Al discharged from the root would account for an Al transport of about 50 nmol h^{-1} . This amount compared with a maximal Al content of 10 nmol (10 mm root tip) $^{-1}$ represents the potential to unload Al from the most Al-sensitive apoplastic sites, the transition zone of the root tip, which has been shown in many plant species to be the most Al-sensitive root-tip zone (Ryan, *et al.*, 1993; Sivaguru and Horst, 1998; Rangel *et al.*, 2007). Furthermore, we showed that Al is primarily accumulated in the meristematic zone of the root tip where the

first three mm account for more than 60 % of the Al content of the 10 mm root tip. Thus, the Al amount which needs to be discharged from the most Al-sensitive root zone is smaller than 10 % of the 10 mm root tip. Hence, the establishment of a 1:1 ratio of Al and oxalate in the root apoplast reduces apoplastic Al injury and, additionally, enhances the Al uptake into the symplast and subsequent translocation to the shoots thus contributing to keeping the apoplastic phytotoxic Al concentration low.

General Discussion

Aluminium toxicity is a major problem affecting crop productivity worldwide. A strategy focusing on the alleviation of Al toxicity by lime applications which is supposed to increase soil pH, thus reducing the activity of rhizotoxic Al species is ineffective (Rao *et al.*, 1993). Lime is not mobile in the soil profile, therefore, at best reducing Al toxicity in the top soil. Additionally, lime is cost-intensive and, therefore, inappropriate particularly in developing countries where Al toxicity is wide spread.

For that reason, other approaches are more promising. Understanding the mechanisms of Al toxicity and resistance of plants is of fundamental importance. Therefore, integrated approaches which focus on genetic resistance mechanisms in crop plants combined with advances in mechanistic understanding of underlying mechanisms represent a more promising procedure. Furthermore, plants like buckwheat which were not bred for certain agronomic traits and additionally adapted to Al toxicity, are expected to conserve more Al resistance genetic information, and will be a good resource to discover important resistance genes (You *et al.*, 2005). As shown in the present work, buckwheat exhibits a well coordinated resistance machinery, involving efficient Al tolerance and Al exclusion mechanisms which provides an important resource of genetic information which could be transferred to other not-resistant crop plants. Simultaneously, unravelling of the molecular basis of underlying mechanisms is a challenge particularly for the Al accumulator buckwheat where all resistance-associated processes are supposed to be expressed constitutively and no gene activation is necessary for the high Al resistance. The Al-exclusion, the Al-tolerance and accumulation-mediating mechanism are most likely expressed constitutively, because Al uptake into the symplast and translocation are quickly occurring which indicates that no *de-novo* protein biosynthesis is necessary. However, this study provides a set of new insights into these mechanisms and it is clearly shown that all involved resistance mechanisms, the exclusion and accumulation of Al are acting in a well coordinated manner and are not mutually exclusive.

The role of the apoplast in Al-accumulating buckwheat

Aluminium is known to interfere directly and immediately with the root tip apoplast (Horst *et al.*, 2007) (Fig 1 A), however buckwheat is well protected (Chapter II, Fig. 6). Oxalate, which detoxifies Al (Fig 1 B), is exuded immediately without a lag phase (Zheng *et al.*, 1998). A lag

phase is found in other plant species, necessary for gene activation and protein synthesis which are either related to the OA synthesis or their efflux (Ryan and Delhaize, 2001). This sudden exudation detoxifies Al directly. Subsequently a concentration ratio of 1:1 (Al:oxalate) is formed in the water free space of buckwheat root tips (Chapter II, Fig. 4). Thus, Al is detoxified to some extent. Nevertheless, due to the high stability constants of Al-pectin complexes Al binds to cell-wall constituents and the detoxification cannot fully protect Al-sensitive sites in buckwheat root tips. The 1:1 ratio of Al and oxalate in the water free space is sustained for extended Al treatment durations (Chapter II, Fig. 2). Notwithstanding, only excessive supplementation of oxalate into the nutrient solution completely alleviated Al-induced root growth inhibition and is also shown to disrupt the Al uptake process into the root symplast (Chapter II, Fig. 8 and 9). The binding of Al to the cell wall is a major site of Al accumulation in not Al-resistant plant species and furthermore in buckwheat (Chapter II, Fig. 3). However, this Al fraction is quantitatively not the most important fraction in buckwheat after Al treatment duration of less than 4 h. In contrast, in Al not accumulating plant species accumulate Al predominantly in the root-tip apoplast. Irrespective of the treatment duration the majority of Al is associated with the cell wall. Only small proportions of Al are found to be localised symplastically. In root tips of buckwheat Al is primarily accumulated in the first 3 mm of the root tip (Chapter I, Fig. 2). Aluminium in this apical root tip region is apoplastically as well as symplastically localized as shown by morin staining and a fractionated extraction which proved to be a suitable measure for analysing Al distribution even in tissues of Al-accumulating plant species (Chapter III, Fig. 5 and Chapter II, Fig 2). The dye morin stained the apoplastic localization of Al, which indicates that Al is also present in a soluble binding stage, rather associated with organic acid anions than with cell wall constituents because these were shown not to be stained by morin (Eticha *et al.*, 2005a). The Al accumulation in non Al-accumulating plant species is characterized by a biphasic uptake pattern where the accumulation in the cell-wall fraction is responsible for a first and rapid binding of Al to negative charges in the apoplast. This rapid phase is followed by a linear phase which is supposed to be related to membrane passage of Al. However, buckwheat exhibits not the same accumulation pattern. Aluminium contents in the cell-wall fraction are increasing linearly and it is not shown that short-term Al treatments lead to an enhanced Al binding compared to treatments for longer terms (Chapter II, Fig. 2). This again could be related to the pattern I response in exudation of oxalate. This execution of the Al exclusion mechanism facilitates the fast development of an equilibrium Al concentration in the WFSF. Apoplastic Al binding is not affected by active metabolic processes, and there were no

enhanced Al binding rates under chilled conditions observed (Chapter II, Fig. 5c). This characterizes the apoplastic binding of Al as passive process. The same is true for the exudation which is also a passive process because there is no difference between the exudation rates of oxalate under low and high temperatures (Chapter II, Fig. 6a). This requires an opening of a pre-existing anion channel without a direct energy turnover. This could be performed by a conformation change of the channel protein only by the free binding energy of Al which is equivalently shown for K⁺ channels (Jiang *et al.* 2002). The concentration of Al in the WFSF is maintained on a moderate level of about 200 μM irrespective of the Al treatment duration (Chapter II, Fig. 2). The Al-activated efflux of oxalate leads to an equivalent concentration in the WFSF suggesting that the root epidermis represents an important diffusion resistance for OAs (Kinraide *et al.*, 2005). This allows efficient detoxification of Al in the WFSF at low carbon costs in the finite volume of the WFS. Additionally, oxalate represents the simplest dicarboxylic acid producing a high stability complex with Al utilising only two carbon atoms per molecule. In comparison, malate utilized by wheat for Al detoxification (Ryan *et al.*, 1995), contains four carbon atoms per molecule and the Al-malate stability constant is much lower. Thus the cost-benefit ratio of the use of malate is lower than of oxalate which could be one reason for the superior Al resistance if buckwheat is compared with wheat.

The bulk Al contents of root tips of various plant species and genotypes often correlate very well with their respective Al resistance or sensitivity (Rangel *et al.*, 2005, Eticha 2005a). This is not the case for buckwheat; Al-sensitive genotypes roughly have the same Al contents compared to Al-resistant genotypes. A screening of 94 buckwheat genotypes revealed that accessions showing lower exudation of oxalate in response to external Al application exhibited the most pronounced Al-induced root growth inhibition (Chapter IV, Fig 10 and 11). Thus, these genotypes were less Al-resistant. However, the Al contents accumulated in the root apices were not significantly different between the genotypes. Even the application of an anion-channel inhibitor, clearly reducing oxalate root-exudation did not increase the apoplastically bound Al. Zheng (2009, Zeijang University, Hangzhou, China, personal information) showed that the application of the anion-channel inhibitor PG also did not affect the total Al content accumulated in the apoplast but lead to a tighter binding of Al to the cell wall. These results support the view (Horst *et al.*, 2010) that also in buckwheat Al-induced inhibition of root elongation is due to stable Al binding to the pectic matrix of the cell wall.

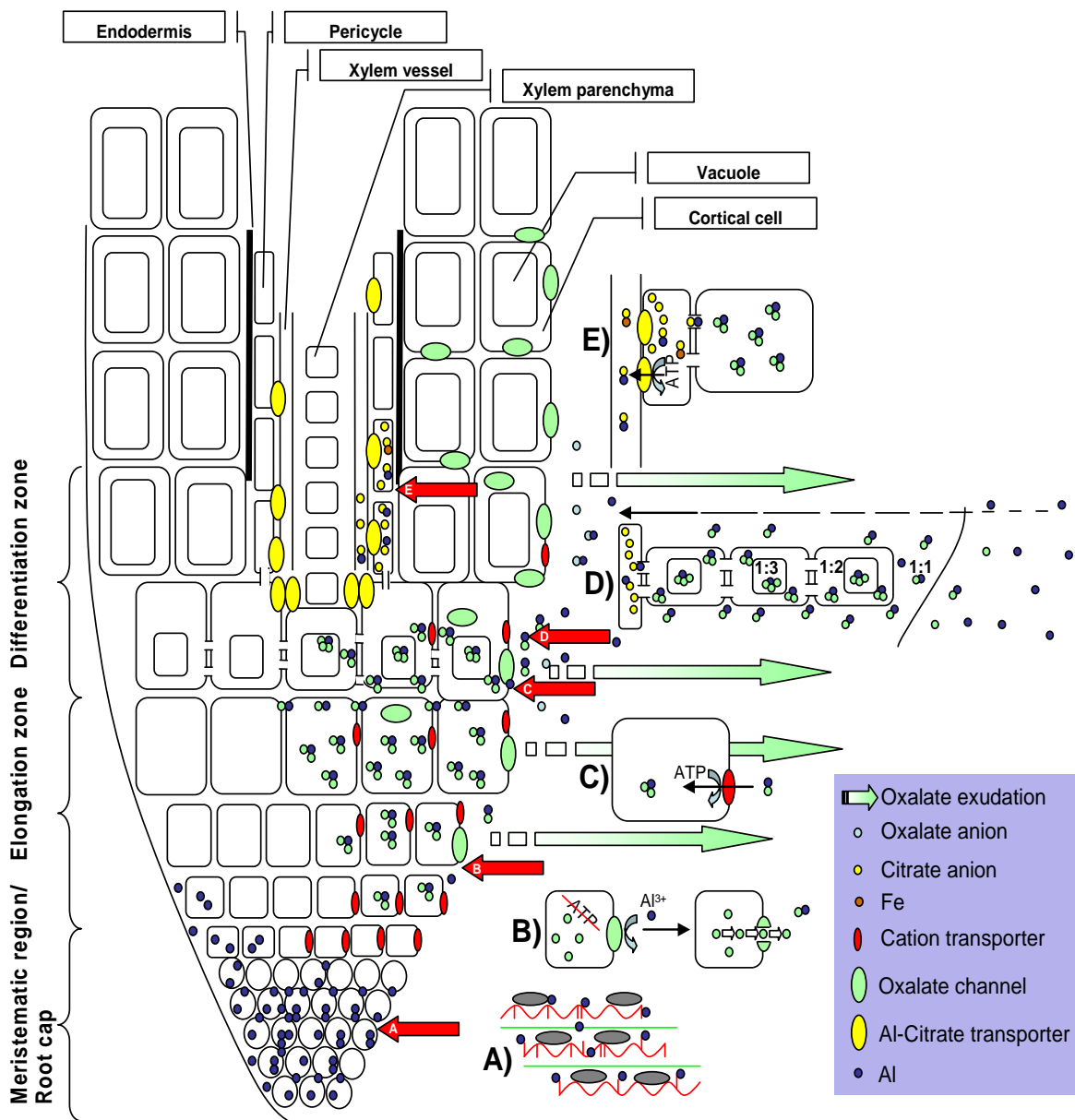


Figure 1. Schematic overview of the key elements involved in Al accumulation, Al resistance and Al tolerance-mediated mechanisms in the root tip of buckwheat. Section A) represents the Al binding to fixed negative charges in the cell wall. Section B) shows the Al-activated but metabolic independent efflux of oxalate anions. Section C) depicts the metabolism-dependent uptake of $\text{Al}(\text{Ox})^+$ by a postulated cation transporter. Section D) represents the Al-activated structuring of a gradient through the formation of Al/oxalate complexes differing in Al:oxalate ratio facilitating Al uptake. Section E) depicts the ligand exchange to citrate in xylem parenchyma cells and the proposed active loading of $\text{Al}(\text{Cit})^{3-}$ into the xylem.

Al uptake and the symplastic contribution to Al resistance in buckwheat

The study indicates that an interaction of Al exclusion and Al tolerance is responsible for the extraordinary performance of buckwheat on acidic and Al-toxic soils (overview in Fig. 1). This was further substantiated by a multiple linear regression, which showed that the Al-exclusion mediating exudation of oxalate as well as the above ground Al accumulation, comprising the internal tolerance mechanism, are positively correlated and both contribute to the growth of buckwheat under Al-toxic conditions, thus the overall Al resistance (Chapter IV, Fig. 12). However, the transport process of Al into the symplast as prerequisite for internal tolerance was virtually unknown. First approaches to unravel Al accumulation in buckwheat suggest that only free Al^{3+} is taken up (Ma and Hiradate, 2000). These results were obtained applying Al or Al-oxalate complexes to the roots in nutrient solution. Under these conditions Al was only taken up in case of the Al^{3+} supply. However, the results presented here clearly show that this does not unequivocally prove that Al^{3+} is taken up by the buckwheat root tips for the following reasons: I) Al uptake and exclusion mechanisms are spatially co-localized, which makes it unlikely that Al is present in the form of Al^{3+} at the plasma membrane surface, if oxalate anions are present at the same time and place in the apoplast (Chapter I). II) It is shown that Al is taken up as Al-oxalate complex if Al and oxalate (Ox) are present in the ratio of 1:1 and the plasma membrane received an Al^{3+} stimulus (Chapter II). III) The results confirm an uptake cascade postulated by Ma and Hiradate (2000) provided that the apoplast represents already the first compartment where $\text{Al}(\text{Ox})^+$ is formed and continues as the more stable $\text{Al}(\text{Ox}_2)^-$ in the cytosol and the even more stable $\text{Al}(\text{Ox}_3)^{3-}$ in the vacuole (Fig 1D). The cytosolic $\text{Al}(\text{Ox}_2)^-$ possibly represents the signal which induces the initiation of Al exclusion mechanisms in root zones which are not in direct contact with Al^{3+} (Chapter I, Fig. 9)

The uptake of Al is rapid and active, because the Al concentration of the external solution is rapidly exceeded in the symplastic solution and in the xylem sap. The Al uptake is strongly reduced if the ambient temperature is decreased to 4°C (Chapter II, Fig 5b) (Fig. 1 C). Furthermore, uptake of Al into the symplast occurs even without transpiration and no negative pressure in the xylem vessels in excised root tips (Chapter I, Fig. 4). Therefore we conclude that Al is taken up by an active cation transporter. However, the results presented do not allow

the final conclusion that it is a specific Al transporter or just an unspecific cation transporter. Uptake and above-ground accumulation of Al is a well conserved trait within 94 tested *Fagopyrum* genotypes originating from almost all over the northern hemisphere which makes a randomly occurring mutation, without an evolutionary advantage unlikely.

Once Al is taken up it is translocated predominantly and fast in radial direction. It is proposed that a tissue-specific orientation of plasmodesmata is responsible for this radial Al transport in a distance of 5-10 mm from the root tip. There are various studies showing that plasmodesmata in different plant tissues show a particular functional diversity. Different root tip regions could be characterized by a specific orientation of plasmodesmata which could influence the dominating flow direction of particular solutes in specific regions of the root tip (Waigmann and Zambryski, 1995; Duckett *et al.*, 1994; Oparka *et al.*, 1995). It is additionally proposed, that the root tip has the highest density or activity of citrate transporters associated to Al-xylem loading. It is further indicated that there are metabolic differences in the cortical and stelar cells of the root tip. In the cortical tissue, $40 \mu\text{mol (cm tissue length)}^{-1}$ oxalate and no citrate, in the stele tissue including the xylem, only $0.8 \mu\text{mol (cm tissue length)}^{-1}$ oxalate and $3.5 \mu\text{mol (cm tissue length)}^{-1}$ of citrate were found. This can explain why a ligand exchange from Al oxalate to Al citrate takes place in the xylem parenchyma. In contrast with the available literature on Al translocation in buckwheat, we observed a pronounced positive response of citrate in the xylem sap to the Al translocation rate. Citrate and Al transport rates were either showing response to spatially differentiated Al application (Chapter I, Fig. 7) or in a genotypic comparison in which the xylem sap Al concentrations were associated with the xylem citrate concentration after short term xylem-sap sampling (Chapter IV, Fig 7A). The xylem-loading Al transporters are under metabolic control because the xylem loading or the unloading of the symplast (Chapter II, Fig. 5b) into the xylem apoplast was temperature-dependent (Bravo-F and Uribe, 1981). The Al transport was linked to the transport of iron (Fe) (Chapter IV, Fig. 7B). A possible explanation for this relation could be that citrate anions represent a common “ferry” for Al as well as Fe (Fig. 1 D). The presence of Al induces an enhanced synthesis of citrate in the xylem parenchyma cells. This high citrate concentration enables enhanced citrate loading via FRD3 transporters, which were shown to facilitate the transport Fe in the xylem (Green *et al.*, 2004; Durett *et al.*, 2007). Additionally, the high concentration of citrate leads to a ligand exchange from Al oxalate to Al citrate in these stelar cells which enables the Al-citrate xylem loading by an unknown transporter.

A systematic *in-situ* Al localization approach revealed significant radial differences in the Al distribution. The apical root-tip region showed highest Al-morin fluorescence or Al

accumulation intensity in the outer cortical cell layers with is in line with the results obtained by the stratified Al application in mini rhizotrons (Chapter III, Fig. 5 and Chapter I, Fig. 4). However, in a distance of 5-10 mm the highest fluorescence and concentrations of Al were analyzed at an early degree of differentiation of pericycle cells at freshly developed xylem vessels substantiating enhanced translocation capacity of these zones.

In conclusion the results clearly present a well coordinated resistance and tolerance machinery which is not only acting at the root tip level but also at a root to shoot level which includes signal transduction and long distance transport processes which continuously discharge Al from Al-sensitive root-tip tissues and translocate it to Al-insensitive tissues and compartments.

Outlook

The results of the present work clearly show spatial and tissue specific differences in the accumulation of Al as well as distinct local differences in the detoxification and transportation involved processes. Moreover, various elements of the tolerance, resistance and transport mediating mechanisms are further characterized and are identified to represent key elements for further research on the Al accumulation in buckwheat. It is known, that for the precise analysis of Al-induced effects in Pattern II plants a strategy focusing on specific tissues will increase the likelihood of success in unraveling molecular mechanisms or in isolating transporters in plants where the Al-toxicity conditions induce specific genes (Ryan *et al.* 2003). In general, a major problem in transcriptomic approaches is the participation of cells or tissues, which are not directly involved in the physiological response reaction caused by a specific treatment. This problem is particularly important in Al-toxicity and/or Al tolerance / exclusion mechanisms because of the spatial characteristic of Al induced mechanisms on root tip level. The comparable high amount of transcripts of non target cells/tissues may mask induced minor changes in the expression of transcripts of interest from target cells/tissues. This tissue specificity was not only shown for pattern I plants (Sivaguru and Horst, 1998), where for instance a zone of ca. 2 mm in root apex, the distal transition zone of maize, is primary responsible for the expression of resistance and sensitivity, but also for pattern II plants like non-accumulators (Rangel *et al.*, 2007) and additionally for accumulators (Zheng *et al.*, 1998) and substantiated and extended in the own work (see chapters above). Moreover, in pattern I plants as buckwheat the analysis of locally defined regions and a comparison of specific tissues provides not only a promising chance, but the comparison of different tissues within one plant will represent most probably the only way for a progress in research on Al uptake and translocation mechanisms in buckwheat, because no induction of genes and *de-novo* protein synthesis might take place (Ma *et al.*, 2001) and no near-isogenic lines are available. Thus a genotypic comparison of two lines which only differ in Al-tolerance will not be possible. Therefore, the consecutive work should be focused into two different approaches following principally the same aim, the molecular unravelling of Al uptake and translocation in buckwheat, particularly on a locally defined level:

I. Expression analysis of physiologically determined candidate genes:

The present study clearly pinpoints the critical steps for Al uptake and translocation and moreover, involved key elements were hypothetically determined. Such possible key elements or candidate genes could code for proteins like for example citrate- and metal-chelate transporters, plasma membrane-located anion channels, for the efflux of oxalate or, proteins which are either involved in the synthesis of oxalate and citrate or their efflux. Furthermore, proteins which show integration into toxicity/sensitivity accounting mechanisms like pectin methyl esterases are of major importance. However, databases are showing a limited number of genomic and cDNA/EST sequences of non-model organism such as buckwheat. The NCBI nucleotide database contains in total only 451 (27.04.2010) nucleotide sequence records from buckwheat, and the biochemical relation to Al uptake and translocation involved genes will be most probably very different. Despite this low state of knowledge in the molecular background of non-model organisms and particularly in buckwheat, database-assisted molecular work even though offers basic *in-silico* research possibilities.

The alignment of sequences originating from several model-organisms or even molecularly better characterized plant species will allow the locating plant-species spanning conserved regions of the coding sequences of potential candidate genes. According to these sequences the design of degenerated primers will enable the amplification of specific homologous *Fagopyrum esculentum* sequences. These unique sequences could be sequenced after cloning into *Escherichia coli*. The knowledge of the specific *F. esculentum* sequence will facilitate to design primers directly for that particular plant species. These primers could subsequently be used for qRT-PCR-based expression analysis. Such expression analysis is not only able to resolve absolute differences in expression levels as expected for induced genes, but also quantitative differences in transcript levels which could be expected for constitutively expressed genes could be detected. Nicolíć *et al.* (2010) showed as well as for the hyperaccumulation of essential Cu and non-essential Cd that the presence of these metals increased the gene expression of tolerance-associated genes in buckwheat, even if the associated proteins are constitutively present. This expression analysis will be performed in different root tissues. The expression of a certain gene within the cortex as compared to its expression in the xylem parenchyma or the total root tip will reveal insights into the proposed stratification of involved mechanisms.

II. Global gene expression profiling in buckwheat tissues

Complex structures such as shoot apices and organ primordia can be micro-dissected into cells from individual constituent cell layers. Laser capture micro dissection (LCM) has the potential to completely resolve one cell type from the other, because individual cells of one type are removed from the tissue context (Kerk *et al.*, 2003). Stelar tissues were already compared with epidermal tissues of maize hypocotyls (Nakazono *et al.*, 2003). Moreover a comprehensive analysis of mRNA expression in rice phloem tissues was performed by Asano *et al.* (2002). Recently, Deeken *et al.* (2008) were able to identify genes required for long-distance RNA-signaling, which was performed by a genome-wide expression profiling of mRNAs isolated from *Arabidopsis* phloem tissue of inflorescence stalks and from leaf exudates. All these studies were able to perform transcriptomic analyses on these specific tissues. The results clearly reflected tissue-specific differences. This tissue-specific expression was either proven by *in-situ* hybridization (Asano *et al.*, 2002) or evaluated by qRT-PCR using specific primers for genes which are exclusively expressed in defined regions or cell types, respectively. The yield of total tissue-specific isolated RNA is limited by the small micro dissected sample volume. Therefore the small amounts of RNA have to be amplified by a T7-polymerase based amplification procedure.

Usually, subsequent to mRNA extraction of particular tissues or cells and the amplification of the RNA, microarrays are utilized to study the gene expression on a global scale. However, this method requires *a priori* knowledge of gene sequences. Therefore, this technique can not be applied as a tool for the discovery of novel transcripts in buckwheat. Since reliable results are usually obtained only for genes that are expressed in high or moderate levels (Liu *et al.*, 2006) the expression levels of low abundance genes cannot be readily assessed by DNA-microarray hybridization, as well.

Experience concerning suppression subtractive hybridization (SSH) technology provides hints for particular shortcomings of SSH-based expression analysis. This could be mainly explained by a limited number of clones analyzed and preferential amplification of cDNA fragments with special characteristics leading to a bias. This influences the obtained results directly and recognition of low-abundance transcripts may be impaired.

SuperSAGE is a new tool in functional Genomics, especially for *in-planta* analysis. This technique uses short cDNA fragments, so called “tags” with a length of 26 bp from a defined position in every transcript of a specific population. This defined specific region is excised by

an elegant application of serial linker ligation and restriction digestions. Subsequently, these tags are connected and cloned in a vector and sequenced in ultra large quantities. An cooperation with Peter Winter and Björn Rotter (GenXpro, Frankfurt, Germany) will guarantee analysis of at least 1,000,000 tags which is around 10,000 times more information of putatively functionally connected genes compared with output obtained by classic SSH analysis. The information about differential expression of specific candidate genes is obtained by advanced bioinformatic analysis. The quantitative information is obtained by a simple count of transcripts and the frequency of each tag directly reflects the abundance of the corresponding mRNA (Velculescu *et al.*, 1995)

Non-model plant species like particularly buckwheat possess numerous important traits not available for study in model plants, which emphasises the need for high-throughput transcript profiling generally applicable to all crop plants (Ceomans *et al.*, 2005). The above mentioned evaluation of specific candidate genes and their particular role in AI translocation and tolerance considers a transformation approach to be indispensable. Methods for *in vitro* regeneration of buckwheat have been elaborated more than two decades ago (Bohanec, 1987; Adachi *et al.*, 1989 and Yamane 1974) and this represents the prerequisite for a molecular approach. After the general susceptibility of buckwheat for *Agrobacterium tumefaciens*, the strain A281 was shown to be the most virulent strain (Nešković *et al.* 1990). The first transformation was performed by using the binary vector system pGA472 (Miljuš-Djukić *et al.*, 1992). Since the *A. tumefaciens*-based transformation is very time consuming, it is important to develop an *in planta* transformation that does not require sterile conditions of tissue culture and enable rapid functional gene analysis which is offered by Bratić *et al.* (2007). This technology allows gene expression and functional promoter analysis of specific buckwheat genes by using the pCAMBIA2301 and pCAMBIA-PL Vector system coupled with a GUS-reporter gene. This vector is electroporated into *A. tumefaciens* (Strain EHA 105) and finally transferred into buckwheat leaves by mild (10^2 Pa for 20 min) vacuum infiltration. Recently, this method has been shown to enhance buckwheat salt resistance via overexpression *AtNHX1*, a vacuolar Na^+/H^+ antiporter gene from *Arabidopsis thaliana*, following *A. tumefaciens* transformation. These plants were able to cope with much higher NaCl concentrations compared with the wild-type (Chen *et al.*, 2008). These both transformation systems allow either a persistent transformation of buckwheat, which produces transgenic plants with pin and thrum clones, which were already allowed to cross-pollinate (Miljuš-Djukić *et al.*, 1992), or the transient transformation for a short-term functional gene expression analysis for example in the root system, where the transformation protocol of

Outlook

Bratić *et al.* (2007) could be adapted to the infiltration of root systems of buckwheat. Additionally, confirmed differentially expressed genes could be used for *in situ* hybridization (Küpper *et al.*, 2007) e.g. for virus induced gene silencing (VIGS) of roots (Valentine *et al.*, 2004) or for the expression in ecotypes which were screened for low Al accumulation performance. This will clarify the physiological role of candidate genes in Al accumulation of buckwheat.

References

- Adachi T, Yamaguchi A, Miike Y, Hoffmann F. 1989. Plant regeneration from protoplasts of common buckwheat (*Fagopyrum esculentum*). *Plant Cell Rep.* 8, 247-250
- Adams F. 1984. Crop response to lime in the southern United States. In: Soil acidity and liming. Adams F. (ed.). American society of Agronomy. Inc. Madison, WI. 211-265.
- Jones LH. 1961. Aluminium uptake and toxicity in plants. *Plant Soil* 13, 297-310
- Ahn SJ, Sivaguru M, Chung GC, Rengel Z, Matsumoto H. 2002. Aluminium-induced growth inhibition is associated with impaired efflux and influx of H⁺ across the plasma membrane in root apices of squash (*Cucurbita pepo*). *J. Exp. Bot.* 53, 1959-1966.
- Amann C, Amberger A. 1989. Phosphorus efficiency of buckwheat (*Fagopyrum esculentum*). *J Plant Nutr Soil Sci* 152: 181-189
- Asano T, Masumura T, Kusano H, Kikuchi S, Kurita A, Shimada H, Kadowaki K. 2002. Construction of a specialized cDNA library from plant cells isolated by laser capture microdissection: toward comprehensive analysis of the genes expressed in the rice phloem. *Plant J.* 32, 401-408
- Barceló J, Poschenrieder C. 2002. Fast root growth responses, root exudates, and internal detoxification as clues to the mechanisms of aluminium toxicity and resistance: a review. *Environ. Exp. Bot.* 48, 75-92.
- Bennet RJ, Breen CM. 1991. The aluminium signal: New dimensions to mechanisms of aluminium tolerance. *Plant Soil* 134, 153-166.

References

- Blamey FPC, Edmeades DC, Wheeler DM. 1990. Role of root cation-exchange capacity in differential aluminum tolerance of *Lotus* species. *J. Plant Nutr.* 13, 729-744.
- Blamey FPC. 2001. The role of the root cell wall in aluminum toxicity. In: *Plant nutrient acquisition: New perspectives*. Ae N, Arihara J, Okada K, Srinivasan A (eds) Springer, Tokyo, 201–226.
- Bohanec B. 1987. Improvements in buckwheat micro-propagation procedures. *Fagopyrum* 7, 13-15
- Borrmann G, Seubert A. 1999. Aluminum speciation by means of anion chromatography and coupled anion/cation chromatography. *Anal. Chim. Acta* 386, 77-88.
- Brady NC, Weil RR. 2008. *The nature and properties of soils*. 14th ed Macmillan Publishing Company. New York, 358-400.
- Bratić A, Majić DB, Miljuš-Djukić JD, Jovanović ŽS, Maksimović VR. 2007. In planta transformation of Buckwheat (*Fagopyrum esculentum* Moench.). *Arch. Biol. Sci., Belgrade*, 59 135-138.
- Brauer D. 2001. Rapid inhibition of root growth in wheat is associated with aluminum uptake as followed by changes in morin fluorescence. *J. Plant Nutr.* 24, 1243-1253.
- Bravo-F P, Uribe EG. 1981. Temperature of the concentration kinetics of absorption of phosphate and potassium in corn roots. *Plant Physiol.* 67, 815-819.
- Briggs GE, Robertson RN. 1957. Apparent free space. *Annu. Rev. Plant Phys* 8, 11-30.
- Browne BA, McColl JG, Driscoll CT. 1990a. Aluminum speciation using morin: I. morin and its complexes with aluminum. *J. Environ Qual.* 19, 65-72.

- Browne BA, Driscoll CT, McColl JG. 1990b. Aluminum speciation using morin: II. principles and procedures. *J. Environ. Qual.* 19, 73-82.
- Brundrett MC, Enstone DE, Peterson CA. 1988. A berberine-aniline blue fluorescent staining procedure for suberine, lignine and callose in plant tissue. *Protoplasma* 146, 133-142.
- Carver BF, Ownby JD. 1995. Acid soil tolerance in wheat. *advances in agronomy* 54, 117-173.
- Chang YC, Yamamoto Y, Matsumoto H. 1999. Accumulation of aluminium in the cell wall pectin in cultured tobacco (*Nicotiana tabacum* L.) cells treated with a combination of aluminium and iron. *Plant Cell Environ.* 22, 1009-1017.
- Chen L-H, Zhang B, Xu Z-Q. 2008. Salt tolerance conferred by overexpression of *Arabidopsis* vacuolar Na⁺/H⁺ antiporter gene *AtNHX1* in common buckwheat (*Fagopyrum esculentum*). *Transgenic Res.* 17,121–132.
- Conner AJ, Meredith CP. 1985. Simulating the mineral environment of aluminium toxic soils in plant cell culture. *J. Exp. Bot.* 36, 870-880.
- Coelho CM, Trick HN, Kochian LV. 2007. A gene in the multidrug and toxic compound extrusion (MATE) family confers aluminum tolerance in sorghum. *Nature Genetics* 39, 1156-1161.
- Coemanns B, Matsumura H, Terauchi R, Remy S, Swennen R, Sági L. 2005. SuperSAGE combined with PCR walking allows global gene expression profiling in banana (*Musa acuminata*), a non-model organism. *Theor. Appl. Genet.* 111, 1118-1126.
- Cuenca G, Herrera R, Medina E. 1990. Aluminium tolerance in trees of a tropical cloud forest. *Plant Soil* 125, 169-175.

- Dalal RC. 1975. Hydrolysis products of solution and exchangeable aluminum in acidic soils. *Soil Sci.* 119, 127-131.
- Deeken R, Ache P, Kajahn I, Klingenberg J, Bringmann G, Hedrich R, 2008. Identification of *Arabidopsis thaliana* phloem RNAs provides a search criterion for phloem based transcripts hidden in complex datasets of microarray experiments. *Plant J.* 55, 746-759.
- Degenhardt J, Larsen PB, Howell SH, Kochian LV. 1998. Aluminum resistance in the arabidopsis mutant *alr-104* is caused by an aluminum-induced increase in rhizosphere pH. *Plant Physiol.* 117, 19-27.
- Delhaize E, Ryan PR, Randall PJ. 1993. Aluminum tolerance in wheat (*Triticum aestivum* L.) II. aluminum stimulated excretion of malic acid from root apices. *Plant Physiol.* 103, 695-702.
- Delhaize E, Ryan PR. 1995. Aluminum toxicity and tolerance in plants. *Plant Physiol.* 107, 315-321.
- Delhaize E, Ryan PR, Hebb DM, Yamamoto Y, Sasaki T, Matsumoto H. 2004. Engineering high-level aluminum tolerance in barley with the ALMT1 gene. *PNAS* 101, 15249-15254.
- Delhaize E, Gruber BD, Ryan PR. 2007. The roles of organic anion permeases in aluminium resistance and mineral nutrition. *FEBS Letters* 581, 2255-2262.
- Downs, AJ. 1993. Chemistry of the group 13 metals: some themes and variations. In: Chemistry of Gallium, Indium and Thallium. Downs AJ (ed.). Blackie Academic & Professional, Glasgow, UK.
- Duckett CM, Oparka KJ, Prior DAM, Dolan L, Roberts K. 1994. Dye coupling in the root epidermis of *Arabidopsis* is progressively reduced during development. *Development* 120, 3247-3255.

- Durrett TP, Gassmann W, Rogers EE. 2007. The FRD3-mediated efflux of citrate into the root vasculature is necessary for efficient iron translocation. *Plant Phys.* 144, 197–205.
- Eticha D, Staß A, Horst WJ. 2005a. Localization of aluminium in the maize root apex: can morin detect cell wall-bound aluminium? *J. Exp. Bot.* 415, 1351–1357.
- Eticha D, Stass A, Horst, WJ. 2005b. Cell-wall pectin and its degree of methylation in the maize root-apex: significance for genotypic differences in aluminium resistance. *Plant Cell Environ.* 28, 1410–1420.
- Eticha D, Thé C, Welcker C, Narro L, Staß A, Horst WJ. 2005c. Aluminium-induced callose formation in root apices: inheritance and selection trait for adaption of tropical maize to acid soils. *Field Crop Res* 93, 252-263.
- Fry SC. 1988. *The growing plant cell wall: chemical and metabolic analysis*. Harlow England, Longman Scientific & Technical, and subsequently, New York, Wiley.
- Glass ADM. 2007. The apoplast: a kinetic perspective. In: *The apoplast of higher plants: compartment of storage, transport and reactions*. Sattelmacher B, Horst WJ, (eds.), Dordrecht, the Netherlands: Springer, 87-96.
- Green, L. S., Rogers, E. E. 2004. *FRD3* Controls Iron localization in *Arabidopsis*. *Plant Phys.* 136, 2523–2531
- Gutierrez, A. C., Gehlen, M. H. 2002. Time resolved fluorescence spectroscopy of quercetin and morin complexes with Al³⁺. *Spectrochim Acta A*, 58, 83-89
- Happel O, Seubert A. 2006. Characterization of stable aluminium-citrate species as reference substances for aluminum speciation by ion chromatography. *J. Chromatogr. A* 1108, 68-75.

- Happel O. 2007. Elementspeziesanalytik anionischer Aluminium-Carbonsäure-Komplexe mittels Ionenchromatographie. PhD thesis, Philipps-Universität Marburg, Marburg, Germany.
- Haug A. 1984. Molecular aspects of aluminum toxicity. *Crit. Rev. Plant Sci.* 1, 345–373
- Hayes JE, Ma, JF. 2003. Al-induced efflux of organic acid anions is poorly associated with internal organic acid metabolism in triticale roots. *J. Exp. Bot.* 54, 1753-1759
- Hede AR, Skovmand B, López-Cesati J. 2001. Acid soils and aluminium toxicity. In: Application of physiology in wheat breeding. Reynolds, M.P., Ortiz-Monasterio, J.I. McNab, A., (eds.), Mexico, D.F., CIMMYT, 172–182.
- Heine G, Tikum G, Horst WJ. 2005. Silicon nutrition of tomato and bitter gourd with special emphasis on silicon distribution in root fractions. *J. Plant Nutr. Soil Sci.* 168, 600-606.
- Heine G, Tikum G, Horst WJ. 2007. The effect of silicon on the infection by and spread of *Phytium aphanidermatum* in single roots of tomato and bitter gourd. *J. Exp. Bot.* 58: 569-577.
- Hokenga OA, Maron LG, Piñeros MA, Cancado GMA, Shaff J, Kobayashi Y, Ryan PR, Dong B, Delhaize E, Sasaki T, Matsumoto H, Yamamoto Y, Koyama H, Kochian LV. 2006. AtALMT1, which encodes a malate transporter, is identified as one of several genes critical for aluminum tolerance in arabidopsis. *PNAS* 103, 9738-9743.
- Horst WJ, Asher CJ, Cakmak I, Szulkiewicz P, Wissemeier AH. 1992. Short-term responses of soybean roots to aluminium. *J. Plant Physiol.* 140, 174-178.
- Horst WJ. 1995. The role of the apoplast in aluminium toxicity and resistance of higher plants: A review. *Z. Pflanzenernähr. Bodenk.* 158, 419-428.

- Horst WJ, Püschel A-K, Schmohl N. 1997. Induction of callose formation is a sensitive marker for genotypic aluminium sensitivity in maize. *Plant Soil* 192, 23-30.
- Horst WJ, Schmohl N, Kollmeier M, Baluška F, Sivaguru M. 1999. Does aluminium affect root growth of maize through interaction with the cell wall – plasma membrane – cytoskeleton continuum? *Plant Soil* 215, 163-174.
- Horst WJ, Kollmeier M, Schmohl N, Sivaguru M, Wang Y, Felle HH, Hedrich R, Schröder W, Staß A. 2007. Significance of the root apoplast for aluminium toxicity and resistance of maize. In: *The apoplast of higher plants: compartment of storage, transport and reactions*. Sattelmacher B, Horst WJ, (eds) Springer, Dordrecht, pp 49-66.
- Horst WJ, Wang Y, Eticha D. 2010. The role of the root apoplast in aluminium-induced inhibition of root elongation and in aluminium resistance of plants: a review. *Annal Bot.* doi:10.1093/aob/mcq053.
- Jansen S, Broadley MR, Robbrecht E, Smets E. 2002a. Aluminum hyperaccumulation in angiosperms: a review of its phylogenetic significance. *Bot. Rev.* 68, 235-269.
- Jansen S, Watanabe T, Smets E. 2002b. Aluminium accumulation in leaves of 127 species in *Melastomataceae*, with comments on the order *Myrtales*. *Annal. Bot.*, 90, 53-64.
- Jiang Y, Lee A, Chen J, Cadene M, Chait BT, MacKinnon R. 2002. Crystal structure and mechanism of a calcium gated potassium channel. *Nature* 417, 515-522.
- Jones LH. 1961. Aluminium uptake and toxicity in plants. *Plant Soil*. 13, 297-310.

References

- Jones DL, Blancaflor EB, Kochian LV, Gilroy S. 2006. Spatial coordination of aluminium uptake, production of reactive oxygen species, callose production and wall rigidification in maize roots. *Plant Cell Environ.* 29, 1309-1318.
- Kataoka T, Iikura H, Nakanishi TM. 1997. Aluminum distribution and viability of plant root and cultured cells. *Soil Sci. Plant Nutr.* 43, 1003–1007.
- Katyal M, Prakash S. 1977. Analytical reactions of hydroxyflavones. *Talanta*, 24, 367-375.
- Kerven GL, Edwards DG, Asher CJ, Hallman PS, Kokot S. 1989. Aluminium determination in soil solution. II. short-term colorimetric procedures for the measurement of inorganic monomeric aluminium in the presence of organic acid ligands. *Austr. J. Soil Res.* 27, 91–102.
- Kinraide TB, Parker DR, Zobel RW. 2005. Organic acid secretion as a mechanism of aluminium resistance: a model incorporating the root cortex, epidermis, and the external unstirred layer. *J. Exp. Bot.* 56, 1853–1865.
- Klein MA, Sekimoto H, Milner MJ, Kochian LV. 2008. Investigation of heavy metal hyperaccumulation at the cellular level: development and characterization of *Thlaspi caerulescens* suspension cell lines. *Plant Phys.* 147, 2006–2016.
- Klug B, Horst WJ. 2010. Spatial characteristics of aluminum uptake and translocation in roots of buckwheat (*Fagopyrum esculentum* Moench). *Physiol. Plant.* 139, 181-191.
- Klug B, Horst, WJ, 2010. Oxalate exudation into the root-tip water free space confers protection from Al toxicity and allows Al accumulation in the symplast in buckwheat (*Fagopyrum esculentum*). *New Phytol.* DOI: 10.1111/j.1469-8137.2010.03288.x
- Kochian LV, Lucas WJ. 1988. Potassium Transport in roots. *Adv. Botany Res.* 15, 93–177.

- Kochian LV. 1995. Cellular mechanisms of aluminum toxicity and resistance in plants. *Annu. Rev. Plant Phys. Plant Mol. Biol.* 46, 237-260.
- Kochian LV, Hoekenga OA, Piñeros MA. 2004. How do crop plants tolerate acid soils? Mechanisms of Aluminum tolerance and Phosphorus efficiency. *Annu. Rev. Plant Biol.* 55, 459-493.
- Kochian LV, Piñeros MA, Hoekenga OA. 2005. The physiology, genetics and molecular biology of aluminum resistance and toxicity. *Plant Soil* 274, 175-195.
- Kollmeier M, Felle HH, Horst WJ. 2000. Genotypical differences in aluminum resistance of maize are expressed in the distal part of the transition zone. is reduced basipetal auxin flow involved in inhibition of root elongation by aluminum? *Plant Physiol.* 122, 945-956.
- Kollmeier M, Dietrich P, Bauer CS, Horst WJ, Hedrich R. 2001. Aluminum activates a citrate-permeable anion channel in the aluminum-sensitive zone of the maize root apex. A comparison between an aluminum-sensitive and an aluminum resistant cultivar. *Plant Physiol.* 126, 397–410
- Köhler B, Raschke K. 2007. Loading of ions into the xylem of the root. In: *The apoplast of higher plants: Compartment of storage, transport and reactions The significance of the apoplast for the mineral nutrition of higher plants.* Eds.: Sattelmacher, B., Horst, W. J., Springer Netherlands
- Kurz H, Schulz R, Römheld V. 1999. Selection of cultivars to reduce the concentration of cadmium and thallium in food and fodder plants. *J. Plant Nutr. Soil Sci.* 162, 323-328
- Küpper H, Seib LO, Sivaguru M, Hoekenga OA, Kochian LV. 2007. A method for cellular localization of gene expression via quantitative in situ hybridization in plants. *Plant J.* 50, 159–175

- Lacombe B, Pilot G, Gaymard F, Sentenac H, Thibaud J. B. 2000. pH Control of the plant outwardly-rectifying potassium channel *Skor*. *FEBS Lett.* 466, 351-354
- Larsen PB, Degenhardt J, Tai C-Y, Stenzler LM, Howell SH, Kochian LV. 1998. Aluminum-resistant *Arabidopsis* mutants that exhibit altered patterns of aluminum accumulation and organic acid release from roots. *Plant Physiol.* 117, 9-17.
- Lazof DB, Goldsmith JG, Rufty TW, Linton RW. 1996. The early entry of Al into root cells of intact soybean roots. A comparison of three developmental root regions using secondary ion mass spectrometry imaging. *Plant Physiol.* 108, 152–160.
- Levesque L, Mizzen CA, McLachlan DR, Fraser PE. 2000. Ligand specific effects on aluminum incorporation and toxicity in neurons and astrocytes. *Brain Res.* 877, 191–202.
- Li YY, Yang JY, Zhang YJ, Zheng SJ. 2009a. Disorganized distribution of homogalacturonan epitopes in cell walls as one possible mechanism for aluminium-induced root growth inhibition in maize. *Ann. Bot.* 104, 235-241.
- Li YY, Zhang YJ, Zhou Y, Yang JL, Zheng, SJ. 2009b. Protecting cell walls from binding aluminum by organic acids contributes to aluminum resistance. *J. Integr. Plant. Biol.* 51: 574-580.
- Li XF, Ma JF, Matsumoto H. 2000. Pattern of Aluminum-induced secretion of organic acids differs between rye and wheat. *Plant Physiol.* 123, 1537-1544.
- Lian H-Z, Kang Y-F, Bi S, Yasin A, Shao D-L, Chen Y-J, Dai L-M, Tian L-C. 2003. Morin applied in speciation of aluminium in natural waters and biological samples by reversed-phase high-performance liquid chromatography with fluorescence detection. *Anal. Bioanal. Chem.* 376, 542–548.

References

- Liao H, Wan H, Shaff J, Wang X, Yan X, Kochian LV. 2006. Phosphorus and aluminum interactions in soybean in relation to aluminum tolerance. Exudation of specific organic acids from different regions of the intact root system. *Plant Physiol.* 141, 674–684.
- Liu J, Magalhaes JV, Shaff J, Kochian LV. 2009. Aluminum-activated citrate and malate transporters from the MATE and ALMT families function independently to confer *Arabidopsis* aluminum tolerance. *Plant J.* 57, 389-399.
- Lombi E, Zhao FJ, McGrath SP, Young SD, Sacchi GA. 2001. Physiological evidence for a high affinity cadmium transporter highly expressed in a *Thlaspi caerulescens* ecotype. *New Phytol.* 149, 53-60.
- Maathuis FJM, May ST, Graham, NS, Bowen HC, Jelitto TC, Trimmer P, Bennett MJ, Sanders D, White PJ. 1998. Cell marking in *Arabidopsis thaliana* and its application to patch-clamp studies. *Plant J.* 15, 843–851.
- Ma G, Rengasamy P, Rathjen AJ. 2003. Phytotoxicity of aluminium to wheat plants in high-pH solutions. *Aust. J. Exp. Agric.* 43, 497–501.
- Ma JF, Hiradate S, Nomoto K, Iwashita T, Matsumoto H. 1997a. Internal detoxification mechanism of Al in *Hydrangea*. *Plant Physiol.* 113, 1033-1039.
- Ma JF, Zheng SJ, Matsumoto H. 1997b. Detoxifying aluminium with buckwheat. *Nature* 390, 569-560.
- Ma JF, Hiradate S, Matsumoto H. 1998. High aluminum resistance in buckwheat II. oxalic acid detoxifies aluminum internally. *Plant Physiol.* 117, 753–759.
- Ma JF, Hiradate S. 2000. Form of aluminium for uptake and translocation in buckwheat (*Fagopyrum esculentum* Moench). *Planta* 211, 355-360.
- Ma JF, Ryan PR, Delhaize E. 2001. Aluminium tolerance in plants and the complexing role of organic acids. *Trends Plant Sci.* 6, 273-278

- Ma JF, Shen R, Zhao Z, Wissuwa M, Takeuchi Y, Ebitani T, Yano M. 2002. Response of rice to Al stress and identification of quantitative trait loci for Al tolerance. *Plant Cell Physiol.* 43, 652-659.
- Ma JF, Furukawa J. 2003. Recent progress in the research of external Al detoxification in higher plants: a minireview. *J. Inorg. Biochem.* 97, 46-51.
- Ma JF, Shen R, Nagao S, Tanimoto E. 2004. Aluminum targets elongating cells by reducing cell wall extensibility in wheat roots. *Plant Cell Physiol.* 45, 583-589.
- MacLean FT, Gilbert BE. 1927. The relative aluminum tolerance of crop plants. *Soil Sci.* 24, 163-176.
- Magalhaes JV. 2003 Molecular genetic and physiological investigations of aluminum tolerance in sorghum (*Sorghum bicolor* L. Moench). Ph.D. thesis, Cornell University, Ithaca, USA.
- Magalhaes JV, Liu J, Guimarães CT., Lana UGP, Alves VMC, Wang Y-H, Schaffert RE, Hoekenga OA, Piñeros MA, Shaff JE, Klein PE, Carneiro NP, Coelho CM, Trick HN, Kochian LV. 2007. A gene in the multidrug and toxic compound extrusion (MATE) family confers aluminum tolerance in sorghum. *Nature Genetics* 39, 1156-1161.
- Magistad, OC. 1925. The Aluminum content of the soil solution and its relation to soil reaction and plant growth. *Soil Sci.* 20, 181-226.
- Marion GM, Hendricks DM, Dutt GR, Fuller WH. 1976. Aluminium and silica solubility in soils. *Soil Sci.* 121, 76-85.
- Mariano ED, Keltjen WG. 2003. Evaluating the role of root citrate exudation as a mechanism of aluminium resistance in maize genotypes. *Plant Soil* 256, 469-479.

References

- Marion GM, Hendricks DM, Dutt GR, Fuller WH. 1976. Aluminium and silica solubility in soils. *Soil Sci.* 121, 76–85.
- Martell AE, Smith RM. 1982. *Critical stability constants*. New York, USA. Plenum press.
- Martin RB. 1986. The chemistry of Aluminum as related to biology and medicine. *Clin. Chem.* 32, 1797-1806.
- Martin RB. 1988. Bioinorganic chemistry of Aluminum. In: *Metal Ions in biological systems Vol 24. Aluminum and its role in biology*. Siegel, H. (ed), Macrel Dekker, New York, NY. 1-57.
- Matsumoto H, Hirasawa E, Morimura S, Takahashi E. 1976. Localization of aluminium in tea leaves. *Plant Cell Physiol.* 17, 627-631.
- Matsumoto H. 2000. Cell biology of Aluminum toxicity and tolerance in higher plants. *International review of cytology – a survey of cell biology*. In: Jeon, K. W. (ed.) Vol 200. Academic press, San Diego, CA. 1-37.
- Milner MJ, Kochian LV. 2008. Investigating heavy-metal hyperaccumulation using *Thlaspi caerulescens* as a model system. *Annal. Bot.* 102, 3-13.
- Miljuš-Djukić J, Nešković M, Ninković S, Crkvenjakov R, 1992. *Agrobacterium* mediated transformation and plant regeneration of buckwheat (*Fagopyrum esculentum* Moench.) *Plant Cell Tiss. Org.* 29, 101-108.
- Miyasaka SC, Buta JG, Howell RK, Foy CD. 1991. Mechanism of aluminum tolerance in snapbeans. Root exudation of citric acid. *Plant Physiol.* 96, 737-743.
- Moyer-Henry K, Silva I, MacFall J, Johannes E, Allen N, Goldfarb B, Rufty T 2005. Accumulation and localization of aluminium in root tips of loblolly pine

- seedlings and the associated ectomycorrhiza *Pisolithus tinctorius*. *Plant Cell Environ.* 28, 111-120.
- Nakazono M, Qiu F, Borsuk LA, Schnable PS. 2003. Laser-Capture Microdissection, a tool for the global analysis of gene expression in specific plant cell types: Identification of genes expressed differentially in epidermal cells or vascular tissues of maize. *Plant cell* 15, 583-596.
- Naumann, A. 2001. Aufnahme und Verlagerung von Aluminium bei Hortensie (*Hydrangea macrophylla*) in Beziehung zur Aluminiumtoleranz und zur Blaufärbung der Sepalen. PhD Thesis, Leibniz Universität Hannover, Germany.
- Naumann A, Horst WJ. 2003. Effect of aluminium supply on aluminium uptake, translocation and blueing of *Hydrangea macrophylla* (Thunb.) Ser. cultivars in a peat-clay substrate. *J. Hortic. Sci. Biotech.* 78, 463-469.
- Nešković M, Vujičić R, Srejšević V, 1990. Differential responses of Buckwheat leaf cells to growth substances stimulating cell division. *Ann. Bot.* 56, 755-760.
- Nikolić DB, Samardžić JT, Bratić AM, Radin IP, Gavrilović SP, Rausch T, Maksimović VR 2010. Buckwheat (*Fagopyrum esculentum* Moench) FeMT3 gene in heavy metal stress: protective role of the protein and inducibility of the promoter region under Cu²⁺ and Cd²⁺ treatments. *J. Agric. Food Chem.* 58, 3488-3494.
- Oparka KJ, Denton AM, Wright P, Wright KM. 1995. Symplastic communication between primary and developing lateral roots of *Arabidopsis thaliana*. *J. Exp. Bot.* 46, 187-197.
- Orvig C. 1993. The aqueous coordination chemistry of aluminum. In: Coordination chemistry of aluminum. Robinson GH (ed.). New York, USA: VCH Publishers Inc., 85–121.

References

- Pellet DM, Papernik LA, Kochian LV. 1996. Multiple aluminum-resistance mechanism in wheat (roles of root apical phosphate and malate exudation) Plant Physiol. 112, 591-597.
- Peng X, Yu L, Yang C, Liu Y. 2003. Genotypic differences in aluminum resistance and oxalate exudation of buckwheat. J. Plant. Nutr. 26: 1767-1777.
- Piñeros MA, Shaff JE, Manslank HS, Carvalho Alves VM, Kochian LV. 2005. Aluminum resistance in maize cannot be solely explained by root organic acid exudation. a comparative physiological study. Plant Physiol. 137, 231-241.
- Pitman MG. 1964. The effect of divalent cations on the uptake of salt by beetroot tissue. J. Exp. Bot. 15, 444-456.
- Pitman MG. 1971. Uptake and transport of ions in barley seedlings. I. estimation of chloride fluxes in cells of excised roots. Aust. J. Biol. Sci. 24, 407-421.
- Pitman MG, Wildes RA, Schaefer N, Wellfare D. 1977. Effect of azetidine 2-carboxylic acid on ion uptake and ion release to the xylem of excised barley roots. Plant Physiol. 60, 240-246.
- Rangel AF, Mobin M, Rao IM, Horst WJ. 2005. Proton toxicity interferes with the screening of common bean (*Phaseolus vulgaris* L.) genotypes for aluminium resistance in nutrient solution. J.. Plant Nutr.. Soil Sci. 168, 607–616.
- Rangel, AF, Rao IM, Horst WJ. 2007. Spatial aluminium sensitivity of root apices of two common bean (*Phaseolus vulgaris* L.) genotypes with contrasting aluminium resistance. J. Exp. Bot, 58, 3895–3904.
- Rangel AP, Rao IM, Horst WJ. 2009. Intracellular distribution and binding state of aluminum in root apices of two common bean (*Phaseolus vulgaris*) genotypes in relation to Al toxicity. Physiol. Plant 135, 162-173.

References

- Rao IM, Zeigler RS, Vera R, Sarkarung S. 1993. Selection and breeding for acid-soil tolerance in crops – upland rice and tropical forages as case studies. *Biosci.* 43, 454-465.
- Rees WJ, Sidrak GH. 1955. Plant growth on fly-ash. *Nature* 176, 352.
- Rengel Z. 1992. Role of calcium in aluminium toxicity. *New Phytol.* 121, 499–513.
- Rengel Z. 1996. Uptake of aluminum by plant cells. *New Phytol.* 134, 389–406.
- Ryan PR, Ditomaso JM, Kochian LV. 1993. Aluminum toxicity in roots: An investigation of spatial sensitivity and the role of the root cap. *J. Exp. Bot.* 259, 437-446.
- Ryan PR, Delhaize E, Randall EJ. 1995. Characterisation of Al-stimulated efflux of malate from the apices of Al-tolerant wheat roots. *Planta* 96, 103-110.
- Ryan PR, Delhaize E. 2001. Function and mechanism of organic acid exudation from plant roots. *Ann. Rev. Plant Phys. Plant Mol. Biol.* 52, 527-560.
- Ryan PR, Dong B, Watt M, Kataoka T, Delhaize E. 2003. Strategies to isolate transporters that facilitate organic anion efflux from plant roots. *Plant Soil* 248, 61–69.
- Roberts SK, Tester M. 1995. Inward and outward K⁺-selective currents in the plasma membrane of protoplasts from maize root cortex and stele. *Plant J.*, 8, 811–825.
- Ryan PR, Delhaize E, Jones DL. 2001. Function and mechanism of organic acid anion exudation from plant roots. *Ann. Rev. Plant Physiol. Plant Mol. Biol.* 52, 527–560.
- Saarl LA, Seitz WR. 1983. Immobilized morin as fluorescence sensor for determination of aluminum(III). *Anal. Chem.* 55, 667-670.

References

- Sasaki T, Yamamoto Y, Ezaki B, Katsuhara M, Ahn SJ, Ryan PR, Delhaize E, Matsumoto H. 2004. A wheat gene encoding an aluminum-activated malate transporter. *Plant J.* 37, 645-653.
- Sawada T, Shibamoto T, Kamada H. 1978. Fluorescence lifetime measurements of morin-metal ion complexes. *B Chem. Soc. Jpn.* 51, 1736-1738.
- Ščančar J, Milačič R. 2006. Aluminium speciation in environmental samples: a review. *Anal. Bioanal. Chem.* 386, 999-1012.
- Schmohl N, Horst WJ. 2001. Cell-wall pectin-content modulates aluminium sensitivity of *Zea mays* L. cells grown in suspension culture. *Plant Cell Environ.* 23, 735-742.
- Shaff JE, Schultz BA, Craft EJ, Clark RT, Kochian LV. 2010. GEOCHEM-EZ: a chemical speciation program with greater power and flexibility. *Plant Soil* 330, 207-214.
- Shen R, Ma JF. 2001. Distribution and mobility of aluminium in an Al-accumulating plant, *Fagopyrum esculentum* Moench. *J. Exp. Bot.* 52, 1683-1687.
- Shen RF, Iwashita T, Ma JF. 2004. Form of Al changes with Al concentration in leaves of buckwheat. *J. Exp. Bot.* 55, 131-136.
- Shen RF, Chen RF, Ma JF. 2006. Buckwheat accumulates aluminum in leaves but not in seeds. *Plant Soil* 284, 265-273.
- Shuman MS. 1992. Dissociation pathways and species distribution of aluminum bound to an aquatic fulvic acid. *Environ. Sci. Technol.* 26, 593–598.
- Siebrecht S, Tischner R. 1999. Changes in the xylem exudate composition of poplar (*Populus tremula* x *P. alba*)- dependent on the nitrogen and potassium supply. *J. Exp. Bot.* 50, 1797-1806.

- Silva IR, Smyth TJ, Moxley DF, Carter TE, Allen NS, Rufty TW. 2000. Aluminium accumulation at nuclei of cells in the root tip. fluorescence detection using lumogallion and confocal laser scanning microscopy. *Plant Physiol.* 123, 543–552.
- Sivaguru M, Horst WJ. 1998. The distal part of the transition zone is the most aluminum-sensitive apical root zone of maize. *Plant Physiol.* 116, 155-163.
- Sivaguru M, Baluška F, Volkmann D, Felle HH, Horst WJ. 1999. Impacts of aluminum on the cytoskeleton of the maize root apex. short-term effects on the distal part of the transition zone. *Plant Physiol.* 119, 1073-1082.
- Sivaguru M, Fujiwara T, Šamaj J, Baluška F, Yang Z, Osawa H, Maeda T, Mori T, Volkmann D, Matsumoto H. 2000. Aluminum-induced 1→3-β-D-glucan inhibits cell-to-cell trafficking of molecules through plasmodesmata. a new mechanism of aluminum toxicity in plants. *Plant Physiol.* 124, 991-1005.
- Stass A, Wang Y, Eticha D, Horst WJ. 2006. Aluminium rhizotoxicity in maize grown in solutions with Al³⁺ or Al(OH)₄⁻ as predominant solution Al species. *J. Exp. Bot.* 57, 4033-4042.
- Stass A, Kotur Z, Horst WJ. 2007. Effect of boron on the expression of aluminium toxicity in *Phaseolus vulgaris*. *Physiol. Plant.* 131, 283-290.
- Sure B. 1955. Nutritive value of proteins in buckwheat and their role as supplements to proteins in cereal grains. *J. Agr. Food Chem.* 3, 793-795.
- Sutheimer SH, Cabaniss SE. 1995. Aqueous Al(III) speciation by high-performance cation exchange chromatography with fluorescence detection of the aluminum-lumogallion complex. *Anal. Chem.* 67, 2342-2349.
- Takano J, Noguchi K, Yasumori M, Kobayashi M, Gajdos Z, Miwa K, Hayashi H, Yoneyama T, Fujiwara T. 2002. Arabidopsis boron transporter for xylem loading. *Nature* 420, 337-340.

- Takeda K, Kariuda M, Itoi H. 1985. Blueing of sepal colour of *Hydrangea macrophylla*. *Phytochem.* 24, 2251-2254.
- Tanoi K, Hayashi Y, Iikura H, Nakanishi M. 2001. Aluminum detection by lumogallion staining method in plants. *Anal. Sci*, 17, 1455-1458.
- Taylor GJ. 1988. The physiology of aluminum phytotoxicity. In: *Metal Ions in Biological Systems*. Sigel H., Sigel, A. (eds.) Vol 24. Marcel Dekker, New York, 123-163.
- Taylor GJ. 1991. Current views of the aluminum stress response: the physiological basis of tolerance. *Curr. Top. Plant Biochem. Physiol.* 10, 57-93.
- Taylor GJ, McDonald-Stephens JL, Hunter DB, Bertsch PM, Elmore D, Rengel Z, Reid RJ. 2000. Direct measurement of aluminum uptake and distribution in single cells of *Chara corallina*. *Plant Physiol.* 123, 987-996.
- Tice KR, Parker DR, DeMason DA. 1992. Operationally defined apoplastic and symplastic aluminum fractions in root tips of aluminum-intoxicated wheat. *Plant Physiol.* 100, 309-318.
- Turner RC, Clark JS. 1966. Lime potential in acid clay and soil suspensions. *Trans. Comm. II & IV Int. Soc. Soil Science*: 208-215
- Ueno D, Iwashita T, Zhao F-J, Ma JF. 2008. Characterization of Cd translocation and identification of the Cd form in xylem sap of the Cd-hyperaccumulator *Arabidopsis halleri*. *Plant Cell Physiol.* 49, 540-548.
- Varfolomeyev SD, Gurevich KG. 2001. The hyperexponential growth of the human population on a macrohistorical scale. *J. Theor. Biol.* 212, 367-372

References

- Vance GF, Stevenson FJ, Sikora FJ. 1996. Environmental chemistry of aluminum-organic complexes. In: The Environmental Chemistry of Aluminum. Spostio, G. (ed.) Boca Raton, USA: CRC Press Inc, 169–220.
- Velculescu, VE, Zhang L, Vogelstein B, Kinzler KW. 1995. Serial analysis of gene expression. *Science* 270, 484-487.
- Verbruggen N, Hermans C, Schat, H. 2009. Molecular mechanisms of metal hyperaccumulation in plants. *New Phytol* 181, 759–776.
- Von Uexkull HR, Mutert E. 1995. Global extent development and economic importance of acid soils. *Plant Soil* 171, 1-15.
- Waignann E, Zambryski P. 1995. Tobacco mosaic virus movement protein-mediated protein transport between trichome cells. *Plant Cell* 7, 2069-2079.
- Walker TS, Bais HP, Grotewold E, Vivanco JM 2003. Root exudation and rhizosphere biology. *Plant Physiol.* 132, 44-51.
- Wang Y, Stass A, Horst WJ. 2004. Apoplastic binding of aluminum is involved in silicon-induced amelioration of aluminum toxicity in maize. *Plant Physiology* 136, 3762–3770.
- Watanabe T, Osaki M, Yoshihara T and Tadano T 1998a. Distribution and chemical speciation of aluminum in the Al accumulator plant, *Melastoma malabathricum* L. *Plant Soil* 201, 165–173.
- Wenzl P, Patiño GM, Chaves AL, Mayer JE, Rao IM. 2001. The high level of Aluminum resistance in signalgrass is not associated with known mechanisms of external aluminum detoxification in root apices. *Plant Physiol.* 125, 1473-1484.

- Wenzl P, Chaves AL, Patiño GM, Mayer JE, Rao IM. 2002. Aluminium stress stimulates the accumulation of organic acids in root apices of *Brachiaria* species. *J. Plant. Nutr. Soil Sci.* 165, 583-588.
- Williams L, Salt DE. 2009. The plant ionome coming into focus. *Curr. Opin. Plant Biol.* 12, 247-249.
- Yang ZM, Sivaguru M, Horst WJ, Matsumoto H. 2000. Aluminum tolerance is achieved by exudation of citric acid from roots of soybean. *Physiol. Plant.* 110, 72-77.
- Yamamoto Y, Kobayashi Y, Devi SR, Rikiishi S, Matsumoto H. 2001. Aluminum toxicity is associated with mitochondrial dysfunction and the production of reactive oxygen species in plant cells. *Plant Physiol.* 128, 63-72.
- Yamane Y. 1974. Induced differentiation of buckwheat plants from subcultured calluses *in vitro*. *Jap. J. Genet.* 49, 139-146.
- Yang JL, Zheng SJ, He YF, Tang CX, Zhou GD. 2005a. Genotypic differences among plant species in response to aluminum stress. *J. Plant Nutr.* 28, 949-961.
- Yang JL, Zheng SJ, He YF, You JF, Zhang L, Yu XH. 2005b. Comparative studies on the effect of a protein-synthesis inhibitor on aluminium-induced secretion of organic acids from *Fagopyrum esculentum* Moench and *Cassia tora* L. *Plant Cell Environ* 29, 240-246.
- Yang JL, Li YY, Zhang YJ, Zhang SS, Wu P, Zheng, SJ. 2008. Cell wall polysaccharides are specifically involved in the exclusion of aluminum from the rice root apex. *Plant Physiol.* 146, 602-611.
- You JF, He YF, Yang JL, Zheng, SJ. 2005. A comparison of aluminum resistance among *Polygonum* species originating on strongly acidic and neutral soils. *Plant Soil* 276, 143–151.

- Yu Q, Tang C, Chang Z, Kuo J. 1999. Extraction of apoplastic sap from plant roots by centrifugation. *New Phytol.* 143, 299-304.
- Zheng SJ, Ma JF, Matsumoto H. 1998. High aluminum resistance in buckwheat. I. Al-induced specific secretion of oxalic acid from root tips. *Plant Physiol.* 117, 745–751.
- Zheng SJ, Yang JL, He, YF, Yu XH, Zhang L, You JF, Shen RF, Matsumoto H. 2005. Immobilization of aluminum with phosphorus in roots is associated with high aluminum resistance in buckwheat. *Plant Physiol.* 138, 297-303.
- Zhou L-L, Bai G-H, Ma H-X, Carver BF. 2007. Quantitative trait loci for aluminum resistance in wheat. *Mol. Breeding* 19, 153-161.
- Zhu Y-G, He Y-Q, Smith SE, Smith FA 2002. Buckwheat (*Fagopyrum esculentum* Moench) has high capacity to take up phosphorus (P) from a calcium (Ca)-bound source. *Plant Soil* 239: 1

Supplemental material

Supplemental material 1. Tabel of screened *Fagopyrum* genotypes. Run ID represents the number used in the graphs. The FAG number is the accession code provided by the gene bank of the Leibniz Institute of Plant Genetics and Crop Plant Research (IPK, Gatersleben, Germany).

Run ID	FAG	Name	Cultivar	Origin
1	21	<i>Fagopyrum tataricum</i> (L.) Gaertn.		
2	26	<i>Fagopyrum tataricum</i> (L.) Gaertn.	Welsford	
3	27	<i>Fagopyrum tataricum</i> (L.) Gaertn.		
4	29	<i>Fagopyrum esculentum</i> Moench var. <i>esculentum</i>	Amurskaja	Sowjetunion
5	30	<i>Fagopyrum esculentum</i> Moench var. <i>esculentum</i>	Bogaty	Sowjetunion
6	31	<i>Fagopyrum esculentum</i> Moench var. <i>esculentum</i>	Belokatajskaja Mestnaja	Sowjetunion
7	33	<i>Fagopyrum esculentum</i> Moench var. <i>esculentum</i>	Tarskaja Mestnaja	Sowjetunion
8	35	<i>Fagopyrum esculentum</i> Moench var. <i>esculentum</i>	Amurskaja Mestnaja	Sowjetunion
9	38	<i>Fagopyrum esculentum</i> Moench var. <i>esculentum</i>	Kazanska	Sowjetunion
10	41	<i>Fagopyrum esculentum</i> Moench var. <i>esculentum</i>	Bogaty	Sowjetunion
11	44	<i>Fagopyrum esculentum</i> Moench var. <i>esculentum</i>	Kalininskaja	Sowjetunion
12	45	<i>Fagopyrum esculentum</i> Moench var. <i>esculentum</i>	Belorusskaja	Belorußland
13	46	<i>Fagopyrum esculentum</i> Moench var. <i>esculentum</i>	Satilovskaja 4	Sowjetunion
14	47	<i>Fagopyrum esculentum</i> Moench var. <i>esculentum</i>	Amurskaja Mestnaja	Sowjetunion
15	48	<i>Fagopyrum tataricum</i> (L.) Gaertn.		Belorußland
16	49	<i>Fagopyrum tataricum</i> (L.) Gaertn.		
17	50	<i>Fagopyrum tataricum</i> (L.) Gaertn.		China
18	66	<i>Fagopyrum esculentum</i> Moench var. <i>esculentum</i>		China
19	67	<i>Fagopyrum esculentum</i> Moench var. <i>esculentum</i>		China
20	68	<i>Fagopyrum esculentum</i> Moench var. <i>esculentum</i>		China
21	69	<i>Fagopyrum esculentum</i> Moench var. <i>esculentum</i>		China
22	70	<i>Fagopyrum esculentum</i> Moench var. <i>esculentum</i>		China
23	72	<i>Fagopyrum esculentum</i> Moench var. <i>esculentum</i>	Serebristaja	Sowjetunion
24	73	<i>Fagopyrum esculentum</i> Moench var. <i>esculentum</i>	Aleksandrovskaja	Sowjetunion
25	74	<i>Fagopyrum esculentum</i> Moench var. <i>esculentum</i>	Burjatskaja	Sowjetunion
26	75	<i>Fagopyrum esculentum</i> Moench var. <i>esculentum</i>	Bogaty	Sowjetunion
27	76	<i>Fagopyrum esculentum</i> Moench var. <i>esculentum</i>	Satilovskaja 4	Sowjetunion
28	77	<i>Fagopyrum esculentum</i> Moench var. <i>esculentum</i>	Slavjanka	Sowjetunion
29	78	<i>Fagopyrum esculentum</i> Moench var. <i>esculentum</i>	Odesskaja	Sowjetunion
30	79	<i>Fagopyrum esculentum</i> Moench var. <i>esculentum</i>	Kalininskaja	Sowjetunion
31	82	<i>Fagopyrum esculentum</i> Moench var. <i>Emarginatum</i> (Roth) Alef.		China
32	83	<i>Fagopyrum esculentum</i> Moench var. <i>Emarginatum</i> (Roth) Alef.		
33	84	<i>Fagopyrum esculentum</i> Moench var. <i>Emarginatum</i> (Roth) Alef.	Krasnoufimskaja 216	Sowjetunion
34	85	<i>Fagopyrum esculentum</i> Moench var. <i>Emarginatum</i> (Roth) Alef.		
35	87	<i>Fagopyrum esculentum</i> Moench var. <i>esculentum</i>	Tokinskaja 356	Sowjetunion
36	88	<i>Fagopyrum esculentum</i> Moench var. <i>esculentum</i>		Deutschland
37	89	<i>Fagopyrum esculentum</i> Moench var. <i>esculentum</i>		Deutschland
38	90	<i>Fagopyrum esculentum</i> Moench var. <i>esculentum</i>		Iran
39	92	<i>Fagopyrum esculentum</i> Moench var. <i>esculentum</i>		CSFR
40	93	<i>Fagopyrum esculentum</i> Moench var. <i>esculentum</i>		CSFR

Supplemental material

41	94	<i>Fagopyrum esculentum</i> Moench var. <i>esculentum</i>		Rußland
42	95	<i>Fagopyrum esculentum</i> Moench var. <i>esculentum</i>	Bogatyry	Rußland
43	98	<i>Fagopyrum tataricum</i> (L.) Gaertn.		Slowakei
44	99	<i>Fagopyrum tataricum</i> (L.) Gaertn.		China
45	100	<i>Fagopyrum tataricum</i> (L.) Gaertn.		Belorußland
46	102	<i>Fagopyrum esculentum</i> Moench var. <i>esculentum</i>		Polen
47	103	<i>Fagopyrum esculentum</i> Moench var. <i>esculentum</i>		Polen
48	104	<i>Fagopyrum esculentum</i> Moench var. <i>esculentum</i>	Chruszowska	Polen
49	105	<i>Fagopyrum esculentum</i> Moench var. <i>esculentum</i>		Slowakei
50	106	<i>Fagopyrum esculentum</i> Moench var. <i>esculentum</i>		Slowakei
51	107	<i>Fagopyrum esculentum</i> Moench var. <i>esculentum</i>		Slowakei
52	108	<i>Fagopyrum esculentum</i> Moench var. <i>esculentum</i>		Slowakei
53	109	<i>Fagopyrum esculentum</i> Moench var. <i>esculentum</i>		Slowakei
54	110	<i>Fagopyrum esculentum</i> Moench var. <i>esculentum</i>		Slowakei
55	111	<i>Fagopyrum tataricum</i> (L.) Gaertn. Subsp. <i>tataricum</i>		Slowakei
56	112	<i>Fagopyrum tataricum</i> (L.) Gaertn. Subsp. <i>tataricum</i>		Slowakei
57	113	<i>Fagopyrum tataricum</i> (L.) Gaertn. Subsp. <i>tataricum</i>		Slowakei
58	114	<i>Fagopyrum esculentum</i> Moench var. <i>esculentum</i>		Slowakei
59	115	<i>Fagopyrum esculentum</i> Moench var. <i>esculentum</i>		Slowakei
60	116	<i>Fagopyrum esculentum</i> Moench var. <i>esculentum</i>		DDR
61	117	<i>Fagopyrum esculentum</i> Moench var. <i>esculentum</i>		Slowakei
62	118	<i>Fagopyrum esculentum</i> Moench var. <i>esculentum</i>		Slowakei
63	120	<i>Fagopyrum esculentum</i> Moench var. <i>esculentum</i>		Slowakei
64	121	<i>Fagopyrum esculentum</i> Moench var. <i>esculentum</i>		Slowakei
65	122	<i>Fagopyrum esculentum</i> Moench var. <i>esculentum</i>		Slowakei
66	123	<i>Fagopyrum esculentum</i> Moench var. <i>esculentum</i>		Slowakei
67	124	<i>Fagopyrum esculentum</i> Moench var. <i>esculentum</i>		Slowakei
68	125	<i>Fagopyrum esculentum</i> Moench var. <i>esculentum</i>		Slowakei
69	126	<i>Fagopyrum esculentum</i> Moench var. <i>esculentum</i>		Slowakei
70	127	<i>Fagopyrum esculentum</i> Moench var. <i>esculentum</i>		Slowakei
71	128	<i>Fagopyrum esculentum</i> Moench var. <i>esculentum</i>		Polen
72	129	<i>Fagopyrum esculentum</i> Moench var. <i>esculentum</i>		Koreanische DVR
73	130	<i>Fagopyrum esculentum</i> Moench var. <i>esculentum</i>		Koreanische DVR
74	131	<i>Fagopyrum esculentum</i> Moench var. <i>esculentum</i>	Steirischer	Österreich
75	132	<i>Fagopyrum esculentum</i> Moench var. <i>esculentum</i>		Koreanische DVR
76	133	<i>Fagopyrum esculentum</i> Moench var. <i>esculentum</i>		Koreanische DVR
77	134	<i>Fagopyrum esculentum</i> Moench var. <i>esculentum</i>		Koreanische DVR
78	135	<i>Fagopyrum acutatum</i> (Lehm.) Mansf. ex Hammer		nn
79	136	<i>Fagopyrum esculentum</i> Moench var. <i>esculentum</i>		Koreanische DVR
80	137	<i>Fagopyrum esculentum</i> Moench var. <i>esculentum</i>	grano sarceno	Italien
81	138	<i>Fagopyrum esculentum</i> Moench var. <i>esculentum</i>	grano sarceno	Italien
82	139	<i>Fagopyrum esculentum</i> Moench var. <i>Emarginatum</i> (Roth) Alef.	grano sarceno	Italien
83	140	<i>Fagopyrum esculentum</i> Moench var. <i>esculentum</i>		Italien
84	141	<i>Fagopyrum esculentum</i> Moench var. <i>esculentum</i>		Italien
85	143	<i>Fagopyrum tataricum</i> (L.) Gaertn.		Italien
86	144	<i>Fagopyrum esculentum</i> Moench var. <i>esculentum</i>		Italien
87	145	<i>Fagopyrum esculentum</i> Moench var. <i>esculentum</i>		Österreich
88	148	<i>Fagopyrum esculentum</i> Moench var. <i>esculentum</i>		China
89	153	<i>Fagopyrum esculentum</i> Moench	Alex	Deutschland

Supplemental material

90	155	Fagopyrum esculentum Moench		Ungarn
91	156	Fagopyrum esculentum Moench	Aral	Niederlande
92	158	Fagopyrum esculentum Moench	Empire	Niederlande
93	159	Fagopyrum esculentum Moench	Skorospelaja 81	Sowjetunion
94	160	Fagopyrum esculentum Moench		Ungarn

Lebenslauf

Name: Benjamin Klug

Geboren: 17.10.1977

Eltern: Rudolf Wilhelm Klug, Dipl. Ing.

Babara Klug, Grosshandelskauffrau

Anschrift: Warstrasse 9

30167 Hannover

Telefon: 0511/3357622

1984 – 1988 Grundschule Herrentor, Emden

1988 – 1990 Orientierungsstufe Wallschule, Emden

1990 – 1997 Gymnasium am Treckfahrtstief, Emden

1997 – 1998 Zivildienst, Ostfriesische Beschützende Werkstätten, Emden

1998 – 1999 Studium, Biotechnologie, Fachhochschule Ostfriesland

1999 Gartenlandschaftsbau, G. Hinrichs, Gartenbau, Emden

1999 Gasthörer, Biologie, Universität Oldenburg

1999 – 2004 Studium, Gartenbau, Universität Hannover

08.11.2004 Abschluss: Dipl. Ing. Gartenbau

ab 01.01.2005 Wissenschaftlicher Mitarbeiter, Institut für Pflanzenernährung,

Leibniz Universität Hannover

Hannover, den 02.05.2010

Scientific Publications:

Klug B, Horst WJ 2010. Spatial characteristics of aluminum uptake and translocation in roots of buckwheat (*Fagopyrum esculentum*). *Physiologia Plantarum* DOI: 10.1111/j.1399-3054.2010.01355.x

Klug B, Horst WJ 2010. Oxalate exudation into the root-tip water free space confers protection from Al toxicity and allows Al accumulation in the symplast in buckwheat (*Fagopyrum esculentum Moench*). *New Phytologist*, accepted.

Klug B, Goldkuhle H, Orlikowski D, Berger RG, Horst WJ 2010. Specific chloride toxicity in strawberries – development of taste and yield related thresholds. *BHGL Tagungsband 27*, ISSN1613-088X

Erklärung

Hiermit erkläre ich, dass ich diese Dissertation selbstständig verfasst und die benutzten Hilfsmittel und Quellen sowie gegebenenfalls die zu Hilfeleistungen herangezogenen Institutionen vollständig angegeben habe.

Erklärung

Hiermit erkläre ich, dass die vorliegende Dissertation nicht schon als Masterarbeit, Diplomarbeit oder ähnliche Prüfungsarbeit verwendet worden ist.

Danke!

Ganz besonderer Dank gilt...

Herrn Prof. Walter J. Horst für die Überlassung dieses interessanten Themas, für die konstruktive Zusammenarbeit, für das entgegengebrachte Vertrauen und nicht zuletzt für alles was er mich gelehrt hat.

Herrn Prof. Goldbach für die Übernahme des Korreferats.

Herrn Prof. Braun für die Übernahme des Prüfungsvorsitzes.

Frau Dr. Angelika Stass dafür, dass sie mich schon mit einer Interessanten Diplomarbeit diesem Arbeitsfeld näher gebracht hat und für eine Vielzahl von Tips, Ratschlägen.

Herrn Dr. Hendrik Führs für die kritische Durchsicht meiner Manuskripte, viel wichtiger aber für die Zusammenarbeit, das Teilen des Büros, den Humor und all seine Unterstützung in allen Situationen die während der Promotion auftraten und natürlich für eine großartige Freundschaft. Ohne Das wäre es wohl sehr viel schwieriger gewesen.

Frau Tanja Frenzel für all die Messungen am ICP, für die Hilfe im Labor und insbesondere dafür, dass sie für alles ein offenes Ohr hatte, für die moralische Unterstützung und dafür, dass es nicht immer nur ernst zugging.

Herrn Dipl. Ing. André Specht für das Teilen seiner großen analytischen Erfahrung und seine uneingeschränkte Hilfsbereitschaft.

Herrn BSc Thomas Kirchner für die optimale Zusammenarbeit, das Interesse an dem Thema und seinen Enthusiasmus.

Frau Dusy für die aktuellsten News, die Sorge um den Zuckerstoffwechsel und besonders für die Hilfe bei der Abwicklung von vielen organisatorischen Dingen.

Meinen Eltern Babara und Rudolf Klug dafür, dass sie mir diesen Weg ermöglicht haben und für die immerwährende Unterstützung.

Meinem Bruder Axel Klug für viele lange Telefonate und seine moralische Unterstützung

Katharina für die Liebe und das Verständnis

Darüber hinaus danke ich allen Mitarbeitern des Institutes für Pflanzenernährung, Herrn Geyer und allen Anderen, die mich unterstützt haben.